POLARIZATION OF RECOIL PROTONS FROM THE PHOTOPRODUCTION OF NEUTRAL PIONS IN HYDROGEN AT 585 AND 660 MEV

Thesis by

John Owen Maloy

In Partial Fulfillment of the Requirements

For the Degree of

Doctor of Philosophy

California Institute of Technology
Pasadena, California
1961

ACKNOWLEDGMENTS

The experiment described in this thesis was undertaken as a joint project of the Synchrotron Laboratory at the California Institute and of the High Energy Physics Laboratory at Stanford University. The support, assistance, and encouragement of the Directors of the two laboratories, Professor Robert F. Bacher and Professor W. K. H. Panofsky, is gratefully acknowledged; Professor Bacher has provided personal support and encouragement.

The initiators of the project were Professor Vincent Peterson at Caltech and Dr. Jerome Friedman and Dr. Henry Kendall at Stanford, who planned and carried out the emulsion exposures at Stanford. The scanning effort at Caltech is the subject of the present thesis; scanning has also been carried out at Rome, under direction of Professor Peterson and Professor A. Manfredini, and at Padua, under the direction of Professor G. A. Salandin. Professor Richard Wilson kindly exposed emulsion to the polarized proton beam of the Harvard Cyclotron.

I am particularly grateful to Professor Peterson, who has sent a continuous flow of advice and privately obtained data from Europe, and to Dr. Friedman and Dr. Kendall for their help and personal encouragement.

In Professor Peterson's absence, Professor Robert Walker has kindly directed the thesis effort. His patient guidance and the benefit of his judgment, both in matters of science and of presentation, are greatly appreciated.

The enthusiasm and ability of the scanning group have contributed

decisively to the successful completion of the experiment. Mrs. Nancy Gross suggested the scanning method eventually used, and she has helped guide the work of the scanners. Over 150 plates were scanned at Caltech, almost entirely by four observers: Mrs. Gross, Miss Geralda Brighouse, Mrs. Cheryl Maloy, and Mrs. Hana Elter. Supporting measurements were made by Mrs. Elaine Motta, Miss Kay Hershey, and Mrs. Sylvia Wilson. Mrs. Nerys Wright verified the data and prepared it for machine computation.

Discussions regarding theory and interpretation with Dr. Carl Iddings and Professor Jon Mathews have been most helpful.

Assistance with numerical computations has been provided by Mr. David Loebakka and Mr. John Link. A number of data reduction and other calculations were performed on the Burroughs 205 and 220 computers at the Institute Computing Center; Mr. H. A. Thiessen was helpful in developing some of the computer programs.

The program was supported by the U. S. Atomic Energy Commission and the U. S. Office of Naval Research, and in Italy by the Italian National Committee for Nuclear Research.

I am personally indebted to the International Business Machines Corporation for a fellowship during the academic year 1959-1960, and to the California Institute for scholarship and other assistance before and after that period.

Besides contributing almost one-third of the data, my wife, Cheryl, has provided continual encouragement and assistance.

ABSTRACT

The polarization of the recoil proton in the photoproduction process $\gamma + p \rightarrow \pi^{o} + p$ has been measured at laboratory photon energies of 585 and 660 Mev, at pion center-of-mass angles of 86 and 77 degrees respectively. Nuclear emulsion was used as a scatterer and detector to analyze the polarization of magnetically selected recoil protons emitted from a liquid hydrogen target. The target was bombarded by bremsstrahlung and electrons from the Stanford Mark III Linear Accelerator. The emulsion was area-scanned for scattering events; no evidence of left-right scanning bias was found. The polarization was calculated from the observed scattering distributions by the method of maximum likelihood, using values of the analyzing power of emulsion obtained at Harwell. Large polarizations were found, 56 ± 14 per cent at 585 Mev and 58 ± 19 per cent at 660 Mev; the 660 Mev value becomes 51 ± 14 per cent if events found in scanning by different methods at Rome and at Padua are included. The polarization is in the direction $\underline{k} \times \underline{p}$, where $\underline{k}$ and $\underline{p}$ are the momentum vectors of the incident photon and recoil proton, respectively. The results are in agreement with measurements made elsewhere. It is shown that the polarizations and angular distributions observed in this reaction are consistent with the choice of odd parity for the second pion resonance, but are not consistent with the choice of even parity.

TABLE OF CONTENTS

LIST OF FIGURES

LIST OF FIGURES (Continued)

I. INTRODUCTION

Since the discovery of the pi-mesons somewhat more than a decade ago, the interactions between the pions and nucleons have been widely studied, most often by the scattering of pions from nucleons and the photoproduction of pions from nucleons by electromagnetic radiation.

As pion and photon beams of higher energy have been available, the pion-nucleon interaction has been found to be surprisingly complex, indicating that a full understanding of the strong interactions may be more remote than was hoped ten years ago.

Both the scattering and photoproduction cross sections show a striking dependence on the energy of the incoming pion or photon. Sharp maxima in the cross sections occur when the total energy in the center of mass system is about 1.25, 1.55, or 1.70 Bev, and a fourth broad maximum has been observed in the pion-proton scattering at about 1.9 Bev. (1-17)

The first maximum appears to arise from a resonant interaction of meson and nucleon in a state of total isotopic spin 3/2, total angular momentum 3/2, and even parity. The photoproduction is excited by magnetic dipole radiation. Strenuous effort has resulted in a modest theoretical understanding of the first resonance, in that the quantum numbers of the resonant state may be derived from first principles, and most of the cross section data can be satisfactorily fitted. (18-21)

A fundamental theoretical explanation of the higher maxima will certainly require an understanding of the interactions between two or

more pions. Even a phenomenological interpretation of the maxima has not yet been obtained. Attempts have been made (22, 23, 24) to interpret the maxima as resonances in definite quantum states, but no resonance model has been shown to be consistent in detail with the observations.

The recoil nucleon from photoproduction or scattering may be polarized even though the beam and target are not. Measurement of the polarization, however, requires high intensity, so that few useful measurements have been made. The experimental difficulties have gradually been reduced by the development of higher-intensity accelerators and of experimental techniques, so that extensive polarization measurements are beginning to contribute to the understanding of the photoproduction process at high energy. It appears that the measurements will prove particularly useful in determining what quantum numbers can be assigned to the higher maxima if they are to be interpreted as resonances in definite states.

A certain amount of information has already been gained from measurements of the total cross sections and angular distributions in photoproduction and scattering. Although the maxima at 1.55 and 1.70 Bev c.m. are observed in the scattering of negative pions in hydrogen, they are not seen in the scattering of positive pions, so that both maxima appear to arise from an interaction in a definite charge state, with total isotopic spin 1/2. The magnitudes of the total photoproduction cross sections also indicate the same assignment. Near the energy of the second maximum, the angular distribution of photoproduced neutral pions is consistent with production in a state of total angular momentum

3/2, by dipole radiation. The parity of the state (that is, whether the exciting radiation is electric or magnetic) cannot be determined from the angular distribution alone, since the shape of a pure multipole distribution is independent of the parity. (25) Interference effects do depend on the parity, but are small and poorly determined in the π^o distributions.

R. R. Wilson at Cornell originally proposed that the second maxima was in fact a resonance with the same angular momentum and parity as the first: unit orbital angular momentum and even parity, excited by magnetic dipole radiation. (22)

However, R. F. Peierls pointed out that the parity assignment made by Wilson leads to difficulty in explaining the energy dependence of the angular distribution of photoproduced positive pions. He concluded that if the second maximum were indeed a resonance, its parity must be odd. (23)

An experimental test of this conclusion was proposed by Sakurai. (26) The nucleon which recoils when a photopion is produced is polarized if at least two multipole amplitudes with the proper spin dependence and phase relation interfere. However, no polarization will be observed at 90 degrees in the center-of-mass system unless two or more states of opposite parity are present. Sakurai pointed out that the Peierls model, in which the first two resonant states have opposite parity, predicted large polarizations, perhaps as high as 80 per cent, at 90 degrees. He argued that the measurement of the polarization of the recoil proton from the photoproduction of neutral pions should lead to an unambiguous result, because the non-resonant production, a confusing factor, is

smaller in the neutral photoproduction, and because the protons recoil in the laboratory with an energy at which their polarization may be found by measuring the asymmetry in the elastic scattering from complex nuclei.

The experiment to be described here is one of several which were undertaken at various laboratories in order to test the predictions of Peierls and Sakurai. The first measurement to be reported was that of Connolly and Weill, at Cornell, using nuclear emulsion as a polarization analyzer; they obtained a polarization of about 30 per cent at 90 degrees c.m. and at a laboratory photon energy of 550 Mev, but with a large statistical uncertainty. (27, 28) Subsequently, P. Stein at Cornell reported counter measurements with a carbon analyzer of the polarizations at 90 degrees. He obtained values of 59 ± 6 per cent at 700 Mev, 30 ± 12 per cent at 550 Mev, and 9 ± 9 per cent at 900 Mev. His values represent averages over a photon energy interval about 150 Mev wide. (28) A more extensive series of measurements, similar in principle to Stein's, is being made at Frascati by R. Querzoli and G. Salvini.

In the present experiment, nuclear emulsions were used as a polarization analyzer, and were exposed to a magnetically analyzed beam of protons recoiling from a liquid hydrogen target. The target was bombarded by electrons and by bremsstrahlung from the Stanford Mark III Linear Accelerator. The protons, most of which come from either the photoproduction or the electroproduction of neutral pions (a process very similar to photoproduction) scatter in the emulsion. Because the protons are polarized, the scattering to left and right is

not symmetric, and from the magnitude of the asymmetry one can determine the polarization of the proton beam. Nuclear emulsion has been previously calibrated as a polarization analyzer by measurement of the scattering asymmetry with a beam of known polarization. (29, 30)

A large degree of polarization, as predicted by Sakurai, is in fact observed. At a photon energy of 585 Mev, at 86 degrees in the center of mass system (pion angle) a polarization of 56 ± 14 per cent is found; at 660 Mev, at an angle of 77 degrees, the polarization is 58 ± 19 per cent. Scanning of the emulsions in the latter exposure was carried out partly at Caltech, and partly at Rome and Padua. The result quoted was obtained from the Caltech data only, and therefore has a large statistical error. Combination of the Caltech data with the data obtained at Rome and Padua yields a result of 51 ± 14 per cent for the polarization at 660 Mev. The polarization is positive in the sense $\underline{k} \times \underline{p}$, where $\underline{k}$ and $\underline{p}$ are the momenta of the incident photon and recoiling proton respectively, in agreement with the other experiments and with the predictions of Peierls and Sakurai.

The prediction of Sakurai has been criticised, (31, 32) on the grounds that an s-wave amplitude or the amplitudes of higher odd-parity resonances could interfere with the even parity states present to give polarization at 90 degrees. Thus, if the second resonance had even parity, as suggested by Wilson, a high polarization might still be observed. Close examination of these suggestions shows that the sign and magnitude of the polarization predicted, at least by the simpler models, does not consistently fit the observations, while the Peierls model not only predicts roughly the observed polarization with the ob-

served sign and energy dependence, but also gives plausible fits to the angular distributions. The fit to the π^o distributions can be improved by including the s-wave amplitude which appears to be present; the effect of this addition is to reduce the calculated polarizations to produce better agreement with experiment. It is not yet clear how well the model can be made to fit the angular distributions of charged photopions.

The same examination shows that a detail which Peierls found troublesome, and which has been cited as an argument against his model, namely, the explanation of the small size of the forward-backward asymmetry in the π^o distributions, is not a source of difficulty at all, especially when s-waves are included. Rather, the size of the observed effect seems to be consistent with the predictions of the model at energies at which the third state is negligible.

Since strong d-waves are also observed in the $\pi^- + p$ scattering, with resonant-like behavior of the phase shift for scattering in the state of total isotopic spin 1/2 and total angular momentum 3/2 (8, 9, 33) the conclusion that the second resonance is indeed a resonance with odd parity seems to be well supported.

With only the presently available data it seems impossible to make any very definite statement about the third maximum, especially since the broad fourth maximum already appears to be important at the energy at which the third occurs. The total angular momentum of the third state appears to be at least 5/2. (17) High energy measurements of the angular distribution and polarization must be obtained before a more definite assignment of the quantum numbers can be made.

II. MEASUREMENT OF THE POLARIZATION OF BEAMS OF FAST NUCLEONS

The polarization of fast nucleon beams is detected by the scattering from complex nuclei, which shows asymmetries proportional to the polarization of the beam. A thorough review of the subject was given in 1956 by Wolfenstein. (34) The following discussion is partly based on the portions of his review which are useful here.

A scattering is described by the relative momentum vectors $\underline{p_1}$ and $\underline{p_2}$ of the two colliding particles before and after the collision. Since the effect of the spin of the target nuclei has been found experimentally to be very small, the discussion may be limited to the case of spinless targets. In this case, the most general non-relativistic scattering amplitude which is invariant under space reflection has the form

$$f(\theta) + g(\theta)\underline{\sigma} \cdot \underline{n}$$

where θ is the scattering angle, $\underline{\sigma}$ is the Pauli spin operator for the nucleon, and $\underline{n}$ is the normal to the scattering plane, a unit vector in the direction of $\underline{p_1} \times \underline{p_2}$. If the beam has polarization P along a direction $\underline{\mu}$, so that $\langle\underline{\sigma}\rangle = P\underline{\mu}$, the scattering cross section is found to be

$$\frac{d\sigma}{d\Omega} = |f|^2 + |g|^2 + 2P\,\mathrm{Re}(f^* g)\underline{n} \cdot \underline{\mu}$$

or

$$\frac{d\sigma}{d\Omega} = \sigma(\theta)[1 + a(\theta)P\underline{n} \cdot \underline{\mu}]$$

where $\sigma(\theta)$ is the scattering cross section for an unpolarized beam. If

the beam is completely polarized, the scattering asymmetry e observed by two ideal counters placed in the plane normal to the direction of polarization at equal angles θ to the left and right of the beam is equal to $a(\theta)$. The scattering asymmetry is defined by

$$e(\theta) = \frac{\text{Number of left counts - Number of right counts}}{\text{Number of left counts + Number of right counts}} .$$

If the scattering is elastic, invariance of the process under time reversal requires that a be also the polarization of an unpolarized beam scattered at angle θ.

The parameter P and the function a are measured experimentally as follows: an unpolarized beam is scattered twice from the same target material at the same angle. After the first scattering, the nucleons scattered elastically at angle θ have polarization $a(\theta)$ in the direction normal to the scattering plane. After the second scattering in the same plane, the asymmetry in the elastic scattering at the same angle θ measured from the polarized beam is $e = a^2$, so that $a = \pm e^{1/2}$. The detector energy resolution must be kept small, so that predominantly elastic scatters are counted.

After the beam polarization has been determined in this manner the second scatterer may be replaced by any desired target and measurements of elastic or inelastic scattering made at other angles. The energy of the beam may be reduced by an absorber without degrading the polarization.

Polarized beams with energies of the order of a few hundred Mev have been produced at a number of cyclotron laboratories. The

scattering of protons and also of neutrons from a variety of targets has been studied at a number of energies. (34-49) At energies greater than 150 Mev strong polarizations, exceeding 90 per cent, have been obtained at some angles. The scattering cross sections and asymmetries show maxima and minima which correspond to the maxima and minima of the diffraction scattering, depending roughly on the quantity $2kR \sin \theta/2$, where R is the nuclear radius and k the wave number. For protons, the polarization in the first diffraction peak is reduced at small angles because the Coulomb scattering dominates the spin-dependent scattering. The Coulomb effect also reduces the polarization in scattering from targets of high atomic number. The polarization decreases at energies below about 130 Mev and becomes quite small below 100 Mev. (34, 35)

The asymmetry in the inelastic scattering from low-lying nuclear levels is essentially the same as in the elastic scattering. However, it decreases more or less linearly with the excitation energy of the target nucleus, becoming small when the excitation energy reaches 30 Mev.(42, 43, 44)

The sign of the polarization, measured absolutely from the scattering of slowed protons in helium (45) is uniformly the same, in the following sense: At angles within the first diffraction maximum, nucleons with spin up scatter preferentially to the left as one looks along the direction of motion of the unscattered particles.

As an example, measurements obtained at Harwell of the asymmetry in the scattering of protons from silver and carbon at about 135 Mev

and from nuclear emulsion at 143, 115, and 91 Mev are shown in figs. 1 and 2. The measured asymmetries have been corrected for the polarization of the incident beam. (35, 30)

The measurements are usually made in the manner described above; a highly collimated polarized beam is incident on a thin foil, and narrow counters are located at precisely equal angles to the left and right of the beam. The angular tolerances are of the order of a few minutes of arc (35) because the single scattering cross sections decrease extremely rapidly with angle. The cross section for silver decreases by about a factor of 10 in the interval from 5 to 10 degrees. To avoid spurious asymmetries, it is therefore essential that the left and right counters be at equal angles from the beam center; the beam must be very well defined in angle, and symmetric. Resolutions of a fraction of a Mev in energy and a fraction of a degree in angle are common; beam intensities are so high, however, that the statistical uncertainties in published measurements seldom exceed 3-5 per cent. Both elastic and inelastic scattering have been studied.

The effects of angular misalignment of the two-counter system have been successfully avoided in some experiments (46) by use of a magnetic field along the beam to rotate the particle spin first to one side and then to the other, so that in principle only a single counter need be used.

These precise double scattering experiments may be regarded as calibrations of the target materials as polarization analyzers for proton beams of a given energy, so that one may refer to the function

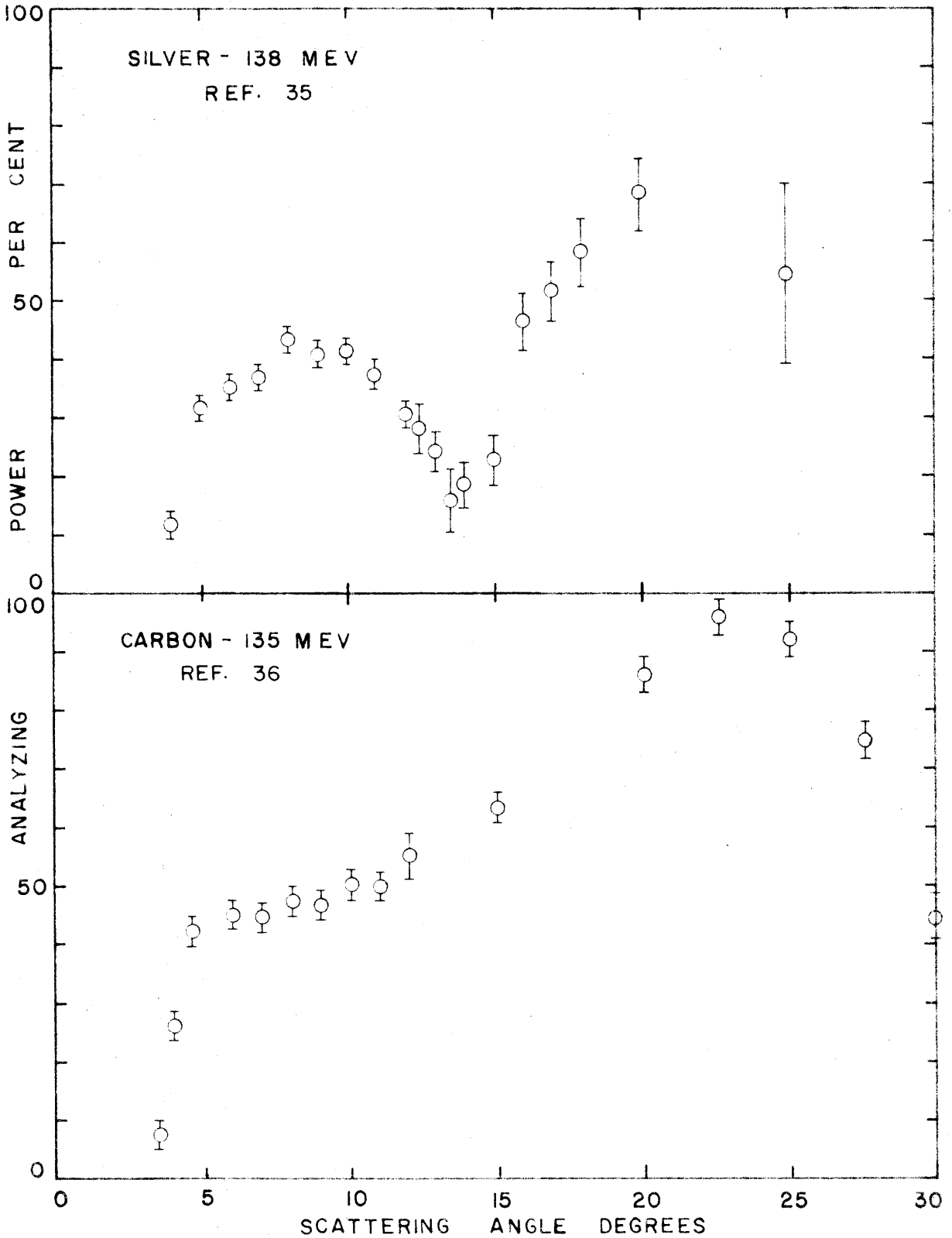

FIGURE 1: PROTON ANALYZING POWER OF SILVER AND CARBON

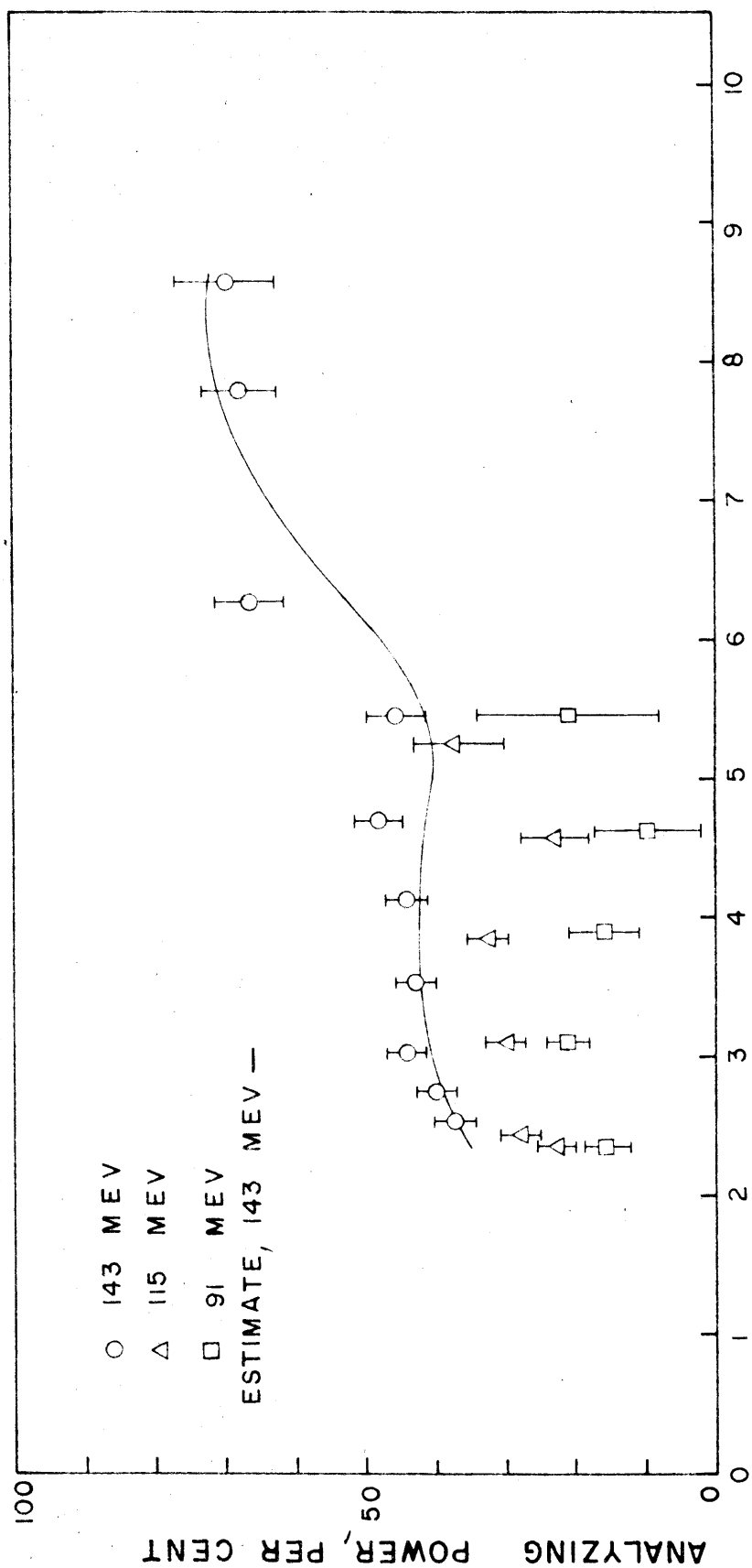

FIGURE 2

PROTON ANALYZING POWER OF NUCLEAR EMULSION

J. RUTHERGLEN, UNIVERSITY OF GLASGOW

$a(\theta)$ as the analyzing power. If the analyzing power is known as a function of angle, energy and energy resolution, there are at least two methods by which one can measure the polarization of a proton beam:

(1) Counter systems can be set up in a fashion already described to left and right of the beam, and the left and right counting rates compared.

(2) A visual detector (bubble chamber or emulsion) can be used to obtain a sample of the angular distribution

$$\frac{d\sigma}{d\Omega} = \sigma(\theta)[1 + Pa(\theta)\underline{n} \cdot \underline{\mu}]$$

of the scatters in the detection medium; the polarization P may then be estimated from the sample by statistical analysis.

In the present experiment the second method was applied to estimate the polarization of the photoproton beam from the reaction $\gamma + p \rightarrow \pi^o + p$ by analysis of the angular distribution of scatters observed in nuclear emulsion.

Not all scattering angles contribute equal statistical weight to the polarization measurement. At small angles the analyzing power is low; at large angles the scattering cross section is low. It seems useful to show how one may arrive at an estimate of the relative utility of different analyzing materials and the relative importance of different angles.

One may define an effective number of counts N_e so that the statistical variance of the polarization is $\sigma^2 = 1/N_e$. The maximum likelihood theorem may be used to show that for a large sample the expected

value of N_e is, from a target of atomic weight A and thickness ρt grams/cm^2 bombarded by an incident flux I_o,

$$N_e = 1/\sigma^2 = \frac{\rho t}{A} I_o N_o \int \sigma(\theta) a^2(\theta) \cos^2\phi (1 + aP \cos\phi)^{-1} \epsilon(\theta, \phi) d\Omega$$

where $\cos\phi = \underline{n} \cdot \underline{\mu}$, $d\Omega = \sin\theta \, d\theta \, d\phi$, $\epsilon(\theta, \phi)$ is the detection efficiency and N_o is Avogadro's number. The other symbols have the same meaning as above.

The integrand has the dimensions of a cross section. A useful quantity, to be called the analyzing cross section, $\sigma_e(\theta, \phi)$, may be obtained by adding the integrands for "left" ($\cos\phi < 0$) and "right" ($\cos\phi > 0$) scattering, assuming unit efficiency. The analyzing cross section is proportional to the number of effective counts obtained from each pair of corresponding elements of solid angle, and is determined as follows:

$$\sigma_e(\theta, \phi) = \frac{\sigma(\theta) a^2(\theta) \cos^2\phi}{1 - a^2 P^2 \cos^2\phi}$$

If aP is small, often the case in practice, a useful approximation to the analyzing cross section is

$$\sigma_e(\theta) \approx \sigma(\theta) a^2(\theta) \cos^2\phi$$

This function determines the relative importance of different angles.

In fig. 3 the values of $a(\theta)$ and $\sigma(\theta) a^2(\theta)$ are plotted for protons on silver and carbon, using the Harwell data at 138 and 135 Mev. (35) The maximum values of the analyzing cross sections are seen to be about 2 barns per steradian for silver at 5 degrees and 0.08 barns

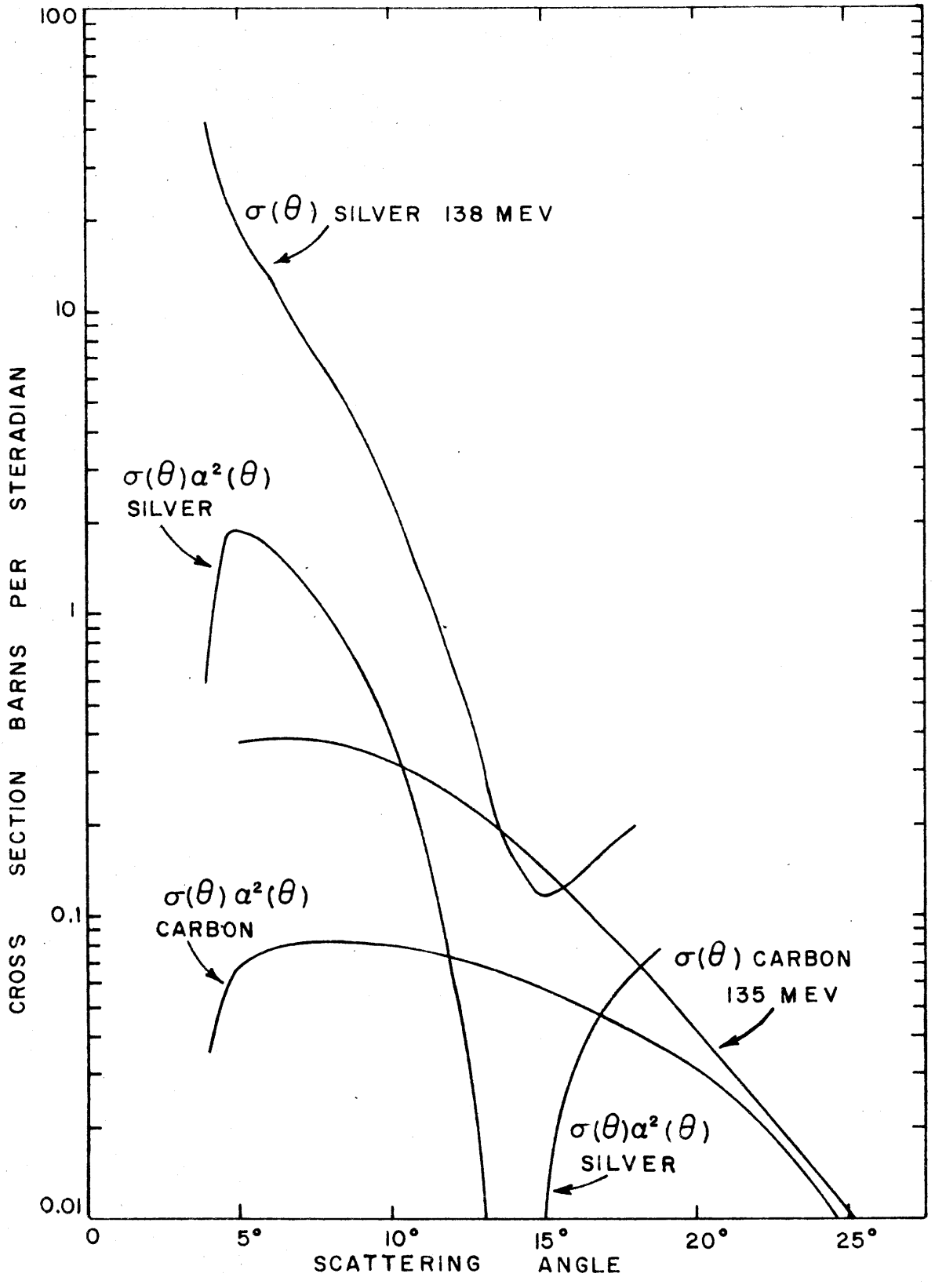

FIGURE 3
SCATTERING AND ANALYZING CROSS SECTIONS FOR SILVER AND CARBON

per steradian for carbon at angles from 5 to 12 degrees.

Another useful quantity is the ratio of effective counts to total counts:

$$\frac{N_e}{N} \approx \frac{\int \sigma(\theta) a^2(\theta) \cos^2\phi \, \epsilon(\theta,\phi) d\Omega}{\int \sigma(\theta) \epsilon(\theta,\phi) d\Omega}$$

The integrals are taken over the range of angles accepted in the experiment. For a visual detector, if all azimuthal angles are accepted with unit efficiency, the average becomes

$$\frac{N_e}{N} \approx \frac{1}{2} \frac{\int \sigma(\theta) a^2(\theta) \sin\theta \, d\theta}{\int \sigma(\theta) \sin\theta \, d\theta}$$

Since the number of effective counts is determined by the statistical accuracy required, the total number of counts varies inversely as the mean square analyzing power.

The material which provides the largest number of effective counts for a given incident flux and target thickness in grams/cm^2 (essentially, that is, for given energy loss) is that which has the largest value of $\sigma(\theta) a^2(\theta)/A$, integrated over the angular interval accepted. To choose the optimum material for a given experiment one must consider, of course, the limitations imposed by multiple scattering, inelastic scattering, and the sources of spurious asymmetry.

III. NUCLEAR EMULSION AS A POLARIZATION ANALYZER FOR 150 MEV PROTONS

Although nuclear emulsion might at first seem inappropriate as a scatterer-detector for polarization analysis, because of the large amounts of scanning time required to obtain a sufficiently large sample of scatters, there are several features which make its use for measurements like the present one attractive. When beam intensities are low, the design of a counter experiment must compromise energy and angular resolution; the elimination of systematic misalignments becomes increasingly difficult. To minimize the effects of experimental asymmetries, a light element is generally chosen as the scatterer, because the elastic analyzing power is somewhat higher compared to the heavier elements; however, the elastic cross sections are lower for the light elements, and the inelastic scattering (of low asymmetry) is higher relative to the elastic, a significant factor if the energy resolution is not narrow (of order 10 Mev).

In such a situation, emulsion has three advantages. First, the effect of angular misalignments and multiple scattering can be eliminated if the scatters are measured directly. Second, the scattering process occurs with a high cross section, so that the effective counting rate per incident particle is higher, as shown by the size of the analyzing cross section for silver in fig. 3; a large solid angle is accepted and the effective target thickness can be made larger. Third, the corrections for inelastic scattering are small, which becomes important if the experimentally accepted energy interval is large.

The effect of inelastic scattering is appreciably larger for the light elements than for the heavy. The cross sections for inelastic scattering have been measured at Uppsala, Harwell, Rochester and Harvard. (40, 41, 47-51) From these cross sections V. Z. Peterson has estimated that if scatters with energy losses up to 50 Mev are accepted, 35 per cent of the scattering from carbon at 135 Mev at an angle of 15 degrees occurs with an energy loss greater than 10 Mev. The fraction is 50 per cent at 180 Mev. If one scales angles inversely as the nuclear radius, the corresponding angle for silver is 7.2 degrees; but with the same energy resolution, only about 5 per cent of the scattering from silver at this angle displays an energy loss greater than 10 Mev. These estimates, which are considered reliable to perhaps 30 per cent, are consistent with direct measurements of the energy losses made in the Pisa propane bubble chamber and in emulsion in the course of the present experiment.

Because of the need for controlling the sources of spurious asymmetries in the counter experiments, the target and detectors must subtend small solid angles, with the result, for example, that appreciable fractions of the running time of major accelerators have been devoted to the measurement of the polarization of the recoil proton in neutral photopion production. If the intensity problems are not severe, however, the rapidity of the counter method in data gathering outweighs the advantages possessed by emulsion, since there is then no need to make experimental compromises. It is also possible that the use of an axial magnetic field to precess the nucleon moment might offer important advantages in making a counter measurement with a low beam intensity.

Even when it appears that the counter method will eventually be the best, emulsion is useful for making exploratory measurements, because its simplicity makes it possible to set up an experiment rapidly, and because the high effective yield (analyzing cross section x solid angle x target thickness) means that the exposure time will be short compared to the time required to make the same exploration otherwise.

After discussing the experimental information available on the calibration of emulsion as a polarization analyzer, it will be possible to give estimates for the scanning time required to obtain a given level of significance, using present scanning methods.

In principle, one should be able to compute the analyzing power of nuclear emulsion from the analyzing powers and scattering cross sections of the pure elements from which emulsion is made. However, the polarization and cross section data are incomplete; in particular, no measurements have been made on bromine, nor have any detailed measurements been made on any element close to bromine in the periodic table.

Nuclear emulsion is a less obnoxious target than bromine, and it can be calibrated directly by the counter technique, using a cyclotron-produced beam of known polarization.

The first measurements were made by direct scanning of emulsion. It was originally shown by J. I. Friedman that nuclear emulsion could be used to analyze the polarization of 300 Mev protons when scanned by the conventional track following technique. (52)

In the energy region of interest here, the first measurement of

the analyzing power of emulsion was that of Feld and Maglić at MIT, who exposed pellicles to the 150 Mev polarized proton beam of the Harvard Cyclotron. (29) Their results are shown in fig. 4, which is taken from their paper. The measurements were not made by direct observation of the scatter, but by counting the numbers of tracks found at equal projected angles to the left and right of the beam direction at a depth of about 2 cm in the emulsion.

Comparison of the Feld-Maglić results with the more recent counter measurements of J. Rutherglen, made at Harwell, and already given in fig. 2, shows an appreciable disagreement at small angles, by almost a factor of two at some angles. (30)

The counter measurement agrees with estimates of the analyzing power of emulsion obtained by combining the Harwell data for silver and carbon, assuming that silver bromide scatters more or less like pure silver. The agreement between the data and the estimate (smooth curve in fig. 2) is seen to be about as good as one might expect. It is worth noting that Rutherglen was able to repeat the previous Harwell measurements on silver and carbon, using the same apparatus employed in the emulsion measurements.

In contrast, the small angle values of the analyzing power obtained by Feld and Maglić do not seem to be consistent with any plausible estimate of the analyzing power based on measurements on the pure elements. Not even the light nuclei have analyzing powers much larger than 0.5 at angles near 6 degrees; the behavior of silver and carbon, shown in fig. 1, is typical of the medium and light elements, respectively.

The conclusion that the MIT results are invalidated by deficiencies

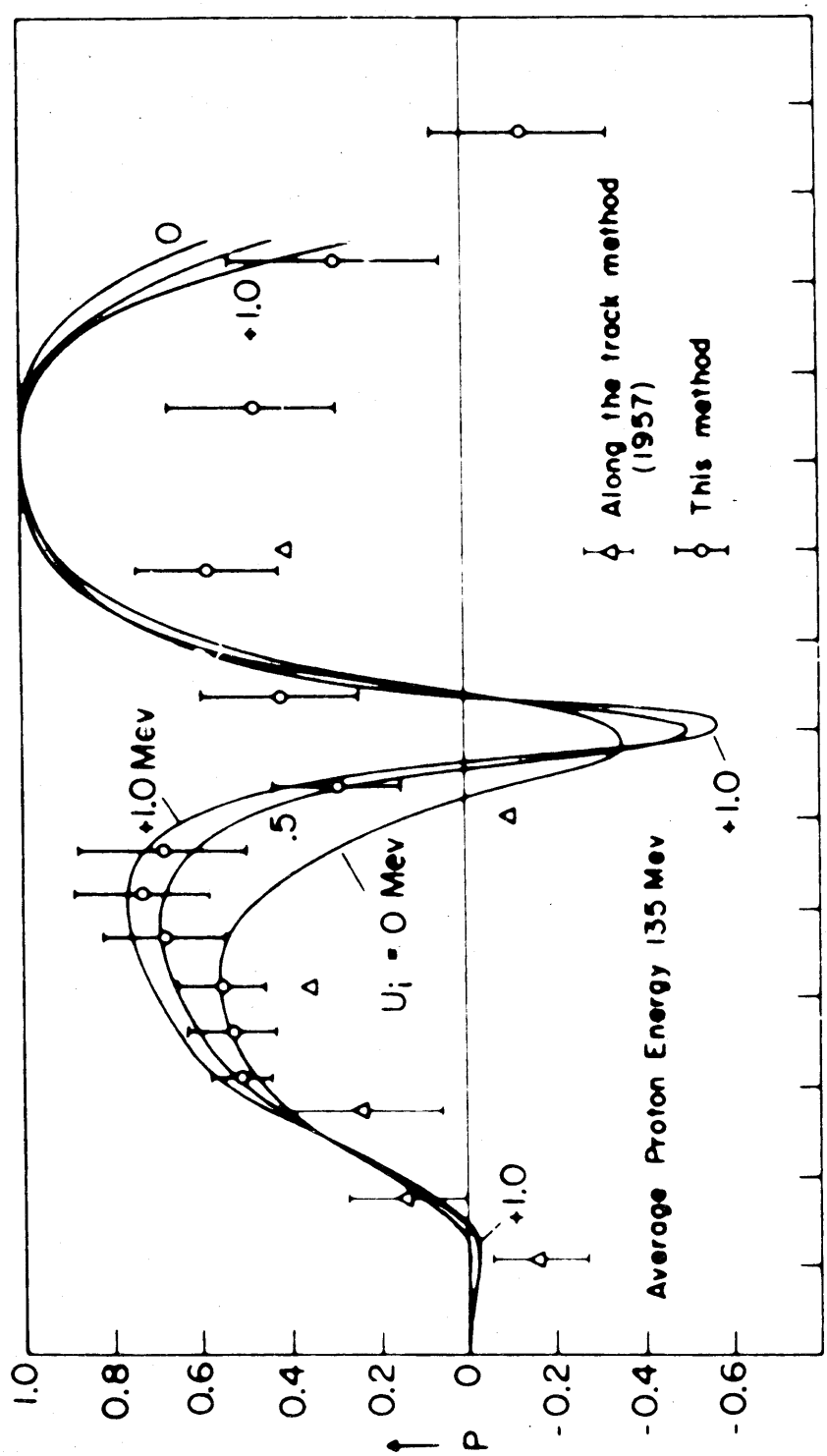

FIGURE 4

ANALYZING POWER OF NUCLEAR EMULSION ACCORDING TO FELD AND MAGLIĆ

in experimental method has been supported by measurements made in the course of the present experiment. The details of these measurements are discussed in Appendix I; it is concluded there that the effects of multiple scattering and of experimental angular misalignments must have been underestimated by Feld and Maglić. It seems clear, therefore, that their values of the analyzing power must be regarded as incorrect. On the other hand, the agreement of Rutherglen's counter measurements with previous Harwell data indicate that they are essentially right, and represent the most satisfactory calibration of nuclear emulsion currently available; the statistical uncertainties are quite small (about 2 per cent) at the most useful energies and angles.

This calibration may be used to estimate the effective counting rate. Using the formula given for the ratio of the number of effective counts to the number of actual counts given in the previous section,

$$\frac{N_e}{N} \approx \frac{\int \epsilon(\theta,\phi)\sigma(\theta)a^2(\theta)\cos^2\phi \, d\Omega}{\int \epsilon(\theta,\phi)\sigma(\theta) d\Omega} ,$$

the values of the analyzing power of emulsion for 143 Mev protons, and an estimated scattering cross section obtained by combining those for silver and carbon, and assuming that scatters with all azimuthal angles are detected with unit efficiency, one obtains the following ratios for scattering into the intervals of scattering angle given:

Scattering Angle Interval	N_e/N
3° - 20°	0.065
6° - 20°	0.10

To obtain a polarization measurement with 10 per cent statistical confidence, therefore, about 1500 and 1000 counts are required in the respective intervals. In the present experiment it has been found that an observer can find slightly less than one event per hour, on the average, in the 3^{o} - 20^{o} interval, so that roughly 2000 hours of scanning are required to make a 10 per cent measurement.

Improvements in the counting rate can probably be made by careful optimization of the exposure conditions, depending on the scanning method used; but it does not seem possible at present to improve this rate by much more than a factor of two without sacrificing the advantages of the emulsion method.

To summarize: As a polarization analyzer emulsion offers the advantages of freedom from systematic errors and high yield per unit exposure time; it suffers from the disadvantage that the analysis time is long. The advantages outweigh the disadvantages when beam intensities are low enough to make the cost of accelerator time relative to scanning time an important factor.

IV. EXPOSURES AND PROCESSING

Stanford Exposures

The measurement of the polarization of the recoil nucleon from photopion production involves severe intensity problems because the nucleons are produced by a process of small cross section and then must be scattered from an analyzer. To avoid contamination from multiple pion production, the electron beam energy must be kept low; synchrotron beam intensities are lower at low energies.

The Stanford Mark III Linear Accelerator operates in the energy region of interest; exceedingly intense bremsstrahlung beams may be obtained. (53) Although the beam pulse is so short that many types of counter experiments are impossible, this limitation does not affect nuclear emulsion, at least in the same way.

The exposures whose analysis is the subject of this thesis were made by Dr. Jerome Friedman and Dr. Henry Kendall of Stanford University and Professor Vincent Peterson, as follows:

The electron beam of the Stanford Linear Accelerator passed through a 1 mil aluminum window in the vacuum pipe which was 15 inches long and struck a copper radiator 11 mils, or 0.017 radiation lengths, thick. The electron beam and the gamma ray beam produced by bremsstrahlung in the copper both irradiated a liquid hydrogen target 8 inches long and one inch in diameter; the target cell was made of 1.2 mil stainless steel. The target was surrounded by an aluminum heat shield 0.25 mils thick, and by a cylindrical vacuum wall 20 inches in diameter. Except for the incoming vacuum pipe and the exit window of 1 mil aluminum, the

vacuum walls were of 5 mil Mylar.

Charged particles coming from the target were analyzed by the 36-inch 180 degree double-focusing magnetic spectrometer described by Hofstadter. (54, 55) The particles passed through two inches of air, the 5 mil Mylar windows of the spectrometer vacuum chamber, and were collimated by the lead entrance slits before entering the spectrometer gap. The slits were 26 inches, and the gap began at a distance of 36 inches, from the center of the target. The rectangular opening of the slits was set to 1 inch in the horizontal plane and 3 inches in the vertical plane, except in early runs where the vertical aperture was 4 inches. A plan view of the target arrangement and the spectrometer and the spectrometer entrance is shown in fig. 5.

The particles leaving the spectrometer were focused onto the emulsion stack, as shown in fig. 6.

Before the exposures were made, a sodium iodide counter was placed at the exit of the spectrometer. The electron beam was monitored with a Faraday cup; (56) the magnet current was the same as that used in the actual exposures. Proton counting rates were measured with the target full and empty and the entrance slits open and closed. The counting rates with the target empty were essentially the same whether the slits were open or closed, and were at most 5 per cent of the counting rate when the slits were open and the target full. After the background runs, the Faraday cup was replaced with a secondary emission monitor. (57)

The emulsion stacks were held between two half-inch aluminum plates by stainless steel pins; the plates fitted into a keyed holder de-

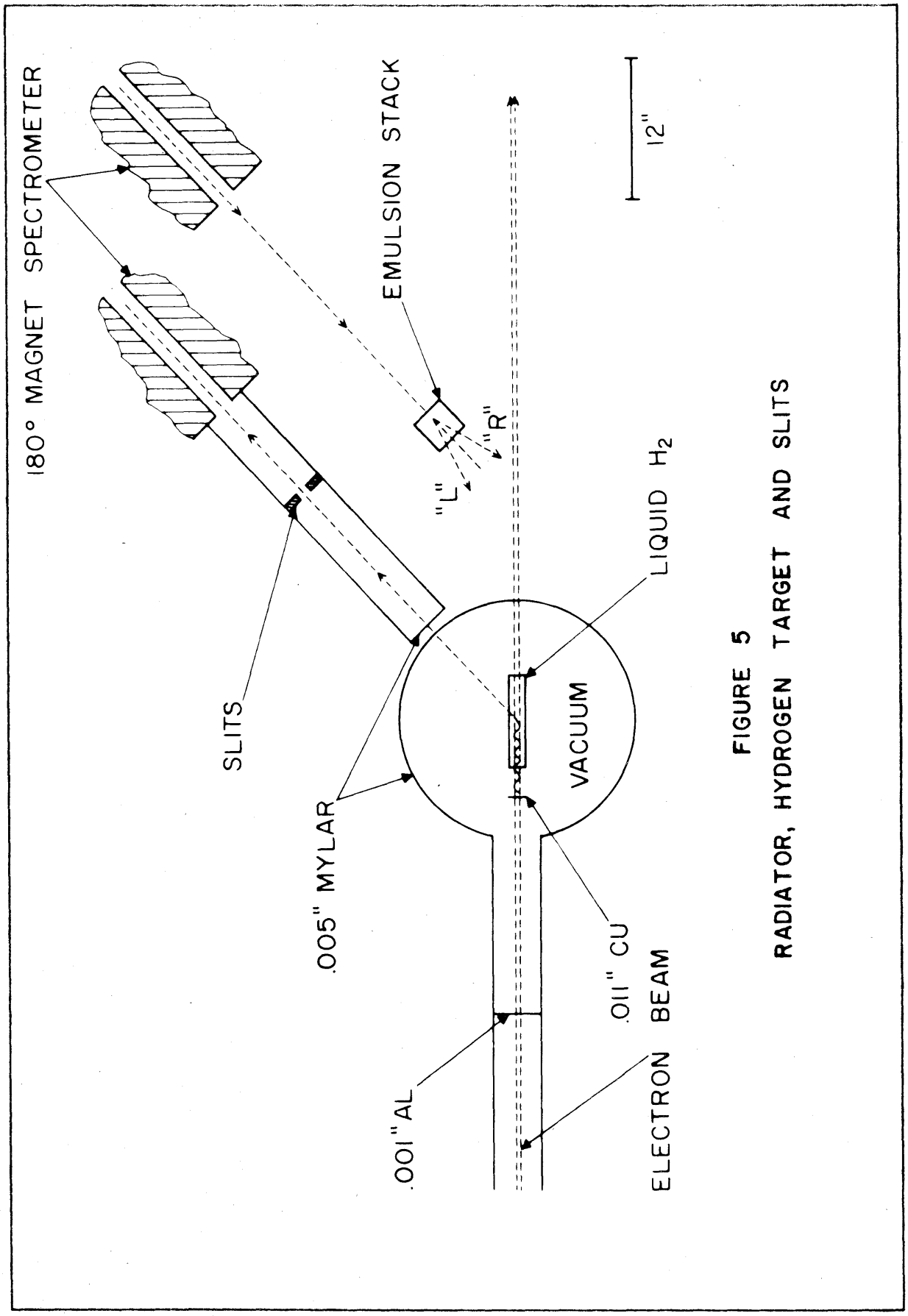

FIGURE 5

RADIATOR, HYDROGEN TARGET AND SLITS

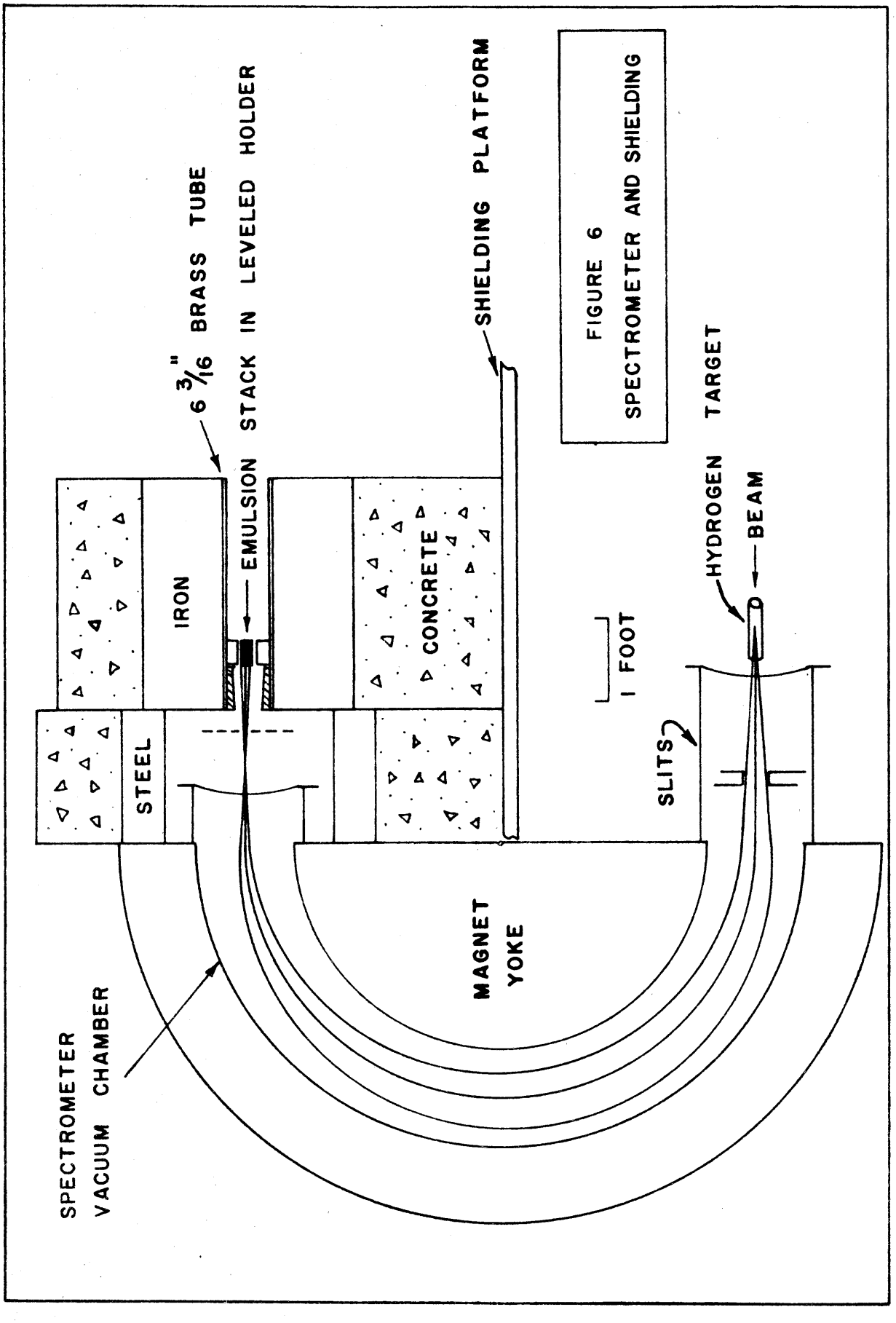

FIGURE 6
SPECTROMETER AND SHIELDING

signed by V. Z. Peterson, who also assembled the stacks. The pellicles were numbered, and a corner was clipped; the assembled stack could only be fitted in one way into the holder, so that no errors in stack orientation could occur. Each stack contained approximately 60 pellicles of 400 micron Ilford K-5 emulsion.

Exposures were made at several laboratory angles and several beam energies, including a run with an empty target.

The maximum momentum which could be focused by the 36 inch spectrometer, about 550 Mev/c, was not quite sufficient to reach an angle of 90 degrees in the c.m. system at each photon energy. At the field strength corresponding to this value of the momentum, the pole tips are partially saturated, and the region where ideal double focusing occurs is radially only about two inches wide. (54)

All of the exposures analyzed here were made with the magnet current set so that the central momentum was 540 Mev/c, according to the momentum-current calibration used at Stanford. The absolute calibration is known to 1 or 2 per cent (58).

The electron beam energies and laboratory angles of recoil, and the corresponding pion center of mass angles, laboratory photon energies, and electron charges delivered are given in the following table:

Stack	Slit Aperture Inches	Target	Electron Energy Mev	Lab Angle Degrees	C. M. Angle Degrees	Lab Photon Energy Mev	Electron Charge Micro-coulombs
A	1x4	Full	650	43.5	86	585	≈1250
C	1x4	Empty	650	43.5	--	--	380
D	1x3	Full	700	47.7	77	660	3000
F	1x3	Full	650	43.5	86	585	2400

Other exposures were made at photon energies of 450 and 520 Mev, and one was made to recoil protons from elastic electron scattering. These exposures have not been analyzed.

On the kinematics diagram, fig. 7, the boundaries of the angle and momentum interval are shown. Two different regions are shown for each exposure; that based on the nominal value of the central momentum and that based on the average momentum estimated from the range of the protons in emulsion, which differs by about 1 per cent.

The electron beam energies were chosen so that recoil photons from two-pion production were not accepted by the spectrometer; at both angles the angle reached by such protons at the maximum bremsstrahlung energy was about 2 degrees less than the inner edge of the laboratory angle interval.

It was considered advisable to allow the electron beam to pass through the hydrogen target, rather than to deflect it with a magnet. Compatibility with other Stanford experiments required that the target chamber be used without modification; it was not suited for use with a deflected beam, since the deflected beam struck the chamber walls. When the beam was deflected, the empty-target counting rate of particles passing through the spectrometer was found to be about 15 per cent of the full-target rate.

Recoil protons from elastic electron scattering were not accepted by the spectrometer unless the electron had previously lost energy by radiation. The (unpolarized) background from this source and from electron scattering with soft photon emission is calculated in the section

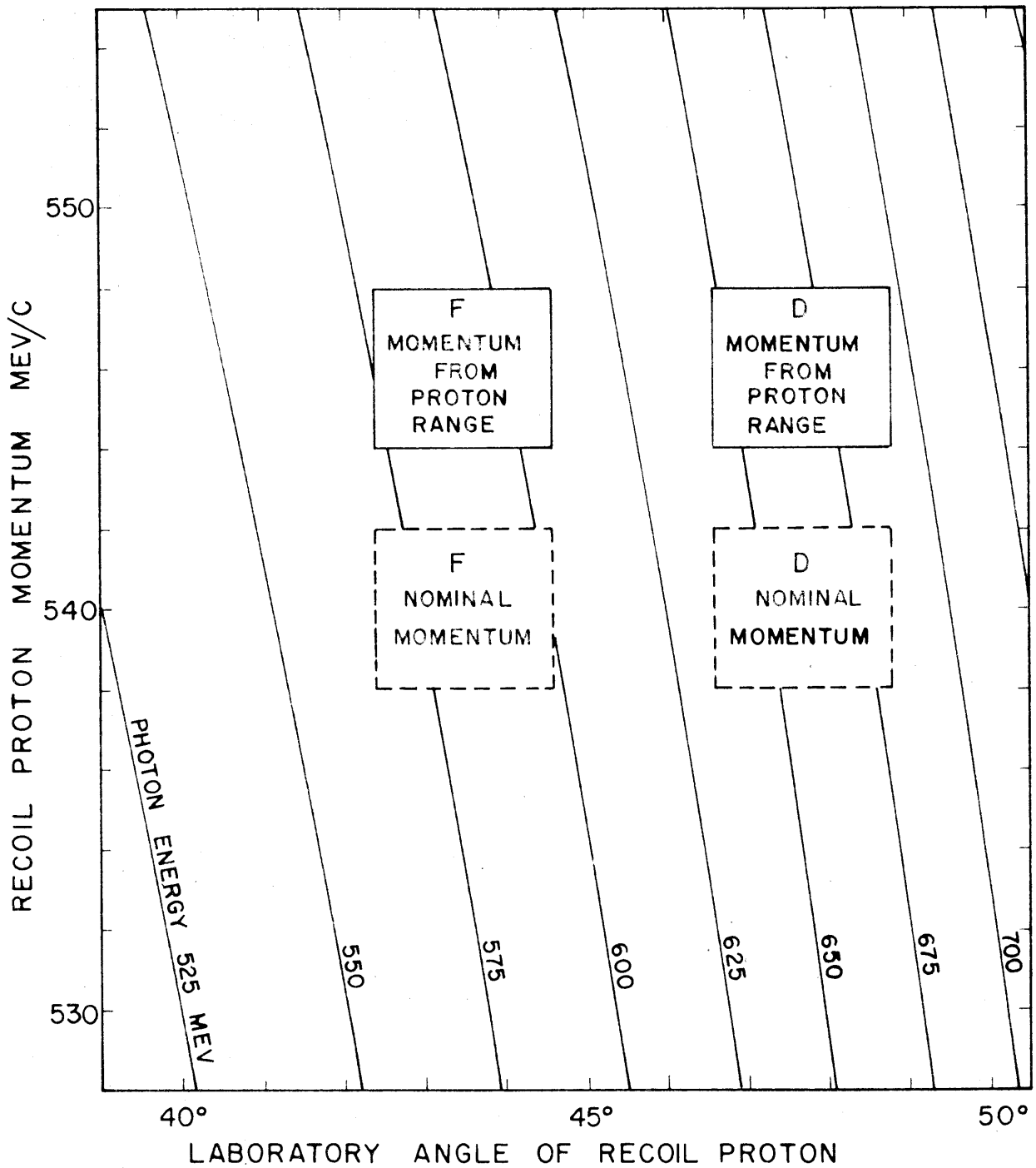

FIGURE 7

PHOTOPRODUCTION KINEMATICS

$\gamma + P \longrightarrow \pi^{\circ} + P$

on Analysis.

The maximum thickness of radiator which could be used was also dictated by the target geometry. The 11 mil thickness of the copper foil corresponds to a radiation length of 0.017; a 20 mil radiator was tried, but was found to produce additional empty-target background, presumably by multiple scattering of the electrons into the steel walls of the target cell. There was no provision for moving the radiator closer to the target, inside the internal heat shield; besides, the amount of heat generated in a radiator by the Stanford beam is generally large enough to make it desirable that the radiator be shielded from the hydrogen cell.

The use of such a thin radiator means that an appreciable fraction (about 40 per cent) of the pions are produced in the electroproduction process $e^- + p \rightarrow e^- + p + \pi^o$, not photoproduced. The two processes are similar; they are almost completely equivalent for forward momentum transfer. The major effect of the electropion process is to smear the kinematics somewhat; the effect is discussed in detail in the section on Analysis.

Because the proton paths are magnetically bent in a plane which contains the proton spin, the precession of the moment must be considered. Including the relativistic precession, the moment rotates 3.068 times more rapidly than the proton momentum vector; the rotation is shown schematically in fig. 8. The approximate result is that protons entering the magnet with spin up leave it with spin down; the detailed effect of the focusing fields on the precession was taken into account in the analysis, described later.

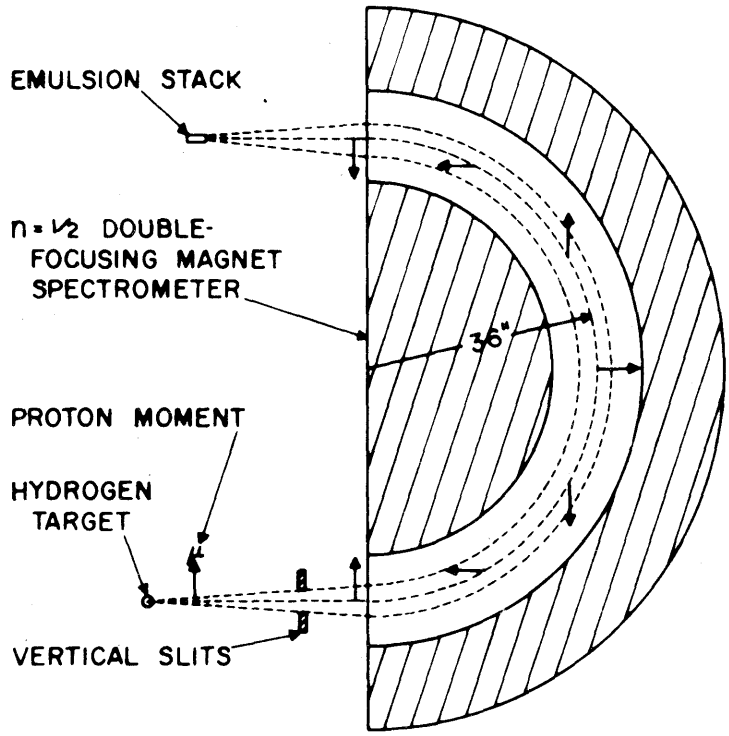

FIGURE 8

PRECESSION OF PROTON MOMENT

Harvard Exposures

Exposures were also made to the polarized proton beam of the Harvard cyclotron, through the kind cooperation of Professor Richard Wilson. Stacks of normal, 2x dilute, and 4x dilute K-5 400 and 600 micron pellicles were exposed to the 144 ± 1 Mev beam, 72 ± 3 per cent polarized. The beam was collimated by lead apertures to an angular width of about 1 degree in both planes.

Processing

After exposure the emulsion pellicles were mounted on glass; the orientation was verified while mounting. The plates were processed using the version of the standard temperature development technique (59) ordinarily employed at Caltech for G-5 emulsion. The results of processing K-5 in this manner were not entirely satisfactory; in some of the processing runs a deposit of developed silver grains appeared at the emulsion-glass interface, causing an annoying reduction in scanning efficiency. The cause of the deposit, whether chemical or other fog, is not well known; it has been found possible to avoid it by wiping the emulsion surface thoroughly before applying the pellicle to the glass slide, so that the plates processed later are free of the deposit. No deposit of this type has ever been experienced with G-5 emulsion.

The Stanford exposures were processed by V. Z. Peterson and H. A. Thiessen.

V. SCANNING

The most straightforward, and the slowest, way to scan nuclear emulsion for scattering events is to follow each track a prescribed distance, following it from plate to plate. This method is very efficient; scatterings with projected angle change as small as 2 degrees can be seen with ease. For this reason the method is generally used in measuring scattering and interaction cross sections. Because the scattering is observed directly with high efficiency, the method is essentially devoid of left-right bias.

Unless special precautions are taken, the trace-through time is larger than the actual following time by an order of magnitude. The rate may be raised if the tracks are not followed from plate to plate; the rate is then determined largely by the time required to record the position of the tracks, so that after following one track the observer may find the next. The rate obtained with either variation of the method depends on the factors which determine the average length of track in a single pellicle: the pellicle thickness, collimation in dip, and multiple scattering.

One may also scan the emulsion area by area, looking for events of the desired kind. The demands on the attentiveness of the scanner are higher, so that this method, although rapid, is less efficient than the track following method. It is not generally used in cross section measurements unless the event looked for is quite distinctive, such as a many-pronged star, or meson decay. The area-scanning rate depends strongly on the density of the events and their visibility.

The scanning method of Feld and Maglić (29), already described briefly, was developed in an attempt to decrease materially the time required to obtain a polarization measurement of a specified level of significance. In their experiment, the incident polarized 150 Mev proton beam was collimated to about ± 1 degree; the projected angle of every track at a certain distance from the incident edge was measured, and the distribution compared with that near the edge. Tracks deviating by more than 5 degrees from the incident beam direction were assumed to have undergone a single scattering; an estimated multiple scattering contribution was subtracted.

With this method the scattering events are not observed directly, and therefore the method is not easily freed of left-right bias; a principal advantage of emulsion is sacrificed for speed. The rate quoted by Feld and Maglić corresponds to a track-scanning velocity of about 8 meters an hour, about 20-50 times faster than the rates that can be obtained with the slower methods.

The Stanford exposures were originally designed to be scanned by the Feld-Maglić method. An attempt to use the method was made by V. Z. Peterson, but the results obtained on Stack A (585 Mev) were felt to be inconsistent; the sign of the asymmetry was opposite to that expected. In Appendix I the Feld-Maglić method is discussed in detail; it was found that the method was invalid at small angles. A sample of tracks which deviated by more than 5 degrees from the beam direction at 23 mm were traced back to the incident edge to determine their history; only 15 per cent of them displayed a single scattering. It appears easily possible that the asymmetry measured by Feld and Maglić was

largely spurious, so that it is not surprising that their values for the analyzing power of nuclear emulsion are implausible.

The method may be modified by following back all wide angle tracks, to eliminate the 85 per cent multiple scattering contribution. Calculations presented in the Appendix show that this procedure (called the "follow-back" method) is also subject to systematic errors which are, however, easier to control; the method is quite inefficient in detecting small angle scatterings.

The pellicles were all mounted on glass with the same orientation. It would have been more desirable to mount half of them upside down, eliminating systematic biases in the scanning process. It is impossible to scan with the plates upside down, viewing the emulsion through the glass, because of the limited working distance of the microscope objectives.

In the circumstances, it appeared undesirable to analyze the existing plates by any method which was sensitive to angular misalignment; it was necessary, therefore, to choose between the track-following and area scan methods. Track following without trace-through was found to be slow, by a factor of two or more, compared to area scanning; accordingly, the Stanford plates were scanned by areas using a procedure designed to avoid a systematic tendency to select scatterings of one sign.

Two of the exposures, Stack F at 585 Mev photon energy, and part of Stack D at 660 Mev, were scanned at Caltech by the area method in the manner to be described. The remainder of the 660 Mev exposure was scanned at Rome under the direction of A. Manfredini and V. Z.

Peterson, using the follow-back method, and at Padua under the direction of G. A. Salandin, by track-following. The data obtained at Caltech represents about half the total.

Area Scan Procedure

Before being mounted on glass the pellicles were printed with a grid which consists of a lattice of numbers at 1 mm intervals and dots at 0.5 mm intervals, arranged in a rectangular coordinate system. The scanning was done under low power,* with a field of view 910 microns in diameter, wide enough to see the 500 micron square bounded by four dots. The scanners searched alternately back and forth, moving normally to the flux of tracks, approaching the same track many times from each side. The emulsion was scanned to a depth of about 23 mm; in some of the plates only the first 10 mm were scanned. The width of the area was adjusted to include the region containing the most tracks, and to exclude the more sparsely-populated areas. Usually the area scanned was about 4 cm wide, containing about 500 to 700 tracks per plate.

The oculars used were without a measuring reticle of any kind, so that there was no line present to provide an angular reference. On most plates, the average direction of the tracks did not differ by more than a degree from the normal to the motion of the microscope stage. Most of the data was contributed by three observers, one of whom

*Objective, 22 X Oil Immersion; Ocular, 10 X wide field.

scanned with the plate reversed on the stage; five other observers also contributed data. Each observer scanned with the plates always in the same position; it was decided that changes in the orientation of the plates by each observer would lead to confusion and errors.

When a scattering was observed, its location was recorded. After the area scan was completed, the scanners measured the projected angle and dip before and after scanning, under higher power.* The projected angle measurements were referred to the normal to the horizontal stage motion, by aligning the reticle hairline with the line of motion of the grains when the stage was moved. The dip of a track was obtained by measuring the difference in optical depth between two points on the track separated horizontally by the length of the reticle, usually 140 microns. The depth of the focal plane can be determined with an accuracy of about 0.5 - 1.0 microns.

The scanners also measured the angle between the stage motion and the grid printed on the pellicle, and the optical thickness after processing of the emulsion. The accuracies of the measurements were as follows: projected angle (including the error in setting the hairline) 0.25°; dip angle in unprocessed emulsion, 1.0°; grid-stage angle, 0.1°; and thickness, 2 per cent.

At the time of measurement the grain density before and after scattering was compared visually so that scattering with large energy loss could be eliminated; it is estimated that, with care, scatterings with energy loss greater than about 30 Mev can be eliminated in this way.

---

*Objective: 53 X Oil Immersion; Ocular: 10X or 15X.

Events were eliminated which did not satisfy certain angular criteria; it was required that the incoming projected angle be less than 8° and that the incoming dip be less than 12 microns per 140 microns in processed emulsion, about 10° in unprocessed emulsion. Events were recorded only if the change in projected angle was greater than 3° and less than 20°, and if the change in dip was less than 24 microns/140 microns in processed emulsion. Tracks whose grain density differed visibly from their neighbors were also eliminated. Meson tracks of the same ionization were readily detected by their multiple scattering: noticeable wandering occurs in a single field of view under high power.

At first the data of all scanners was checked for errors in measurement or the erroneous inclusion of events. It was later found necessary to check in detail only the scanning of the less experienced observers. All data was carefully reexamined twice for errors in recording or transcription.

About two-thirds of the plates of Stack D, exposed at 660 Mev, and almost all of the plates of Stack F, exposed at 585 Mev, were area-scanned at Caltech. Some of the Harvard plates were also scanned, although the scanning was stopped when the analyzing power data of Rutherglen became available.

Scanning Rate

The rate was found to depend strongly on the visibility and density of the tracks and clarity of the plates. The deposit, already described, at the emulsion-glass interface of some of the Stanford plates (especially

those exposed at 660 Mev) decreased the rate and the efficiency. The average rate on all plates was about 0.25 cm^2 per hour; allowing for the density of tracks and the width of the area scanned, this rate corresponds to a track-following rate of about 40 cm per hour.

Scanning Efficiency and Bias

If the scanning method is not entirely efficient, so that a certain percentage of the scattering events remain undetected, it is possible that the selection may be biased, that is, that there be a greater probability for the detection of a scattering to one side than to the other. If the detection is not biased, the difference of the efficiency from unity affects the confidence in the value of the scattering asymmetry only through the increased statistical uncertainty resulting from the detection of fewer events.

The area scanning procedure just described is less efficient than track following; it is more difficult to pick events out of a confused field of tracks than to detect a kink in a single track which is being followed attentively. The efficiency of the technique is also sensitive to any imperfections which obscure the field of view.

The scanning procedure was chosen to minimize systematic bias. Because of the random nature of the search, bias effects should be small: any bias must come from a psychological tendency for the scanners to see left-handed rather than right-handed kinks in the tracks, or the reverse.

The efficiency was measured by repeated scanning of about 15 per cent of the 585 Mev stack. The detection efficiencies were measured

separately for scattering to the left and to the right, and found to be equal within a small statistical uncertainty. The details of the efficiency and bias estimates are given in the section on results.

Additional Scanning and Measurements

Energy loss in a sample of wide-angle scattering events was measured by grain-counting the track before and after scattering, in order to determine the value of the energy loss which resulted in a visible change in grain density. Losses greater than 70 Mev were measured by finding the range of the scattered prong. A very detailed study of the distribution of the energy loss was made by the Padua group, so that it was not required that the measurements at Caltech be extensive.

The grain counting was carried out by Mrs. Elaine Motta, using a 100 X Objective and 10 X Ocular; the length of the reticle scale was 60 microns. At least 400 grains were counted before and after the scattering point. The measurement of ionization by grain counting is not entirely trivial at the range of ionization of interest; the grains are so close together that they often join. Merely counting the density of the black blobs is inadequate; the blob density decreases both at high and low ionizations. At low ionization there are few grains, and at high ionization there are few gaps. The maximum density occurs near the ionization of interest, so that the blob density is a very insensitive measure of the ionization. The remedy is to adapt a convention for handling oversize blobs; the technique must be calibrated, and its reproducibility investigated. (60) In the present measurements, any blob

which filled more than one small division of the reticle (0.5 micron) was counted as more than one grain; the number of grains assigned to such a blob was equal to the number of divisions entirely filled. The calibration was obtained by counting a number of tracks in the plates exposed at 660 Mev; the technique was found to be reproducible within statistics. The grain density-energy calibration obtained is shown in fig. 9. The average slope is such that the counting of 400 grains before and after scattering enables one to determine the energy loss to about 7 Mev.

During the scanning of some of the plates of the 585 Mev stack (F), the scanners recorded all stars which had gray prongs that could be confused with an incident proton. They also recorded the inelastic scatterings recognized by a visible change of grain density.

The number of tracks per cm^2 entering the stacks was measured as a function of the position on the entering face. The track densities were also measured in the plates of the hydrogen-out exposure, Stack C.

The ranges of the stopping protons were measured in both the Stanford and Harvard stacks. The absolute momentum calibration of the spectrometer was known only to about 1-2 per cent, so that the range distribution of the protons provided a useful independent measure of the beam momentum.

As a part of the original attempt to use the Feld-Maglić scanning method, the angular distributions in both projected angle and dip were measured at a distance of 3 mm from the incident edge. The most complete measurements were made on the plates of the first 585 Mev exposure (Stack A). The measurements are consistent with a roughly rectan-

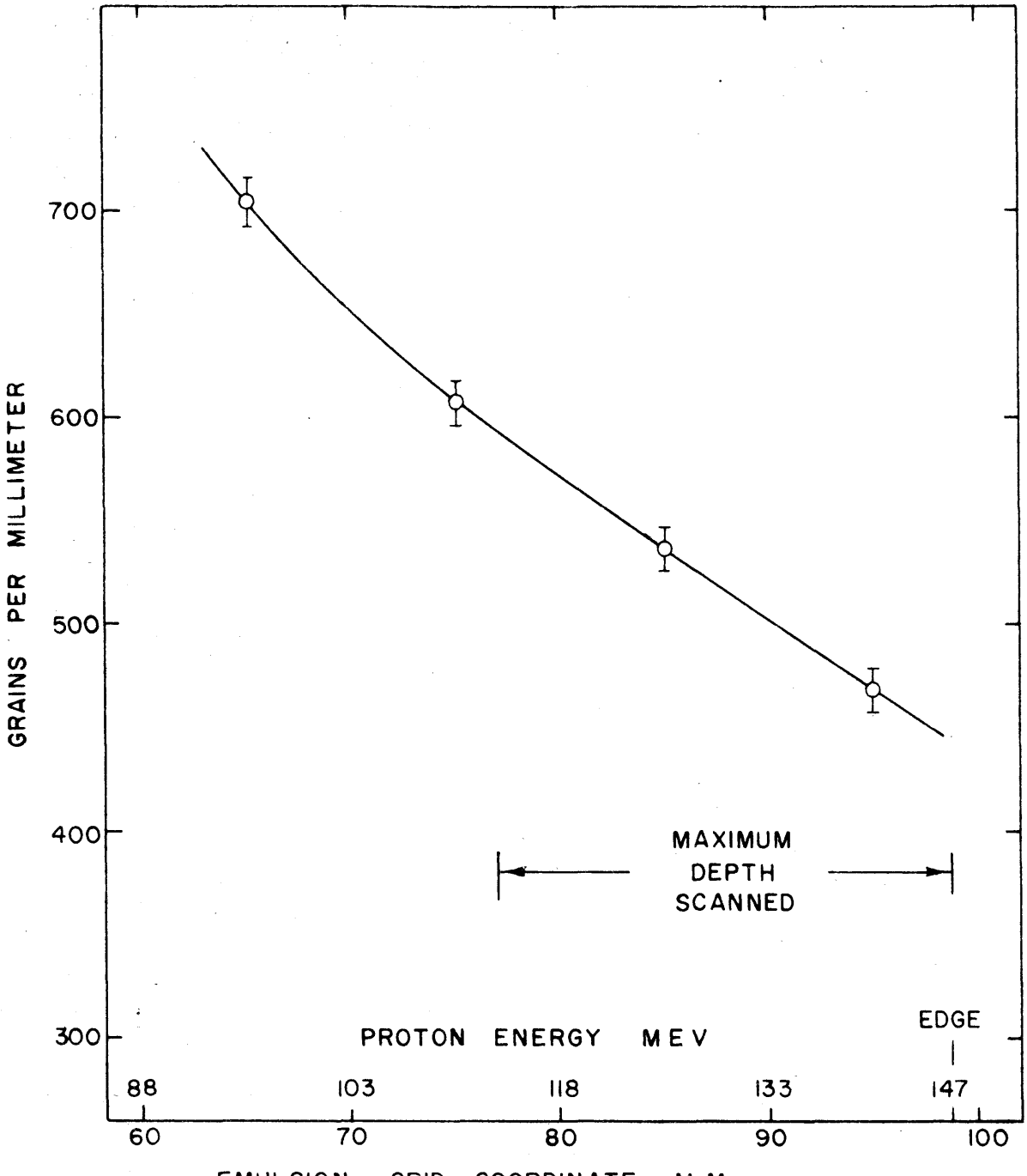

FIGURE 9

GRAIN DENSITY — ENERGY CALIBRATION

STACK D

gular distribution of the incoming angles, whose width is determined by the angular width of the entrance aperture and the angular magnification of the double-focusing magnet (1.17) obtained using the usual optical theory. (61) Sample distributions at 3 mm are shown in fig. 10; the solid curves are calculated assuming a rectangular beam and Gaussian multiple scattering.

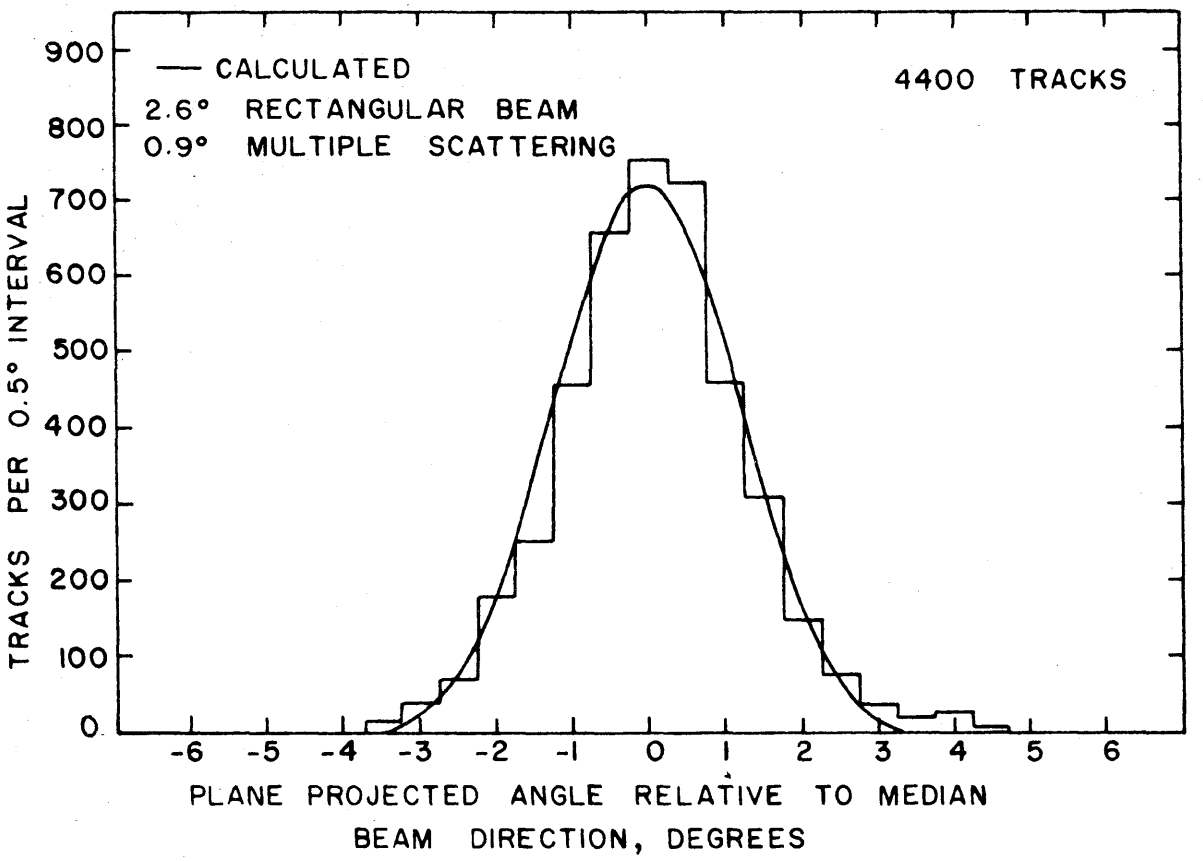

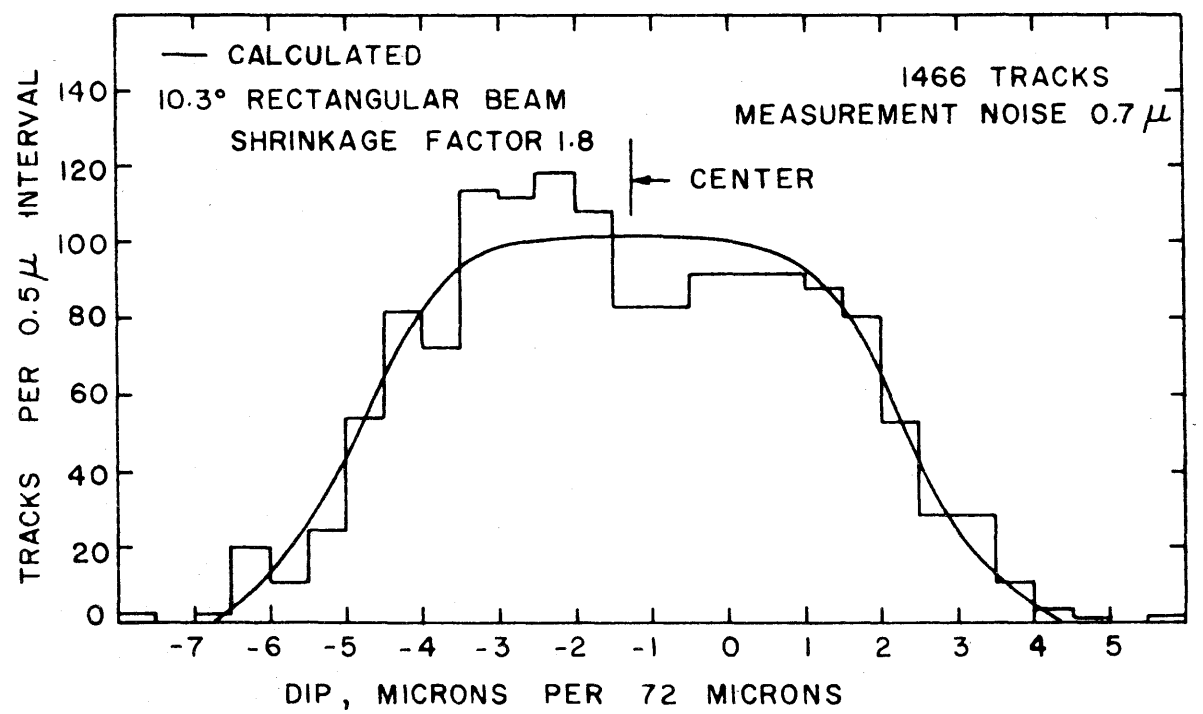

FIGURE 10

ANGULAR DISTRIBUTIONS AT 3 M M, STACK A

VI. ANALYSIS

The analysis of the data poses two independent problems. The first is that of correctly determining the polarization of the proton beam emerging from the double-focusing spectrometer; the second is that of determining how the measured polarization is related to the polarization of the protons recoiling from π^{o} photoproduction: not all of the protons came from this process.

A. Measurement of the Beam Polarization

Statistical Analysis

To estimate the polarization of theemergent proton beam one may simply compare the number of scatterings to left and right, dividing the computed asymmetry by a suitably constructed average of the analyzing power over the chosen interval in angle and energy.

This procedure, while simple, has several disadvantages. The scattering distribution is multidimensional; the scattering angle, azimuthal angle, and the energy of the protons at the scattering point vary appreciably, and are all measured for each scatter. The averaging over all these variables produces a loss of information; furthermore, the construction of the average analyzing power requires that one integrate over the three-dimensional distribution, including the effects of the detection efficiency and the geometrical factors required to convert space angles to projected angles. The product of the detection efficiency and the cross section must therefore be known as a function of the several variables. The calculation must be repeated whenever

the geometrical or other criteria are changed; the data of different groups scanning in different ways cannot be directly compared.

These complications can be avoided by use of the maximum likelihood procedure. The method has four advantages: first, the estimate obtained is statistically optimum, in the sense that the distribution of estimates obtained from successive independent samples has minimum variance; second, the information obtained in the multidimensional measurements is not lost, or incorrectly averaged over, but is all used properly weighted; third, the computations are quite simple; fourth, the cross section and scanning efficiency need not be known, although the efficiency must be unbiased.

The maximum likelihood method is frequently used to estimate a parameter in a distribution from a very small sample, so that the method is often regarded, with some justification, as a device for drawing reliable conclusions from unreliable data. However, it is to be emphasized that the method is both powerful and convenient if the samples are large and multidimensional; the minimum-variance property is an additional dividend.

For the present purposes the maximum likelihood theorem can be stated as follows: Let $f(x_i;P)$ be a normalized probability distribution of known analytical form in an m-dimensional random variable x_i $(i = 1, 2, 3, \ldots, m)$ and an unknown parameter P. Let successive samples S_k $(k = 1, 2, 3, \ldots)$ be taken, each sample containing n values of the m-dimensional variable x_i, denoted by x_{ij} $(j = 1, 2, 3, \ldots, n)$. Then, if there exists <u>any</u> estimate P_k^* of the parameter P from the data of sample S_k which has the property that the distribution of the

successive values of P_k^* has minimum variable, the estimate P_k^* is unique, and is the value of P which maximizes the likelihood function $L(n, k, P)$ for the sample S_k, defined by the product

$$L(n, k, P) = \prod_{j=1}^{n} f(x_{ij}; P) \qquad (x_{ij} \in S_k)$$

The maximum condition may be stated as follows:

$$\left[\frac{\partial}{\partial P} \log L(n, k, P) \right]_{P = P_k^*} = 0$$

As the size of the samples increases $(n \to \infty)$, the distribution of the estimates P_k and the likelihood function both tend to a Gaussian distribution whose variance is estimated from a given sample by

$$\sigma_k^2 = - \left\{ \left[\frac{\partial^2 \log L(n,k,P)}{\partial P^2} \right]_{P=P_k^*} \right\}^{-1}$$

The theorem holds if certain conditions of regularity, which guarantee the existence of a relative maximum of the likelihood function and the existence of a minimum variance estimate, are satisfied; a discussion of these conditions and the proof are given by Cramer. (62)

For a small sample, the theorem provides an estimate of the parameter P but does not give the distribution of the estimate to be expected in successive samplings. It is usual to give a plot of the likelihood as a function of the parameter P to show the shape of the maximum. For large samples, however, the theorem is more powerful; the distribution of the estimates is nearly Gaussian.

Except in the simplest cases, the solution of the likelihood equation

$$\frac{\partial}{\partial P}\Big[\log L(P)\Big]_{P=P^*} = 0$$

for the estimate P^* must be numerical. The solution is, however, always straightforward for a large sample: the likelihood is nearly Gaussian, its logarithm nearly quadratic, and the derivative of its logarithm nearly linear in P. Iterative solution of the likelihood equation, almost a linear equation in P, by a succession of linear approximations (Newton's method) will in general converge promptly. The maximum can also be found graphically, although the former method is better suited to machine computation.

In the present application one wishes to estimate the value of the parameter P in a sample from the distribution

$$f(\theta, \phi, T; P) = \epsilon(\theta, \phi, T)\sigma(\theta, T)[1 + a(\theta, T)P \cos \phi]$$

where, as before, $\epsilon(\theta, \phi, T)$ is the detection efficiency, assumed unbiased,* $\sigma(\theta, T)$ is the unpolarized cross section, $a(\theta, T)$ is the analyzing power, and θ and ϕ are respectively the space scattering angle and the azimuthal angle between the direction of polarization and the normal to the scattering plane. The logarithm of the likelihood function for a sample of n values (θ_j, ϕ_j, T_j), $j = 1, 2, 3, \ldots, n$, is therefore

---

*That is, $\epsilon(\theta, \phi, T)$ is assumed to be an even function of $\cos \phi$.

$$\log L = \sum_{j=1}^{n} \log \epsilon_j \sigma_j + \sum_{j=1}^{n} \log (1 + P y_j)$$

$$y_j = a(\theta_j, T_j) \cos \phi_j$$

and the condition for the maximum is obtained by differentiation:

$$\left[\frac{\partial \log L}{\partial P}\right]_{P=P^*} = \sum_{j=1}^{n} \left[\frac{y_j}{1 + P^* y_j}\right] = 0$$

Notice that the unpolarized cross section and the detection efficiency do not appear in this formula. The variance is determined by the next higher derivative:

$$\frac{1}{\sigma^2} = -\left[\frac{\partial^2 \log L}{\partial P^2}\right]_{P=P^*} = \sum_{j=1}^{n} \left[\frac{y_j}{1 + P^* y_j}\right]^2$$

Space Angles

The use of these formulas involves the calculation, from the measurements of projected angle and dip, of the space angles of scattering: the scattering angle θ between the ingoing and outgoing momentum vectors, and the azimuthal angle ϕ between the normal to the scattering plane and the direction of polarization.

Scattering in emulsion is experimentally represented in terms of the projected angles and dips before and after scattering, as shown in fig. 11. The momentum vectors before and after scattering, $\underline{p}_1$ and $\underline{p}_2$, may be resolved into the rectangular coordinate system shown in the figure; the rectangular components of a vector $\underline{p}$ are given in terms

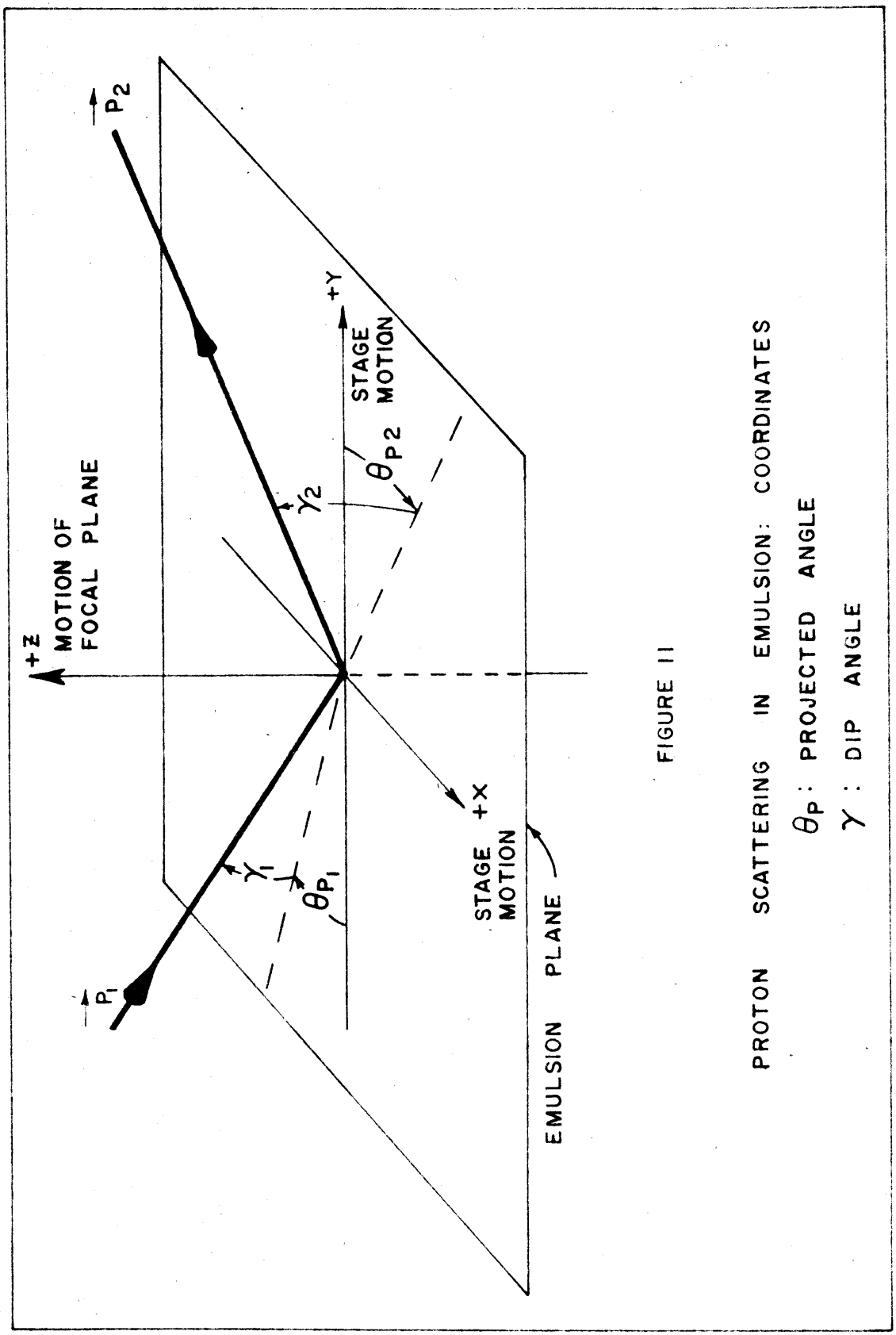

FIGURE 11

PROTON SCATTERING IN EMULSION: COORDINATES

θ_P : PROJECTED ANGLE

γ : DIP ANGLE

of the projected angle θ_p and the dip by

$$p_x = p \cos \gamma \sin \theta_p$$

$$p_y = p \cos \gamma \cos \theta_p$$

$$p_z = p \sin \gamma$$

The space angle of scattering may then be calculated by taking either the vector or scalar product of the two momentum vectors:

$$\sin \theta = |\underline{p}_1 \times \underline{p}_2| / p_1 p_2$$

$$\cos \theta = \underline{p}_1 \cdot \underline{p}_2 / p_1 p_2$$

The components of the normal to the scattering plane are the components of $\underline{p}_1 \times \underline{p}_2 / \sin \theta$.

If the polarization vector $\underline{\mu}$ is fixed in space, the calculation of $\cos \phi = \underline{n} \cdot \underline{\mu}$ is trivial. However, in the Stanford exposures, the effect of the spin precession and the finite dip distribution in producing a distribution of the polarization vector in space must be considered.

Spin Precession

In passing through the spectrometer the proton moment rotates $\Omega = (1 + aE/m) = 3.068$ times faster than the linear moment. (34)* In this formula, a is the anomalous part of the proton moment (1.79 nuclear magnetons); E is the total energy and m is the rest energy of the protons. The numerical value applies to protons of 540 Mev/c momentum.

*I am indebted to Dr. Carl Iddings for providing a short derivation of this formula.

Measurements on the Stanford spectrometer show that the central bending angle is 180. 7 $\pm$ 0. 1 degrees (58); the dip distributions in emulsion confirm these measurements within the experimental error quoted. The total precession angle on the central orbit at a momentum of 540 Mev/c is accordingly 554. 4 $\pm$ 0. 3 degrees, 14. 4 $\pm$ 0. 3 degrees in excess of 1. 5 revolutions. (In fig. 8 the precession angle is schematically represented as 540 degrees, or exactly 1. 5 revolutions.)

Since the polarization is transverse,* the moment is normal to the path at the entrance of the magnet; a finite spread in dip ($\pm$ 3. 3°) was accepted by the slits, so that the distribution of the entering moments had a similar spread. This spread is magnified by the focusing action and the precession; a proton which enters the magnet with dip γ leaves it with dip $M\gamma$, where M is the angular magnification of the double-focusing lens. The total bending angle is therefore less than the central bending angle by an angle $(1 + M)\gamma$. Allowing for the initial position of the moment at the entrance, the angle between the moment at the exit and the direction of the moment on the central ray is found to be $[1 - \Omega(1 + M)]\gamma$. The magnification M may be estimated using the formulas given for a double-focusing lens system by Judd. (61) For the Stanford magnet, where the object distance is equal to the radius, the computed value of the angular magnification is 1. 17. It has already been remarked that the magnet was operated at a rather high field strength, so that there was partial saturation of the pole tips; however,

---

*A small longitudinal polarization, about 5 per cent at most, may be contributed by the direct production process $e^- + p \rightarrow e^- + p + \pi^o$.

the widths of the angular distributions observed in emulsion (fig. 10) do not seem to differ greatly from the widths predicted by the double-focusing theory. Assuming the theoretical value of the magnification, therefore, one finds that the spread of $\pm$ 3.3 degrees at the entrance of the magnet is magnified to a spread of $\pm$ 22 degrees at the exit, so that the total precession angle lies between 532 and 576 degrees.

The precession angle relevant to a given track can be calculated from the dip observed at the entrance of the stack, if the double-focusing formulas are assumed to hold. The exit dip, entering dip, and precession angle are uniquely related; having obtained the direction cosines of the moment vector $\underline{\mu}$, the factor $\underline{n} \cdot \underline{\mu} = \cos \phi$ is readily obtained.

The dip observed immediately before scattering is not uniquely related to the dip entering the stack, because of multiple scattering, which produces a further spread in dip comparable to the entering spread. To determine the dip at the entrance, it is necessary to trace the tracks back to the incident edge. The expenditure of the labor required to trace all the tracks did not appear to be justified by the size of the effect; if the vector $\underline{n}$ is held fixed the scalar product $\underline{n} \cdot \underline{\mu}$ varies by at most 20 per cent as the components of $\underline{\mu}$ vary over the allowed range.

The factor $\underline{n} \cdot \underline{\mu}$ in the maximum likelihood formula for the polarization was evaluated for each event using the conditional means of the components of the moment vector, given that the dip and projected angle before scattering had the observed values. In this fashion the correlation between the observed angles and the orientation of the moment was included. The formulas used to calculate the components

of the moment vector are listed and justified in Appendix 2; in deriving them it was assumed that the multiple scattering is Gaussian, that the distributions of incident dips and projected angles were rectangular, and that the optical parameters calculated from the double-focusing theory are sufficiently accurate.

The interaction of the moment with the radial focusing fields was also investigated, and found to be negligible.

Inelastic Scattering

Measurements made at Uppsala of the analyzing power as a function of angle and energy loss in scattering show that for the elements studied, the analyzing power decreases roughly linearly with energy loss, becoming essentially zero when more than 30 Mev is lost. (42) Scattering which excites nuclear levels lying only a few Mev above the ground state displays an asymmetry similar in magnitude to the asymmetry in scattering from the ground state.

The inelastic scattering is roughly isotropic and uniformly distributed in energy loss, unless individual levels are resolved; the cross sections increase slowly with atomic number. The elastic scattering, on the other hand, increases rapidly at small scattering angles and with increasing atomic number. The possible advantage of using the heavier elements as polarization analyzers has already been pointed out.

It is possible to measure the energy loss of each scattering occurring in emulsion, either by grain counting, or--since the incident beam was highly monoenergetic--by measuring the range of the scattered prong. A resolution of the order of 5 Mev may easily be obtained.

If the energy loss is not directly measured, scattering with energy loss greater than about 30 Mev can be eliminated by visual comparison of the grain density before and after scattering.

A careful study of the inelastic scattering in the 660 Mev exposure has been made at Padua, where the energy losses of 280 events were measured. The results show that the ratio of inelastic to elastic scattering is sufficiently small that the inelastic scattering can be accounted for as a small correction to the data obtained in the Caltech area scan, without measuring the energy loss of each scattering except by visual comparison of the grain density before and after scattering. The manner of making the correction will now be described.

The distributions in scattering angle and energy loss obtained at Padua are shown in fig. 12. About half the Padua data is included; the data shown is representative. The elastic peak manifests itself plainly; the distribution in energy and angle of inelastic scattering is seen to be roughly uniform. To make the correction it was assumed that the analyzing power decreases linearly with energy loss, becoming zero at an energy E_o, and that it is zero if the loss is greater. It was also assumed that the dependence of the cross section on energy loss could be expressed as the sum of the elastic cross section, a delta function in energy loss, and a uniform inelastic spectrum. The analyzing power and cross section per unit angle are then written

$$a = a_o(\theta)(1 - \frac{E}{E_o}) \qquad E \leqslant E_o$$

$$= 0 \qquad E \geqslant E_o$$

$$\sigma = \sigma_o(\theta)\delta(E) + \sigma_i$$

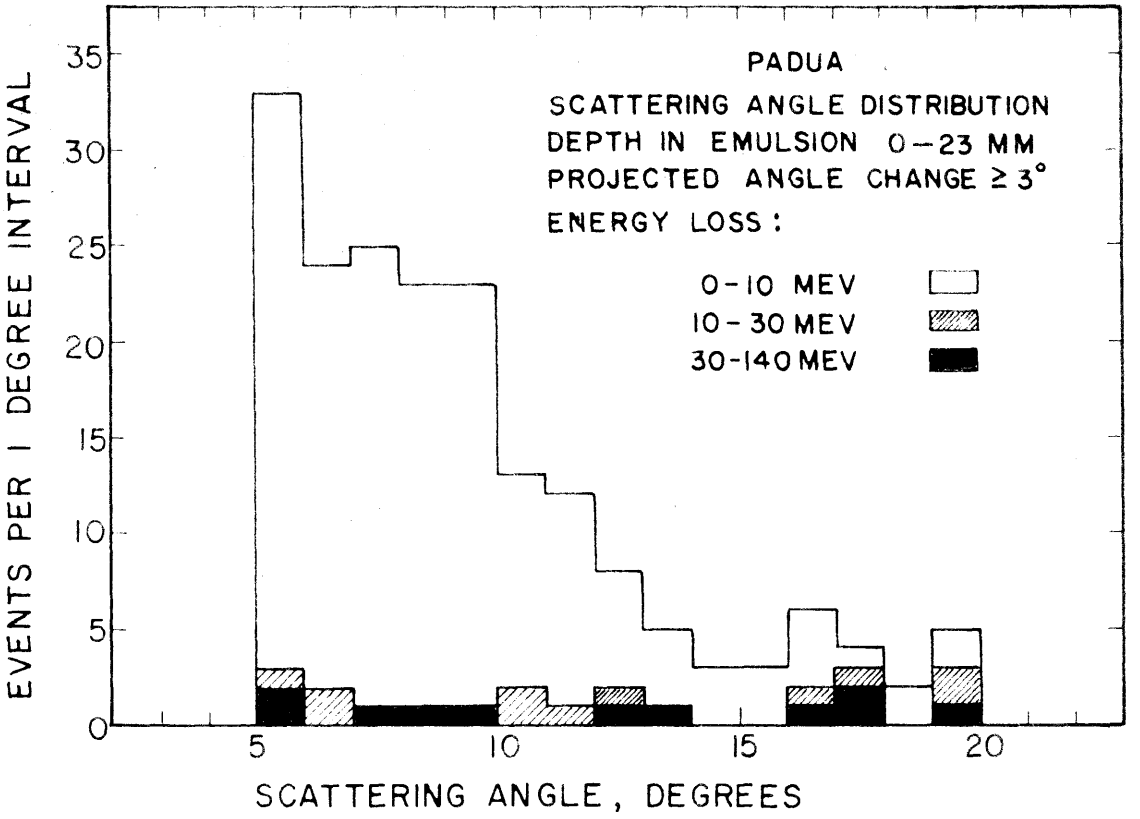

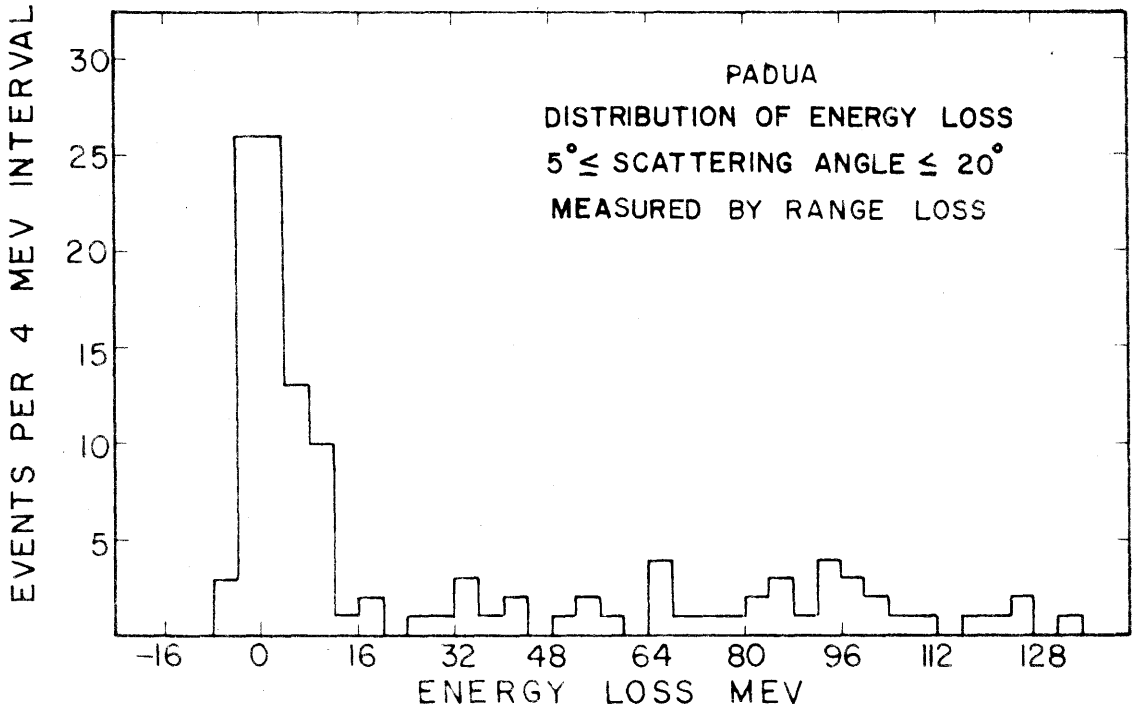

FIGURE 12

TYPICAL RESULTS OF PADUA TRACK SCAN
STACK D

where σ_o is the strength of the elastic delta function, and σ_i is the magnitude of the inelastic scattering per unit energy loss; a_o is the analyzing power in scattering from the ground state and the low-lying levels included in the calibration experiment.

If energy losses up to a maximum value of E_m are accepted, the average value of the analyzing power is

$$\bar{a}(\theta) = \frac{\int_o^{E_m} a(\theta, E)\sigma(\theta, E)dE}{\int_o^{E_m} \sigma(\theta, E)dE}$$

or, if $E_m \geqslant E_o$,

$$\bar{a}(\theta) = a_o(\theta)\left[1 - \frac{1}{2}\,\frac{\sigma_i E_o}{\sigma_o + \sigma_i E_m}\right]$$

The parameters σ_o and σ_i were determined from the Padua data. The elastic cross section per unit angle was taken to be proportional to the number of events in the interval of energy loss $0 \leqslant E \leqslant 10$ Mev, and the inelastic intensity σ_i was taken to be proportional to the average number of events per unit energy loss and per unit angle in the interval $10 \leqslant E \leqslant 30$ Mev. It was assumed that the detection efficiency was essentially unity at the angles shown.

The maximum energy loss accepted in the area scan was taken to be 30 Mev. The results of the measurements of energy loss by grain-counting wide angle tracks, described previously, or by measuring the range of the scattered prong, are shown in fig. 13 (lower histogram). No event accepted in the area scan was found to lose more than 27 Mev. Some scatters rejected because the grain density changed visibly upon scattering were grain-counted; the smallest energy loss found was 15 Mev.

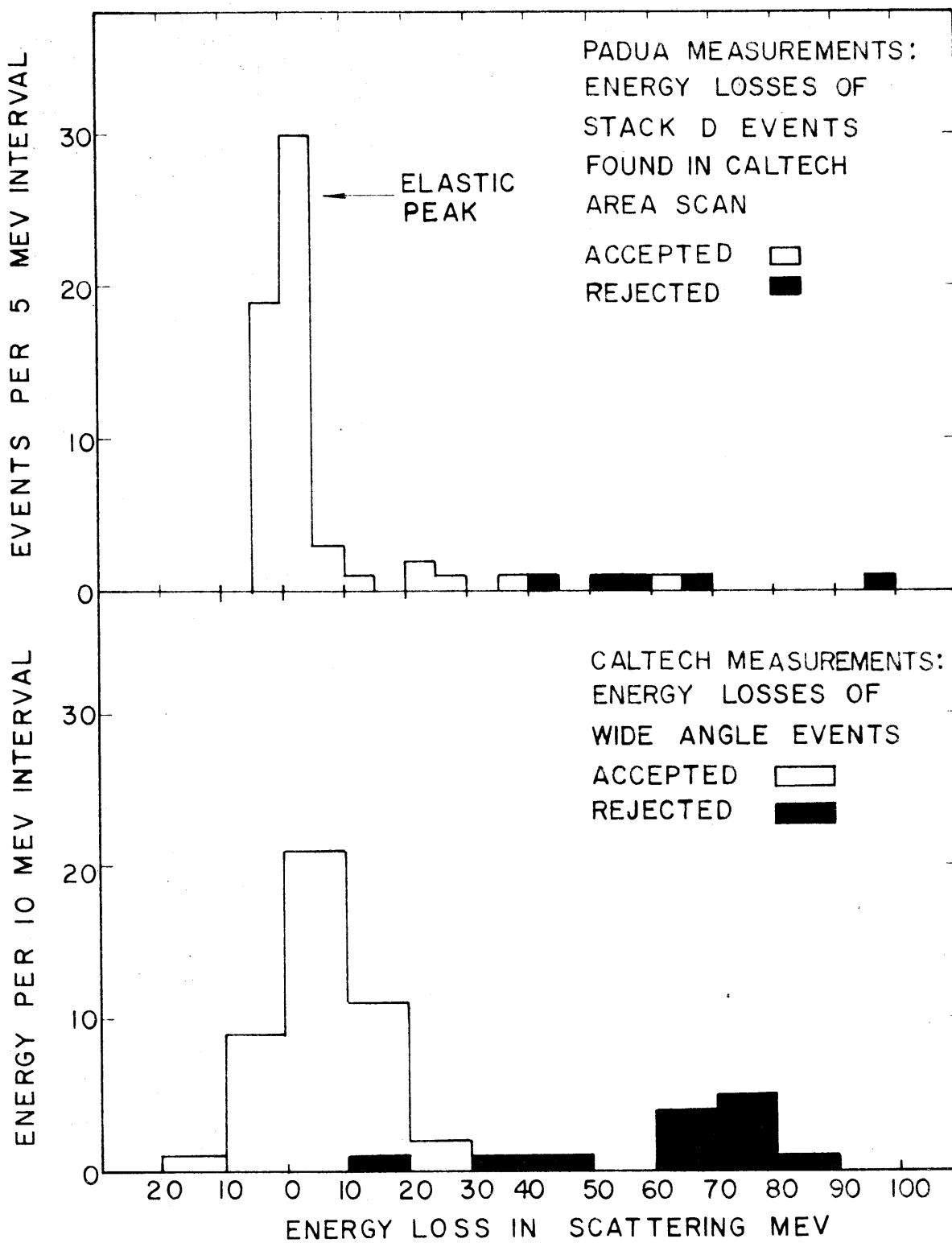

FIGURE 13

ENERGY RESOLUTION OF AREA SCAN
FROM VISIBLE CHANGE IN GRAIN DENSITY

A similar determination (upper histogram) was obtained by identifying events accepted in the area scan of the 660 Mev exposure at Caltech which were also detected at Padua, where their energy losses were measured; two events with an energy loss greater than 30 Mev were accepted, and several others rejected.

Using the parameters derived from the data, supplemented at wide angles by the elastic cross section estimated for emulsion by V. Z. Peterson from the Harwell data shown in fig. 3, the following correction was obtained:

θ, deg.	$\Delta a_o/a_o$, %	
6	-2.0	
8	-2.4	
10	-3.1	
12	-5.8	
14	-11.2	
16	-13.8	Elastic Minimum
18	-12.5	
20	-14.6	

The magnitude of the correction for a given sample depends on the angular distribution of the sample; the correction to the Caltech data will be given in the section on Results. The correction is quite small, since only about 15 per cent of the events found in the area scan and used in the analysis scatter more than 12 degrees; in fact, the statistical uncertainties in the analyzing power at wide angles are as large as the correction.

Data Reduction Procedure

The calculation of the polarization was performed in two steps:

First, the space scattering angle, the scalar product $\underline{n} \cdot \underline{\mu}$, and the kinetic energy at the point of scatter were computed for each event. The angular factors were calculated in the manner outlined above, and the kinetic energy was obtained from the depth in emulsion at which the scattering occurred, using the range-energy relation published by Barkas (63), allowing for the measured density of the emulsion. The range of the protons disagreed slightly with the value predicted using the nominal value, 540 Mev/c, of the incident proton beam. In the stacks exposed at Harvard, however, the measured range agreed very well with the range predicted from beam energy of 144 $\pm$ 1 Mev; it was therefore assumed that the momentum calibration of the Stanford spectrometer (known to about 1 or 2 per cent) was in error by about 1 per cent. The incident momentum was taken to be 546 Mev/c.

Second, the effective analyzing power $y = a(\theta, T)\underline{n} \cdot \underline{\mu}$ was calculated for each event and the maximum likelihood solution obtained by linear iteration; the likelihood was then computed as a function of the polarization to display the shape of the maximum. The analyzing power data furnished by Rutherglen (fig. 2) was approximated by a table in the variable $\theta \sqrt{T/mc^2}$ for each of the three proton energies (91, 115, and 143 Mev) at which measurements were made. The value of the analyzing power for each event was found by interpolation. At small angles the 143 Mev data was supplemented by the Harwell measurements on silver at 138 Mev (fig. 1). The decrease in the analyzing power at

the two lower energies was estimated from the corresponding decrease for carbon; the low-energy analyzing power of carbon has been measured at Harwell. (36) The values of the analyzing power used in the calculation are shown in fig. 14, except that the analyzing power was set to zero at angles beyond $\theta\sqrt{T/mc^2} = 8.0$ degrees, furnishing a cutoff at about 21.5 degrees in scattering angle to the average energy of 130 Mev. The effects of inelastic scattering and the uncertainty in the analyzing power at wide angles and low energy were investigated by modifying the analyzing power at wide angles.

The numerical computations were performed with the Burroughs 220 computer. Mr. H. A. Thiessen assisted in developing the programs. Most of the data was prepared for the computer either by Mr. Thiessen or by Mrs. Nerys G. Wright. The preparation of the data was thoroughly checked for errors in recording or in translating the data to the form accepted by the computer. After proofreading, the data for each plate was summed as it was punched on paper tape; the sum was checked after the tape was read by the computer. The space angles program was designed to use the data in raw form as originally recorded, without preliminary processing.

Other programs were used to sort the space angle and energy data into histograms, and to sort the values of the effective analyzing power, $y = a(\theta, T)\underline{n} \cdot \underline{\mu}$. It is estimated that the cost of such simple but tedious sorting operations is 20-30 times less if done by machine rather than by hand.

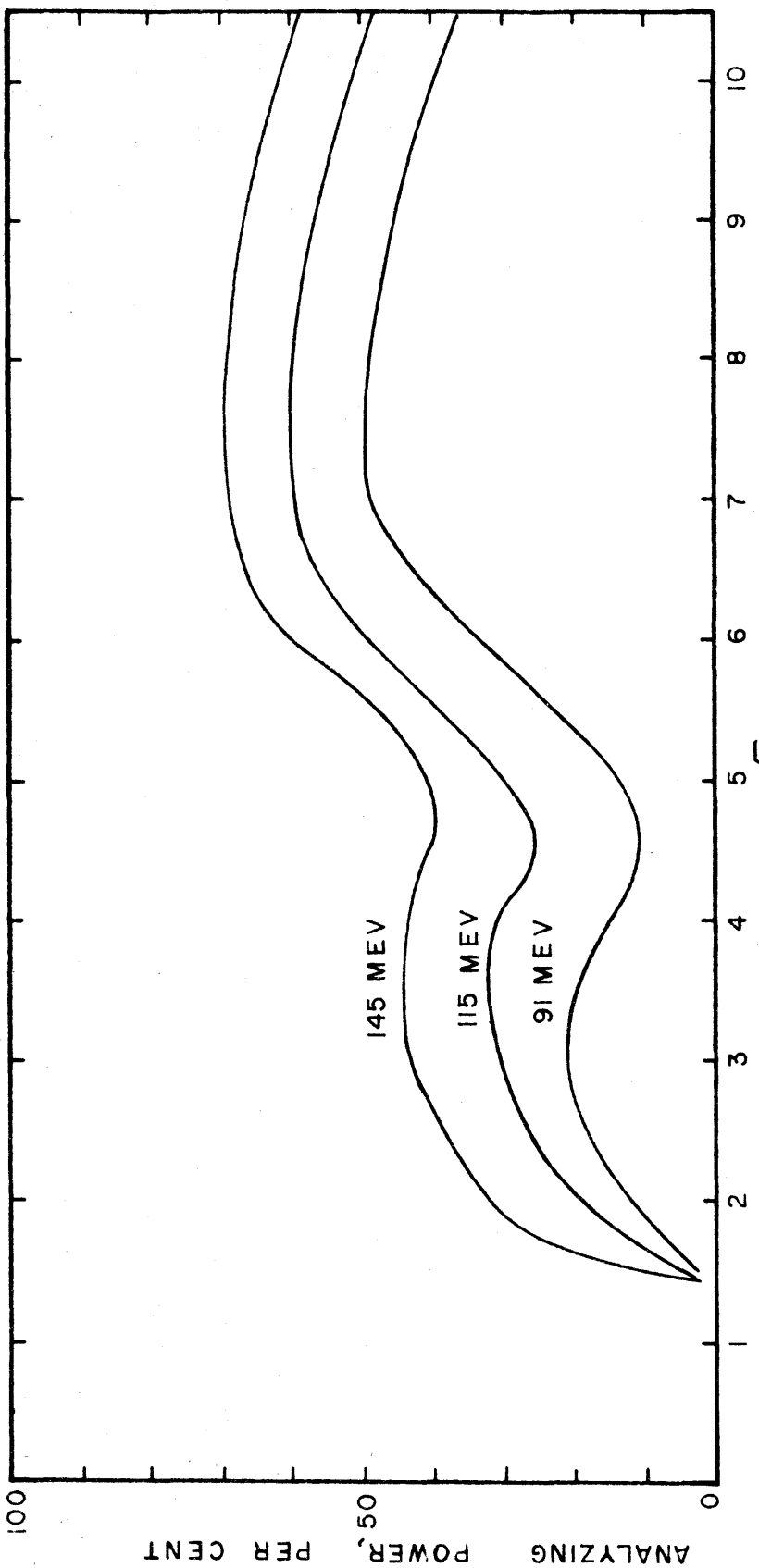

FIGURE 14

ANALYZING POWER ASSUMED FOR NUCLEAR EMULSION
(ESTIMATED AT WIDE ANGLES AND LOW ENERGY)

B. OTHER PROCESSES

When the electron beam passed through the target a number of recoil protons were accepted by the spectrometer which came from processes other than the photoproduction of neutral pions or the scattering of electromagnetic radiation (assumed to be negligible). One of these processes was the direct production of pions in the reaction $e^- + p \rightarrow e^- + p + \pi^o$; also, protons were accepted which recoiled from the scattering of electrons with soft photon emission, in the reaction $e^- + p \rightarrow e^- + p + \gamma$, or from the elastic scattering of electrons which had previously lost energy by radiation. The contributions from all of these processes can, however, be estimated.

Electron Scattering

The cross section for the scattering of electrons from protons with a point charge and point anomalous magnetic moment has been calculated by Rosenbluth in first Born approximation from the following diagram, on which the amplitudes for the emission, absorption, and propagation of the virtual photon are shown in Feynman's notation (64) apart from a numerical factor:

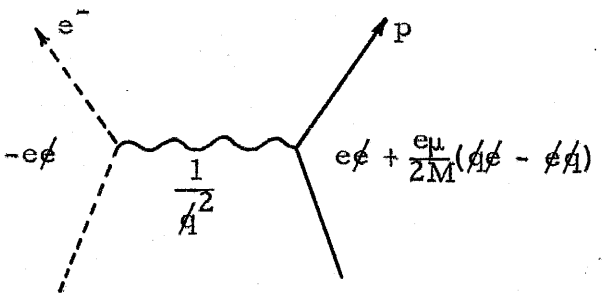

The electron scattering experiments at Stanford have shown that the

Rosenbluth formula correctly represents the data if it is multiplied by a form factor, which is a function only of the invariant four-momentum transfer, to take account of the finite size of the proton. The form factor for the charge and the Dirac moment seems to have the same shape as the form factor for the anomalous moment. The radius of the charge-moment distribution seems to be about 0.8×10^{-13} cm. (54, 55)

The radiative correction to the elastic scattering, to allow for inelastic emission of soft photons, has been calculated by Schwinger and by Schiff. (65, 66) The correction is in the form of a factor multiplying the Rosenbluth cross section, which depends on the experimental energy resolution, and which gives the energy spectrum of the radiative scattering. The cross section and the correction are given, in terms of the laboratory angle and energy of the recoil proton, in the paper by Tautfest and Panofsky.* (67) The radiative correction factor has the following form:

$$\Delta = \frac{\alpha}{\pi}\left\{\left(\log\frac{q_e}{mc} - \frac{1}{2}\right)\left[\log\left(x + \frac{1}{x} - 2\right) + x + \frac{11}{6}\right] - \frac{17}{18} - 4\phi(\theta)\right\}$$

$$x = \frac{q_e}{q_m}$$

where α is the fine-structure constant, q_e is the laboratory momentum if the recoil protons from elastic scattering, and q_m is the minimum laboratory momentum accepted; $\phi(\theta)$ is a function of the laboratory angle of recoil.

---

*There is an error in the formula for the Rosenbluth cross section in this paper; the linear factor in the total proton moment $\mu + 1$ should be squared.

In the present exposures the recoil protons from elastic scattering were not accepted by the spectrometer: the elastic recoil momentum q_e was above the upper limit of the momentum window. The contribution which fell within the narrow window was estimated by multiplying the derivative of the spectrum factor with respect to q_m by the width of the momentum window and by the Rosenbluth cross section and the square of the experimental form factor. (54)

The number of protons from the elastic scattering of electrons slowed by radiation was calculated using the Rosenbluth cross section and experimental form factor, evaluated at the incident electron energy which produced a recoil accepted by the spectrometer.

To compare the contribution from the scattering processes with the contributions from photoproduction and electroproduction, the number of useful protons per incident electron was calculated from the known radiation probability in the radiator, target windows, and liquid hydrogen. The bremsstrahlung intensity from the copper radiator and steel windows was computed using the thin-target spectrum derived by Bethe and Heitler. (68) The radiation in hydrogen, comparable in magnitude, was determined from the recent calculation of Becker, DeStaebler, and Panofsky, based on the Wheeler-Lamb estimate of the radiation from the atomic electron. (69, 70).

The laboratory photopion yields per unit proton energy were obtained from the data of Vette. (14) A summary of the details of the calculation of the relative contributions of the two electron-scattering processes is given in Table I. The contributions are expressed in terms of the ratios of the yields per unit solid angle and per unit proton energy.

TABLE I

SUMMARY OF ELECTRON SCATTERING CONTRIBUTION

I. RECOIL PROTONS FROM PROCESS $e^- + p \rightarrow e^- + p + \gamma$

A. Energy Distribution (Radiated Energy per Unit Energy) of Real and Virtual Photons: kN(k)/incident electron

Stack	Copper-SS Window	Hydrogen	Electropion Prod.	Total
D	0.0173	0.0080	0.0144	0.0397
F	0.0168	0.0091	0.0164	0.0423

B. Numerical Results

		D	F	
1.	Rosenbluth cross section xF^2	9.65×10^{-32}	7.6×10^{-32}	cm^2/ster.
2.	Radiative correction factor (per Mev proton kinetic energy)	1.60×10^{-3}	0.98×10^{-3}	Mev^{-1}
3.	Cross section x rad. corr. x electrons/photons per Mev	2.6	1.0	μb/ster.
4.	Photon cross section $\frac{d\sigma}{d\Omega'_\pi} \frac{d\Omega'_\pi}{d\Omega} \frac{dk}{dT}$	28.6	26.2	μb/ster.
5.	Ratio (3)/(4)	9.0%	3.8%	

TABLE I (Continued)

II. RECOIL PROTONS FROM PROCESS:

$$e^- + A \rightarrow e^{-\prime} + A + \gamma \qquad \text{Bremsstrahung}$$

$$e^{-\prime} + p \rightarrow e^{-\prime} + p \qquad \text{Elastic scattering}$$

Results:

		D	F	
1.	Electron energy: E To give acceptable scatter	620	520	Mev
2.	Photon energy $E_o - E$	80	90	Mev
3.	Ratio, electrons/real + virtual photons per Mev	7.6	5.3	Mev
4.	Cross section x F^2	0.134	0.112	μb/ster.
5.	dE/dT: electron energy per unit proton energy	3.24	2.79	
6.	(3) x (4) x (5) (cross section/photon.)	3.3	1.7	μb/ster.
7.	Pion cross section (lab) $\frac{d\sigma}{d\Omega'_\pi} \frac{d\Omega'_\pi}{d\Omega} \frac{dk}{dT}$	29	26	μb/ster.
8.	Ratio	11.5%	6.3%	

III. TOTAL

$e^- + p \rightarrow e^- + p + \gamma$	9.0%	3.8%
$e^- + A \rightarrow e^{-\prime} + A + \gamma$	11.5%	6.3%
$e^{-\prime} + p \rightarrow e^{-\prime} + p$		
	20.5%	10.1%
$\frac{\text{Signal + Noise}}{\text{Signal}} = 1 + B$	1.20	1.10

Correct observed polarizations by these factors.

The protons which recoil from the two scattering processes have essentially zero polarization. To show that the scattered recoils are unpolarized in the first Born approximation, even if the anomalous-moment scattering is included, is straightforward.

In the Dirac theory, the spin operator is $i\gamma_5 \not{W}$, where $\not{W}$ is the operator constructed from the four-vector W_λ: $\not{W} = W_t\gamma_t - W_x\gamma_x - W_y\gamma_y - W_z\gamma_z$. The four-vector W_λ must be chosen so that its scalar product with the particle's four-momentum is zero. (71) If the scattering amplitude is f, the polarization in the direction of the three-vector $\underline{W}$ is then the expected value of the spin operator:

$$P = \frac{f^+ i\gamma_5 \not{W} f}{f^+ f}$$

The numerator and denominator of this expression must be appropriately summed and averaged over the final and initial spins of the proton and electron, keeping only positive energy states.

The scattering amplitude is proportional to the matrix element, computed to lowest order by the usual Feynman rules. The matrix element contains two factors, one involving proton operators and one involving electron operators. The square of the matrix element may be evaluated in the usual way by inserting the projection operators constructed from the Dirac equation, which leave only the positive energy states; one may then perform the sums over the spins efficiently by taking the trace of the resulting matrix. (71, 72) The electron factors, whether for elastic scattering or scattering with radiation, cancel out in the polarization expression, so that the final formula for the polarization is the following:

$$P = \frac{\sum_e \mathrm{Tr}\{(\not{p}_2 + m)[\not{e} + \frac{\mu}{2m}(\not{q}\not{e} - \not{e}\not{q})]\, i\gamma_5 W (\not{p}_1 + m)[\not{e} + \frac{\mu}{2m}(\not{e}\not{q} - \not{q}\not{e})]\}}{\sum_e \mathrm{Tr}\{(\not{p}_2 + m)[\not{e} + \frac{\mu}{2m}(\not{q}\not{e} - \not{e}\not{q})]\,(\not{p}_1 + m)[\not{e} + \frac{\mu}{2m}(\not{e}\not{q} - \not{q}\not{e})]\}}$$

In this formula, p_{1_λ} and p_{2_λ} are the four-momenta of the proton before and after scattering, q_λ is the four-momentum transfer $p_{2_\lambda} - p_{1_\lambda}$, μ is the anomalous moment, and m is the proton mass; e_λ is the polarization vector of the virtual photon, to be summed over.

Straightforward evaluation of the numerator, using the commutation rules for daggered operators

$$\not{a}\not{b} + \not{b}\not{a} = 2a_\lambda b_\lambda$$

$$\not{a}\gamma_5 + \not{a}\gamma_5 = 0$$

gives a zero result, regardless of the choice of e_λ.

Since the protons from the scattering processes have known (zero) polarization, it is easy to correct the magnitude of the measured polarization to obtain the polarization resulting from the pion processes. The polarization obtained by combining two beams of polarizations P_1 and P_2 of intensities N_1 and N_2, is the arithmetic mean

$$P = \frac{N_1 P_1 + N_2 P_2}{N_1 + N_2}$$

If R is the ratio N_2/N_1, and P_2 is zero, one obtains

$$P_1 = (1 + R)P$$

The correction, therefore, consists of multiplying the observed polarization by a factor equal to the ratio of the total number of protons to the

number from the pion processes. The ratios are 1.10 and 1.20 for the 585 Mev and 660 Mev exposures respectively.

Electropion Production*

Having determined the polarization of the protons which recoil from the photoproduction and electroproduction of neutral pions, the differences in the polarization of the protons produced in the two processes must be investigated.

The electroproduction process may be considered as photoproduction by a virtual photon, as shown by the following pair of diagrams:

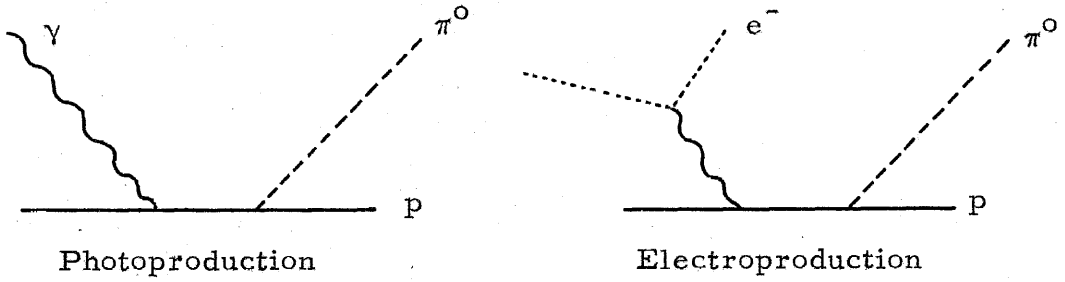

Photoproduction Electroproduction

The processes differ in two ways: First, the pion-nucleon final state can be excited by longitudinal as well as transverse photons, that is, by a direct coulomb interaction as well as by radiation; second, the excitation of the final state cannot be uniquely determined by measuring the energy and angle of one of the outgoing particles, since the final state contains three particles.

For forward electron scattering the excitation of the pion-nucleon final state and the kinematics of the electroproduction process differ from photoproduction only by a trivial energy difference, arising from

---

*Dr. Carl Iddings has assisted materially in the following analysis.

the finite rest energy of the electron. The contribution from longitudinal photons is negligible, and the ratio of the transverse contributions is a known function of energy.

Although the cross section for the production of pions is found by integrating over all angles of the scattered electron, small angle scattering is strongly favored, because the cross section for scattering into a given direction is inversely proportional to the square of the invariant momentum transfer, that is, to*

$$\begin{aligned} k^{\mu}k_{\mu} &= (p^{\mu} - p'^{\mu})(p_{\mu} - p'_{\mu}) \\ &= -2[m^2 + \underline{p} \cdot \underline{p}' - p_o p'_o] \\ &\approx 2pp'(1 - \cos\theta_e) + m^2(p - p')^2/pp' \end{aligned}$$

where p and p' are the initial and final four momenta of the scattered electron, $\underline{p}$ and $\underline{p}'$ are the corresponding three-momenta, m is the electron mass, and θ_e is the electron scattering angle.

The cross section for electropion production is conveniently expressed in terms of the ratio of the number of electroproduced pions to the number of photoproduced pions in a target bombarded by equal intensities of electrons and photons respectively. Because of the importance of small angle scattering, this ratio is almost independent of the details of the meson-nucleon interaction. In the approximation that one

---

*The notation in this section follows that of Dalitz and Yennie (73); in particular, the scalar product of two four-vectors is defined by $a^{\mu}b_{\mu} = a_1b_1 + a_2b_2 + a_3b_3 - a_ob_o = \underline{a} \cdot \underline{b} - a_ob_o$.

can replace slowly-varying terms in the cross section by their values for forward scattering, the electropion/photopion ratio can be estimated analytically; recent estimates are given by Dalitz and Yennie (73).

Good agreement with this approximation to the ratio has been obtained in the experiments of Panofsky, Woodward, Newton and Yodh, who measured the cross section for the electroproduction of positive pions from hydrogen. For example, in one case (60 Mev pions at 75° lab, at a beam energy of 600 Mev) the predicted ratio was 0.0200 and the observed ratio was 0.0193 ± 0.010, indicating that the wide angle scattering does not produce deviations greater than at most a few per cent, at this energy. (74, 75, 76)

Information about the behavior of the cross section off the energy shell has been gathered by Panofsky and Allton, who measured the cross section for wide angle electron scattering with associated pion production. The pions were not observed, so that the meas ured quantity was the total cross section for charged and neutral pion production by virtual photons of given invariant momentum transfer. The kinematical conditions were such that the pions were produced resonantly in the 33 state. No evidence for a large longitudinal contribution was found, although the resonant state can be excited by certain longitudinal multipoles. The finite size of the proton was evidenced by the decrease of the cross section with increasing invariant momentum transfer. (77)

Polarization, however, arises from interferences not detected in a total cross section measurement. Assuming that the contribution from longitudinal multipoles is of the same magnitude as the experimental errors in the Panofsky-Allton experiment, one concludes that it is

quite possible that the longitudinal multipoles are as large as the non-resonant transverse multipoles at energies near the second resonance, where the total cross section has only about one-seventh the value it has at the first resonance.

It is therefore necessary to discover if the kinematic favoring of small angle scattering does in fact permit only a small contribution from longitudinal terms, and to investigate the effect of the three-body kinematics on the resolution in center of mass angle and energy.

Dalitz and Yennie have derived an expression for the ratio of the number of electroproduced pions to the number of pions photoproduced by a bremsstrahlung spectrum $\phi(k, p)$. The ratio is $N_e/\phi(k, p)$ where

$$N_e = \frac{\alpha}{\pi} \frac{4k_f^2}{pp_f'} \int \frac{\Phi_e}{\Phi_{ph}} \frac{p'^2}{k^\mu k_\mu} \frac{d\Omega}{4\pi}$$

$$\Phi_{ph} = (\mathrm{Tr}\ |j_t|^2)_f$$

$$\Phi_e = \frac{1}{2}\,\mathrm{Tr}\,\{4|p \cdot j_t|^2 + k^\mu k_\mu |j_t|^2$$

$$+ 4\,\mathrm{Re}\,(p \cdot j_t)^2 (k \cdot j_\ell) k^\mu k_\mu (p^2 - p'^2)/k_o^2 k^2$$

$$+ |k \cdot j_\ell|^2 [(p+p')^2 - k^2](k^\mu k_\mu)^2/k^4 k_o^2\}(k^\mu k_\mu)^{-1}$$

In these formulas, Φ_{ph} and Φ_e are proportional to the sum over spins of the squares of the matrix elements for photoproduction and electroproduction respectively, j_t is the transverse current operator, j_ℓ is the longitudinal current operator, and the subscript f implies evaluation for forward electron scattering, F^2 is the form factor which allows

for the finite size of the proton, measured by Panofsky and Allton.

The electroproduction term Φ_e is Lorentz invariant, although this fact is not obvious from the formula given. To identify the transverse amplitudes with those known (or thought) to be present in photoproduction, it is desirable to evaluate the indicated traces in the pion-nucleon center of mass system, separating the factors which vary rapidly with electron scattering angle. The evaluation of the traces, in terms of generalized longitudinal and transverse production amplitudes, is similar to the corresponding evaluation for photoproduction performed in Appendix IV. It was found that the four terms in the expression for Φ_e consist of products of quantities which depend only on the energy and angle in the pion-nucleon c. m. system with coefficients which depend sensitively on the electron scattering angles. The coefficients of the two longitudinal terms are as follows:

1. Coefficient of longitudinal-transverse interference term:

$$L_1 = 4(p^2 - p'^2)(\underline{p} \cdot \underline{r}_t)/k_o^2 kr$$

where $\underline{r}_t$ = transverse component of recoil proton momentum $\underline{r}$.

2. Coefficient of pure longitudinal term:

$$L_2 = [(p + p')^2 - k^2]\, k^\mu k_\mu / k^2 k_o^2$$

If the momentum transfer is forward, only the pure transverse terms can contribute; the longitudinal coefficients given are zero for forward scattering: $(\underline{p} \cdot \underline{r}_t)_f = 0$, $k^\mu k_\mu \approx 0$.

The principal objection to the small angle approximation conventionally made is that the variation of the recoil electron momentum with electron scattering angle is neglected. It is not obvious that the neglect is justified, because the recoil momentum appears squared in

integrand of the electroproduction cross section, and at wide angles the electron can carry off a large share of the momentum. If the recoil momentum in the forward direction is small (as it was in the present exposures), it can be relatively quite large at wide angles.

To obtain a quantitative idea of the seriousness of this effect in allowing contributions from longitudinal multipoles and in smearing the kinematics, the following viewpoint was taken: Assuming that the production amplitudes are slowly varying functions of angle and energy, the density of states factor $W = p'^2 \sin\theta_e / k^\mu k_\mu$ determines the relative contributions of different scattering angles, and therefore the distribution of values of the energy and angle in the pion-proton center of mass system, of the invariant momentum transfer, or other kinematical quantity.

For a specified momentum and angle of observation of the recoil proton, the electroproduction process is kinematically determined if the two angles determining the direction of the scattered electron are given: the angle θ_e between the incident and scattered momenta, and the angle ϕ between the beam-proton and beam-electron planes. The distribution of a given kinematical quantity $Q(\theta_e, \phi)$, such as the square of the invariant momentum transfer, may be determined by integrating the weight W (multiplied by the appropriate Jacobian) along lines of constant Q.

The resolution in the energy and angle in the pion-proton c. m. system, and in the magnitude of the invariant momentum transfer, $k^\mu k_\mu$, were calculated for the kinematical conditions of the Stanford exposures. The necessary integrals were computed using a simple numerical

method: the angular range in θ_e, ϕ was broken into small elementary areas, and the value of the quantity Q whose resolution function was to be determined was computed for each cell, using the formulas given in Appendix III; the values of Q found were weighted according to the value of W for the cell, and the weighted counts were sorted into groups. The cells were made smaller in regions where the factor W varied rapidly. The Burroughs 220 computer was used to make the necessary kinematical calculations and to tally the counts.

This calculation would be exact if the square of the electroproduction matrix element were independent of the direction of electron scattering. More representative resolution functions were obtained by approximately including the angular dependence of the coefficient of the second transverse term in Φ_e, $4 \text{ Tr } |\underline{p} \cdot \underline{j}_t|^2 / k^\mu k_\mu$, using a modified weighting factor, $W' = W(1 + 4\underline{p} \cdot \underline{p}_t / k^\mu k_\mu)$. In this factor, $\underline{p}_t$ is the transverse part of the incident electron momentum in the pion-proton center of mass system. The approximation implied, $\text{Tr } |\underline{p} \cdot \underline{j}_t|^2 = \underline{p} \cdot \underline{p}_t \text{ Tr } |j_t|^2$, is good at small angles.

The results obtained using the improved weighting factor are shown in figs. 15, 16, and 17. The excitation of the pion-proton center of mass system has been expressed in terms of the energy of the real photon which photoproduces the same final state, to facilitate comparison with photoproduction. The width of the peak in photon energy is seen to be about 20 Mev; there is, however, a long low energy tail. The corresponding distribution in the photoproduction process is, of course, a delta function. The resolution in center-of-mass angle is seen to be about 3-5 degrees. More than half of the area under the

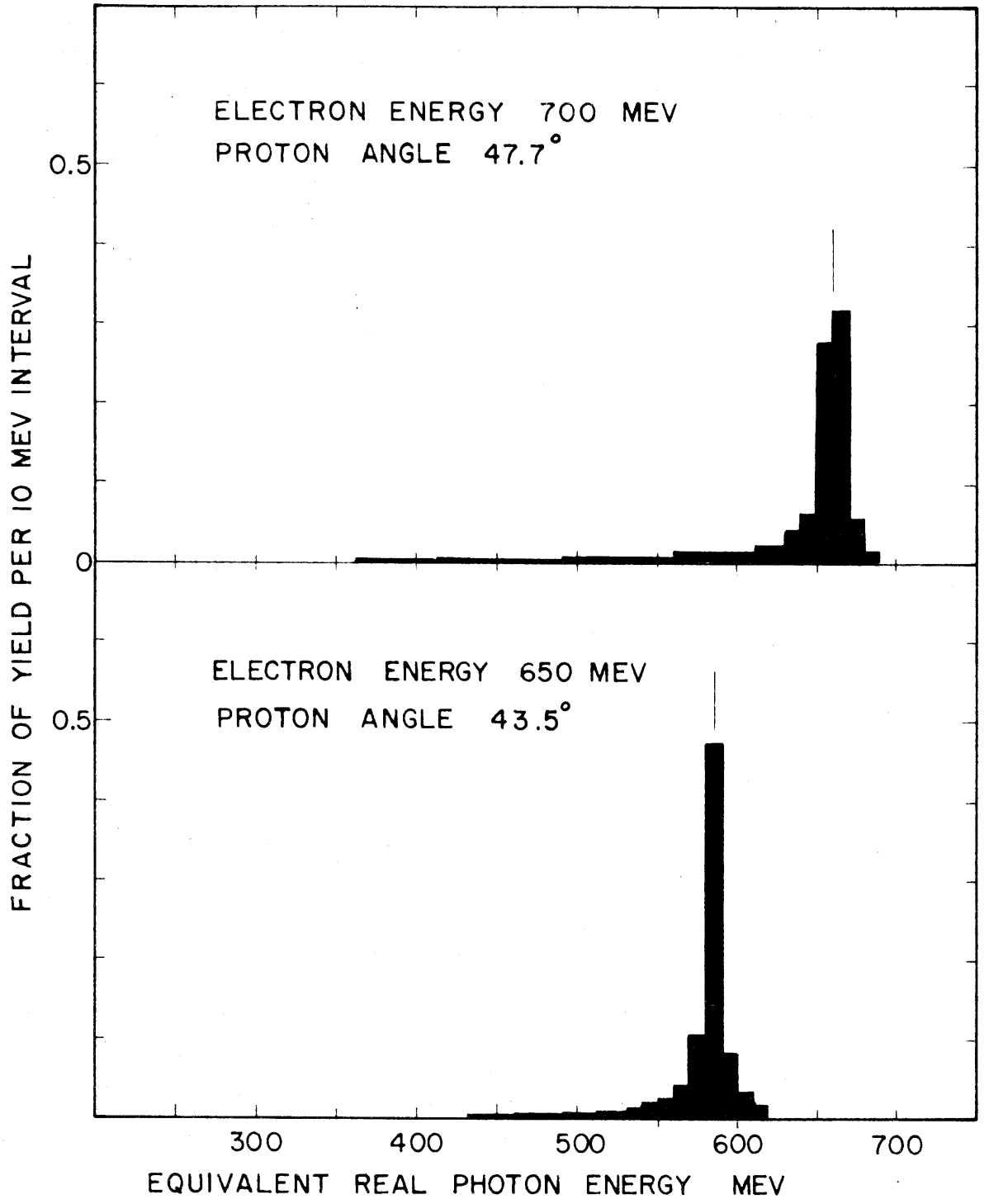

FIGURE 15

PION-PROTON C.M. ENERGY RESOLUTION, $e^- + p \rightarrow e^- + p + \pi^\circ$, EXPRESSED IN TERMS OF LABORATORY PHOTON ENERGY REQUIRED TO PHOTOPRODUCE SAME STATE

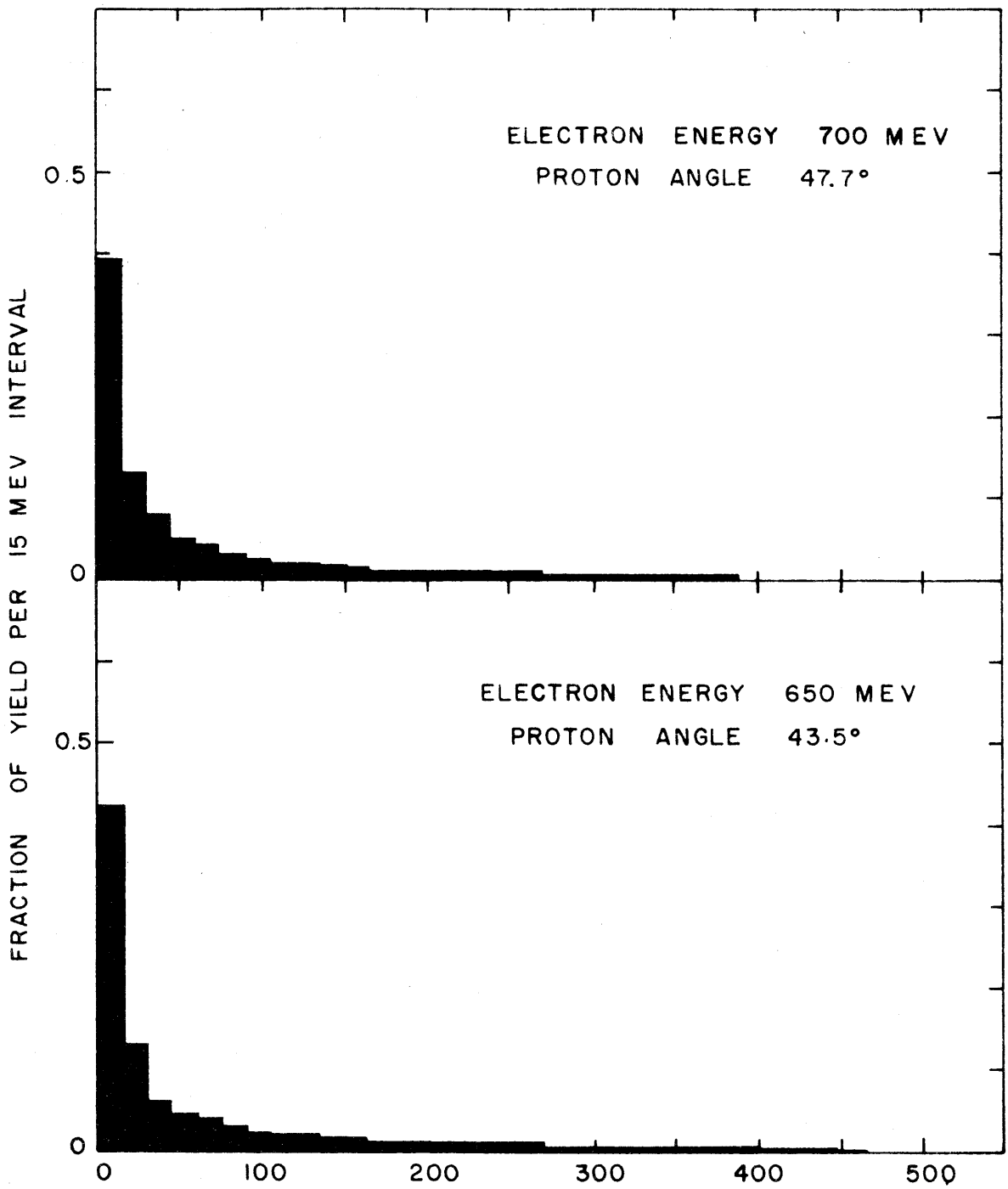

FIGURE 16

RESOLUTION IN INVARIANT MOMENTUM TRANSFER

$e^- + p \longrightarrow e^- + p + \pi^\circ$

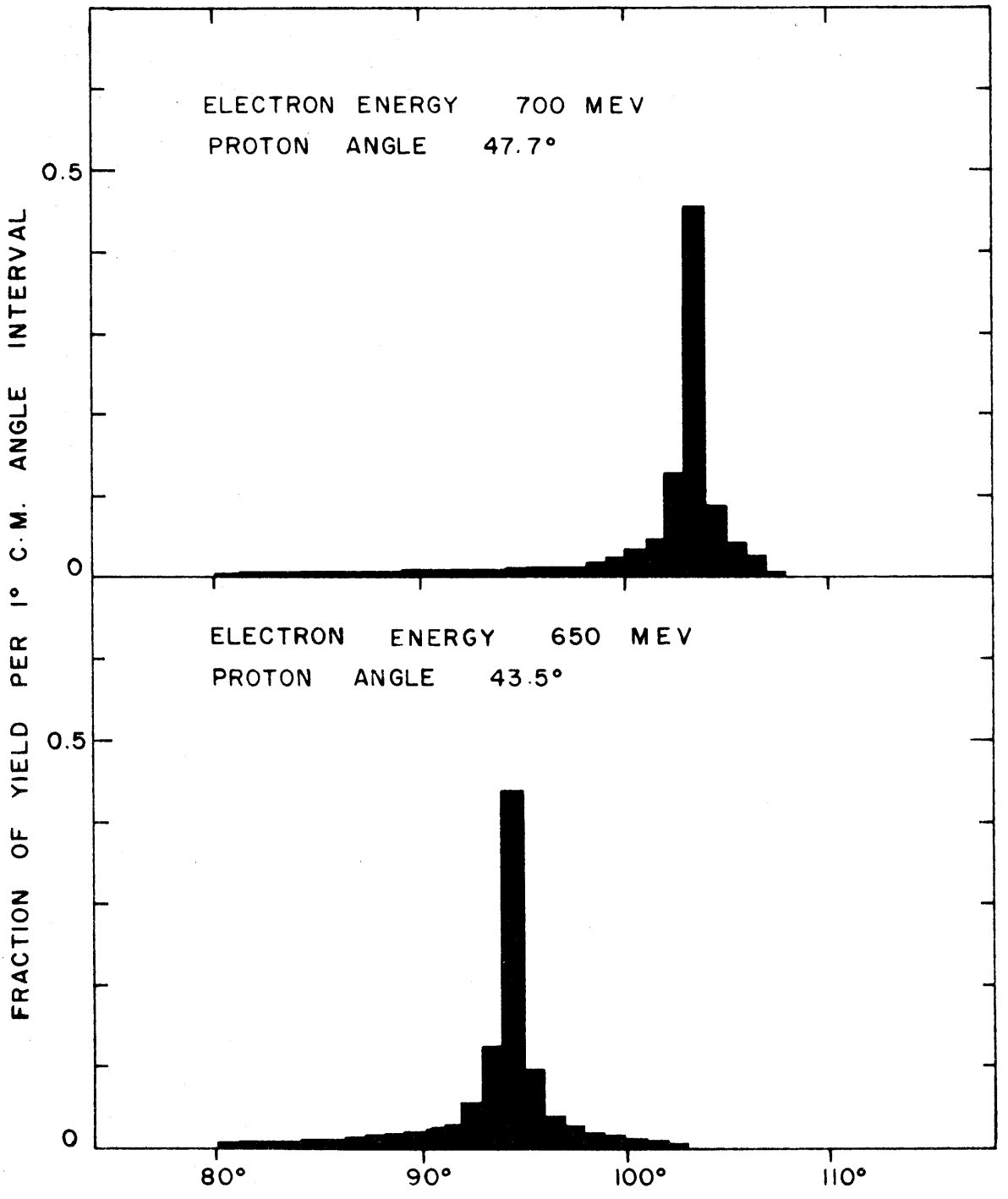

FIGURE 17

RESOLUTION IN CENTER OF MASS ANGLE

$e^- + p \rightarrow e^- + p + \pi^\circ$

resolution curves for invariant momentum transfer corresponds to transfers smaller than 20 Mev.

An estimate of the possible magnitude of the longitudinal contributions was obtained by using the resolution program to determine the distribution of values of the longitudinal coefficients. The average values of the coefficients were calculated from the distributions obtained; the calculation was done only for the 660 Mev exposure, the worst case. The ratios of the average transverse coefficients were as follows:

$$L_1/(1 + 4\underline{p} \cdot \underline{p}_t) = 0.20$$

$$L_2/(1 + 4\underline{p} \cdot \underline{p}_t) = 0.09$$

Therefore, if the longitudinal amplitudes were exactly the same in magnitude and phase, and in energy and angular dependence, as the transverse amplitudes, the longitudinal production would amount to 29 per cent of the transverse production.

Near the second resonance, the non-resonant production appears to contribute perhaps 20 per cent of the total photoproduction cross section. Assuming that the longitudinal amplitudes have, as an upper limit, a magnitude corresponding to this non-resonant production, one estimates that about 10 per cent of the electroproduction is excited by longitudinal virtual photons.

The electropion/photopion ratios were computed from the equation for N_e using the values of the integrals found. The results agree with those obtained using the small angle approximation given by Dalitz and Yennie. The ratios are given in Table I; about 40 per cent of the pions

are electroproduced. It is concluded, therefore, that longitudinal production may amount to about 5 per cent of the total. The uncertainties in the polarization are of comparable magnitude. It should be noted that this uncertainty may be reduced when more information about the electroproduction process becomes available.

Besides this uncertainty, the main effect of the inclusion of electroproduced recoils is to degrade the resolution. The effective resolution in laboratory photon energy for the two exposures was obtained by combining the rectangular distribution of real photon energies accepted with the smeared distribution of equivalent photon energy representative of electroproduction. The results are shown in fig. 18.

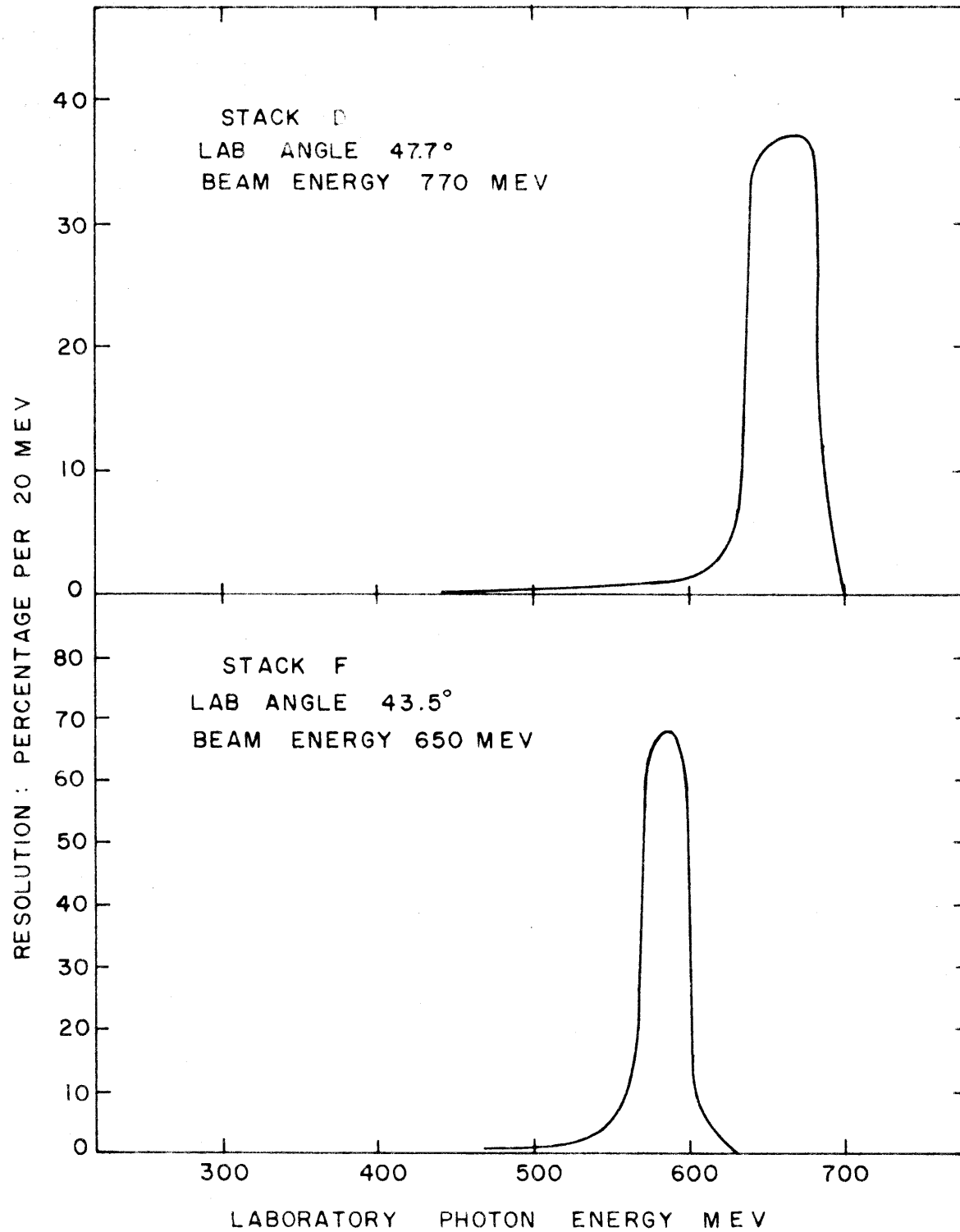

FIGURE 18

EFFECTIVE RESOLUTION IN LABORATORY PHOTON ENERGY, NOMINAL MOMENTUM VALUES

VII. RESULTS

Distributions in Angle and Energy

In figs. 19 and 20 the distributions in space scattering angle of the events found in the area scan of the 660 and 585 Mev exposures are shown. In the analysis of the 585 Mev exposure, some plates were scanned to a depth of only 10 mm; the higher average energy, and an evident gain in the small-angle detection efficiency, account for the larger proportion of small angle scatterings.

For comparison, the angular distribution of the scatterings found at Rome by the follow-back method is shown as well. In the Rome scan, only scatterings with a projected angle change of at least 6 degrees were retained. The selection criteria applied at Padua were essentially the same as those used in the area scan; scatterings with a projected angle change of at least 3 degrees were recorded. In the sample Padua distribution, fig. 12, only scatterings of 5 degrees or more in space are shown.

The distributions in energy before scattering and in the cosine of the azimuthal angle ($\cos \phi = \underline{n} \cdot \underline{\mu}$) obtained in the area scan of the 660 Mev exposure are shown in fig. 21. The cosine distributions are given separately for positive and negative values; the dependence of the asymmetry on the value of the cosine is well illustrated.

Efficiency and Bias

The efficiency of the area scan was measured by repeated scanning, mostly of the 585 Mev plates. The efficiencies for the detection of scat-

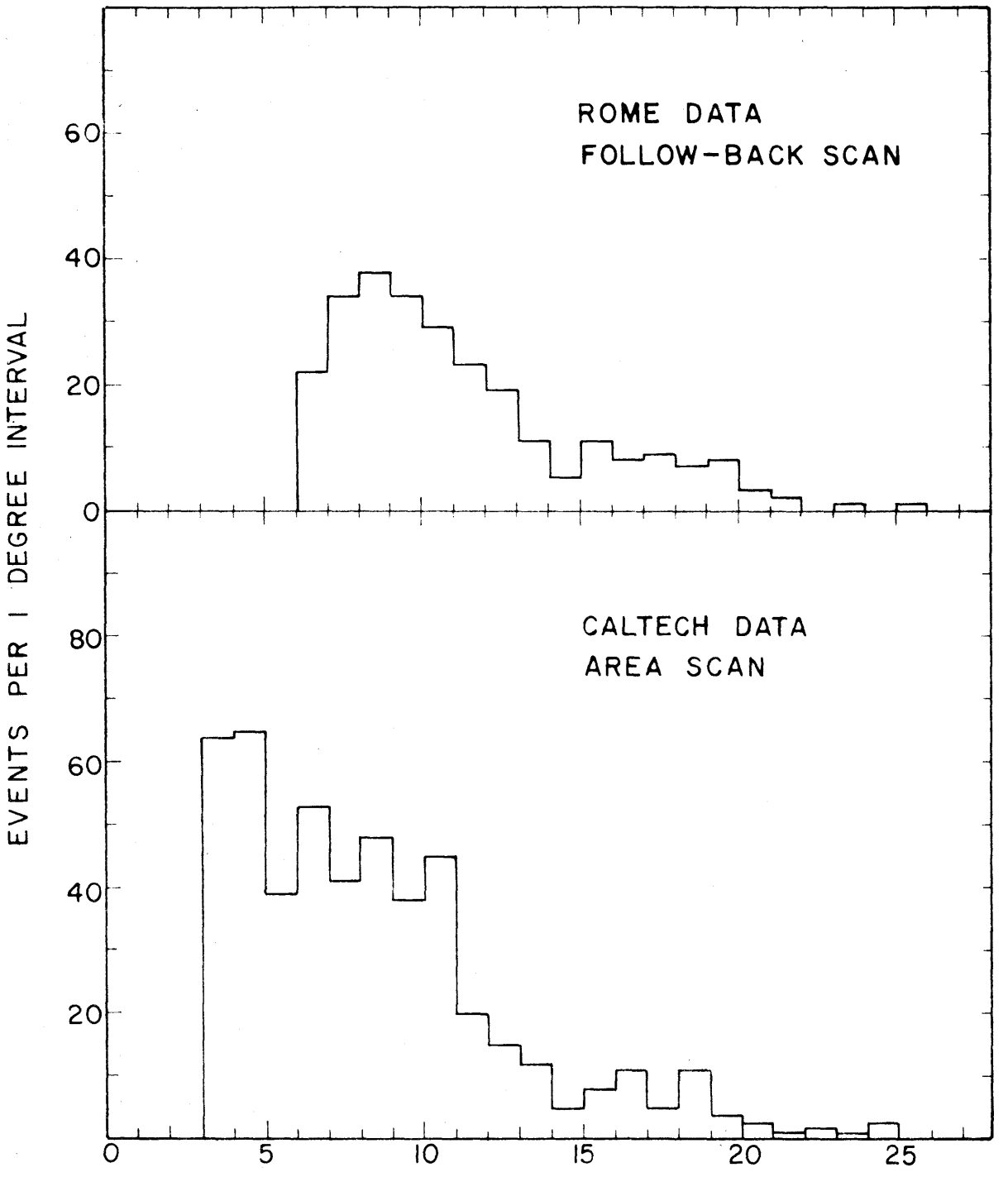

FIGURE 19

SCATTERING ANGLE DISTRIBUTIONS, STACK D

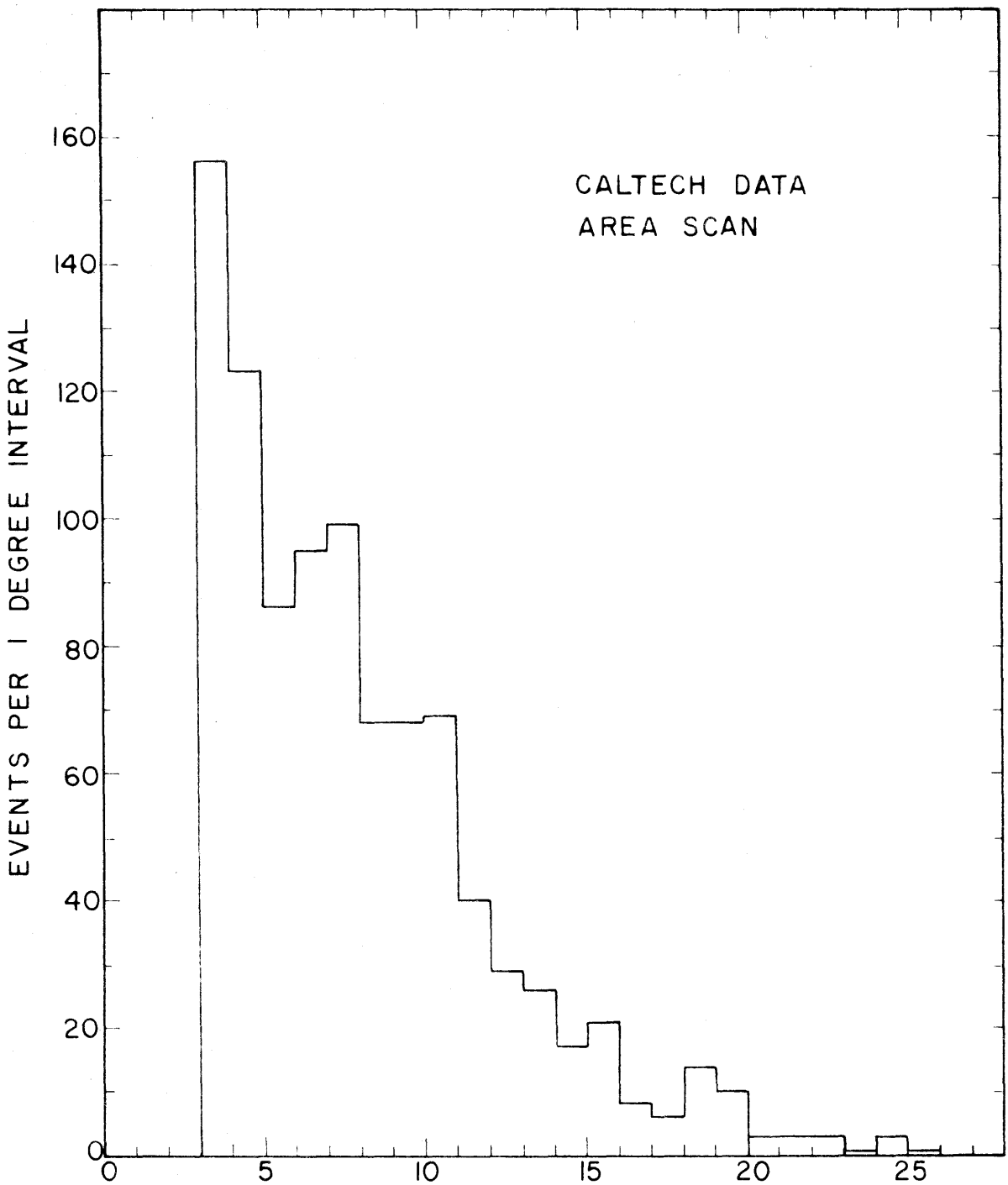

FIGURE 20

SCATTERING ANGLE DISTRIBUTION, STACK F

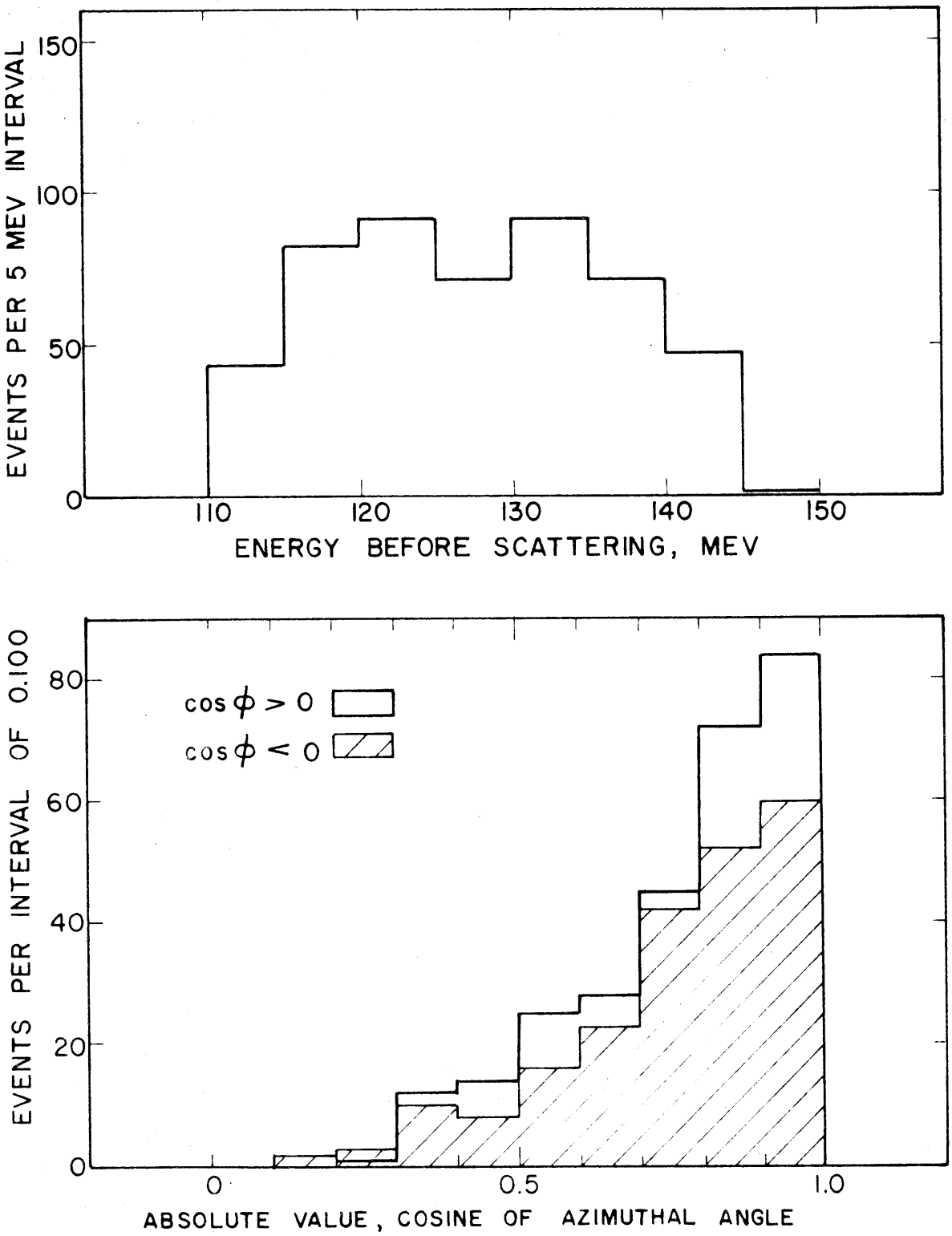

FIGURE 21

DISTRIBUTIONS IN ENERGY AND AZIMUTH, STACK D

CALTECH AREA SCAN

tering to the left and right were measured separately, providing an accurate measure of the bias, defined as the difference of the left and right efficiencies divided by the sum. The efficiencies in the area scan of the 660 Mev plates were obtained by comparison with the scanning of the same areas at Rome and Padua. The results of the measurements and comparisons follow:

1. Double scanning results: both exposures: Scatterings with projected angle change $3 - 20^{\circ}$:

	Left $\cos\phi < 0$	Right $\cos\phi > 0$	Sum or Average
Found by first scanners only	14	6	20
Found by second scanners only	10	18	28
Found by both	56	63	119
Average efficiency, first scanners	$81 \pm 3\%$	$84 \pm 3\%$	$83 \pm 2\%$
Average bias, all scanners			$2 \pm 3\%$

The data from two early check-scans on the 660 Mev plates used is not included; for these plates the efficiency was as low as 20 per cent, although the bias was zero within statistics. The above efficiencies are therefore characteristic of the fully-developed scanning method, with clear plates; there is no evidence of significant bias. It is worth emphasizing that such a bias would have been detected, even if all scanners were equally biased.

2. Rome-Caltech comparison: 660 Mev exposure, scatterings with projected angle change 6 - 20 degrees:

	Left $\cos\phi < 0$	Right $\cos\phi > 0$	Sum or Average
Found by Caltech only	31	41	72
Found by Rome only	32	31	63
Found by both	31	44	75
Caltech efficiency	49 ± 4%	59 ± 4%	54 ± 3%
Caltech bias			9 ± 6%
Rome efficiency	52 ± 4%	50 ± 4%	51 ± 3%
Rome bias			2 ± 6%

Some events were missed at Rome because the scattered tracks entered plates which were not line-scanned; the efficiencies given include these losses and are therefore lower than estimated, and are not typical of the method, although they are representative of the experiment, and provide a measure of bias.

3. Padua-Caltech comparison: 660 Mev exposure, scatterings with projected angle change 3 - 20 degrees:

	Left $\cos\phi < 0$	Right $\cos\phi > 0$	Sum or Average
Found by Caltech only	47	68	115
Found by Padua only	19	27	46
Found by both	23	31	54
Caltech efficiency	54 ± 4%	54 ± 4%	54 ± 3%
Caltech bias			-1.2 ± 5%
Padua efficiency	33 ± 4%	31 ± 3%	32 ± 3%
Padua bias			-2.4 ± 8%

The Padua efficiencies are also lowered by losses of events which would have been traced from plates not scanned, or of events lost in plates

scanned by track-following without trace-through, where the scattered track did not cross the starting line.

There appears to be little evidence of scanning bias in any of the three scanning methods, although the bias values obtained from the Rome and Padua comparisons have rather large uncertainties. Bias in follow-back method used at Rome was also monitored by comparison of the numbers of multiply-scattered tracks found in the left and right acceptance intervals (see the discussion in Appendix I). The average spurious asymmetry was found to be quite small, corresponding to an angular misalignment of at most 0.05 degrees. It is therefore legitimate to combine the data to obtain a final polarization value.

The difference of the scanning efficiency on the 585 and 660 Mev plates was caused by the use of the latter plates for training and the fact that they were less transparent.

Background from Empty Target and Star Prongs

Eight of the plates of the hydrogen-out exposure, Stack C, were line-scanned for tracks meeting the criteria applied to proton tracks during the area scan. Only 15 tracks were found; the same area in Stack F contains about 2800 acceptable tracks. Allowing for the difference in exposure, the background from the empty target is found to be 3.5 ± 1 per cent, presumably almost entirely from elastic electron scattering in the target walls and hence unpolarized.

In scanning some of the plates of the 585 Mev exposure, a record was kept of all stars which had one or more gray prongs whose grain density was similar to that of the proton tracks. The number of star

prongs per unit volume which satisfied the acceptance criteria for proton tracks was less than 1 per cent of the number of acceptable tracks.

Polarization Values

The polarizations obtained from the maximum likelihood calculations described earlier are given in the following table:

Photon Energy Mev	Scanning Group	Useful Events	Polarization Values, Per Cent With Inelastic Correction	Without Inelastic Correction
585	Caltech	959	49 ± 13	48 ± 13
660	Caltech	470	47 ± 19	45 ± 18
660	Rome	265	28 ± 18	24 ± 17
660	Padua (Energy loss 0-30 Mev)	232	90 ± 24	80 ± 22
660	All, less duplications	830	41 ± 13	37 ± 12

Sample plots of the likelihood as a function of polarization are given in fig. 22. The likelihood function differs from a Gaussian by at most 1 or 2 per cent. Typical distributions of the values of the effective analyzing power, $a(\theta)\cos\phi$, for the events used in the maximum likelihood calculation are shown in fig. 23.

The efficiency and bias measurements indicate that the data of the different scanning groups may be validly combined, and that the rather large differences in the 660 Mev results are statistical in origin. A more complete comparison of the Caltech and Italian results is in progress, but it is not expected that the above values will change greatly.

The calculation has been checked in a number of ways. The 660

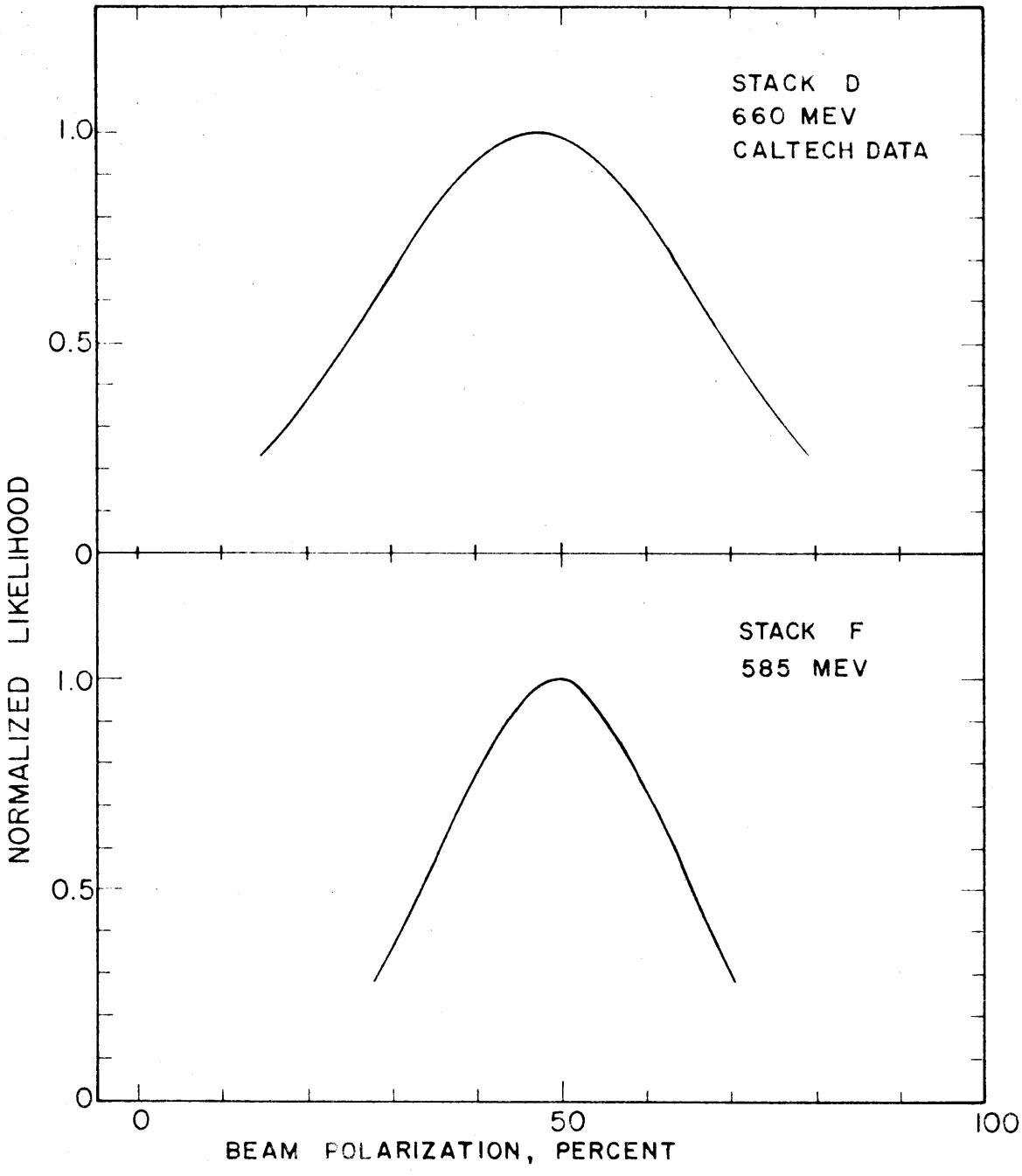

FIGURE 22

LIKELIHOOD AS A FUNCTION OF POLARIZATION

INELASTIC CORRECTION INCLUDED

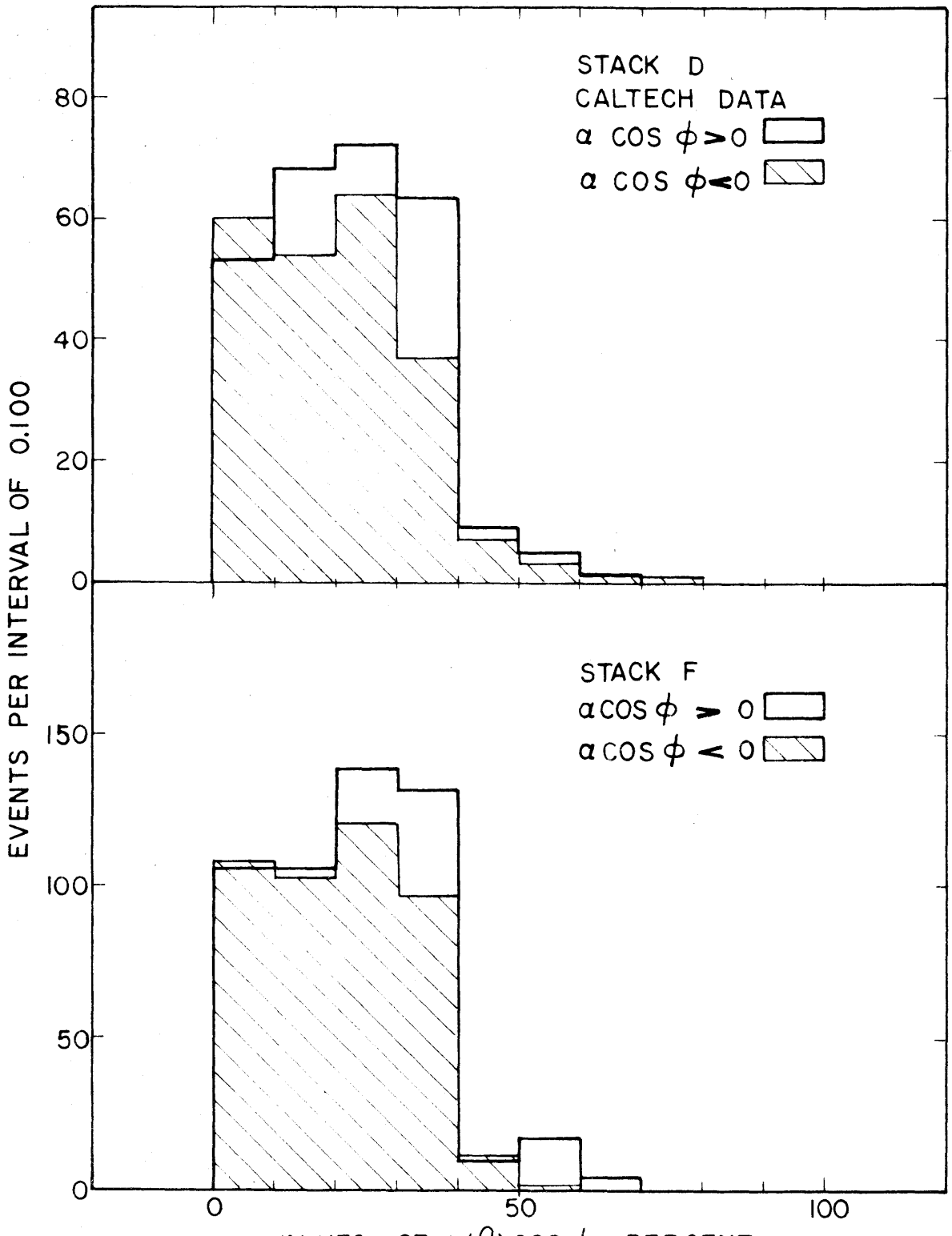

FIGURE 23

DISTRIBUTION OF EFFECTIVE ANALYZING POWER

UNCORRECTED

Mev polarization (combined data) was computed excluding scattering with space angles less than 5 degrees, and with the angle between scattering plane and proton moment less than 45 degrees; the polarization changed by only 4 per cent. The 660 Mev polarization (Caltech data) was also recomputed using the average precession of the proton moment for all tracks. The polarization changed by the expected amount, less than one per cent.

Only the statistical uncertainty is shown. The uncertainty in the polarization resulting from uncertainty in the analyzing power is estimated to be at most 4 per cent. The estimate allows for the statistical error in the analyzing power and for the 10-20 per cent uncertainty in the assumed values of the analyzing power at wide angles and low energy, and is based on an investigation of the changes in the calculated polarization when the analyzing power was modified within the limits of uncertainty; no deviation greater than 4 per cent was found.

The final values, corrected for background, and including the uncertainty in the analyzing power, but not the uncertainty from electropion production, or the uncertainty in the bias measurements, estimated to be at most 3 per cent, are as follows:

Photon Energy, Mev	Pion c. m. angle	Polarization, per cent
585	86°	56 ± 14
660 Caltech data	77°	58 ± 19
660 Combined data	77°	51 ± 14

The scattering in emulsion was predominantly to the right, looking along the tracks from the top. The spin of the protons was therefore

down, since protons with spin up scatter predominantly to the left. (34) Because the spectrometer, which was placed on the left side of the beam (fig. 5), reversed the spin direction, the protons were emitted from the target with spin up, in the direction $\underline{k} \times \underline{p}$, where $\underline{k}$ and $\underline{p}$ are the momentum vectors of the incident photon and recoil proton respectively. The sign of the polarization agrees with that found by Stein. (28)

These polarizations are plotted with the results obtained by others (28, 78) as functions of the laboratory photon energy in fig. 24; the counter data of Salvini and Querzoli is preliminary. The agreement between the different experiments is in general good.

The solid curves in fig. 24 are model calculations, to be discussed in the following section.

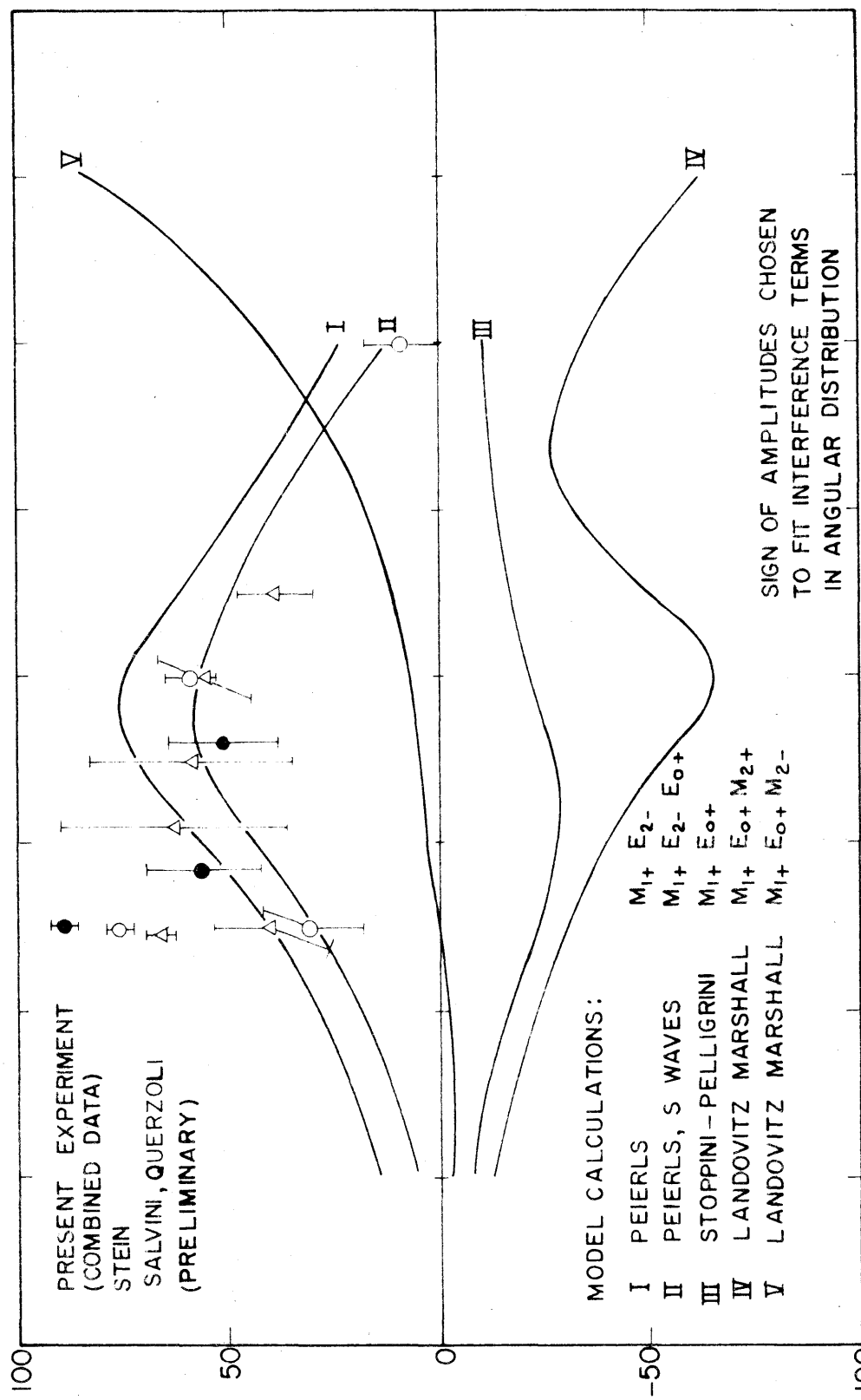

FIGURE 24

MEASURED POLARIZATIONS AND MODEL CALCULATIONS

VIII. DISCUSSION

As a first step in understanding the higher-energy maxima in pion nucleon scattering and photoproduction, it is desirable to discover if the angular distributions and polarizations observed are actually consistent with the assumption that the observed maxima are resonances in given state of angular momentum, isotopic spin, and parity.

The two higher maxima do not appear in the $\pi^+ + p$ scattering,* so that it seems that, whether resonant or not, they are produced by interactions in a state of total isotopic spin 1/2. From the π^o angular distributions it seems clear that the second maximum in photoproduction arises from an interaction in a state of total angular momentum 3/2, excited by dipole radiation: Near the energy where the maximum occurs the distribution is similar to the $5-3\cos^2\theta$ distribution characteristic of this choice of quantum numbers, and seems to include little quadrupole contribution, of the form $1 + \cos^2\theta$. The third maximum seems to involve interaction with a total angular momentum of at least 5/2. It is quite possible that both quadrupole and octupole radiation contribute; the quadrupole and octupole distributions for angular momentum 5/2 have a similar shape, so that it is difficult to rule out either choice using the present sketchy π^o data, or the more complete, but more complicated, π^+ data. Furthermore, there is a fourth maximum observed in the $\pi^+ + p$ and $\pi^- + p$ scattering, at a center of mass energy of about 1.9 Bev; this

*It is not entirely certain that the third maximum does not appear in $\pi^+ + p$ scattering; recent data seems to show that the fourth maximum has a shoulder at the energy of the third peak in the $\pi^- + p$ scattering. (7, 79) The isotopic spin dependence of the higher resonance is currently being argued. (80, 81)

maximum is quite broad, and may already complicate matters at the energy of the third maximum. It has been suggested that the third level may have a total angular momentum 3/2, while the higher value of 5/2 applies to the fourth level. (32)

Different level schemes have been proposed in efforts to explain the observed maxima by resonance models. The schemes which have been seriously discussed are the following:

Author	Level	Total Angular Momentum	Orbital Angular Momentum	Parity	Exciting Multipole (Lowest Order)
Wilson (22)	II	3/2	1	Even	Magnetic Dipole
Peierls (23, 24)	II	3/2	2	Odd	Electric Dipole
	III	5/2	3	Even	Electric Quadrupole
Landovitz, Marshall (32)	II	3/2	1	Even	Magnetic Dipole
	III	3/2 or 5/2	2	Odd	Electric Dipole Magnetic Quadrupole

In each scheme the first level (the 33 resonance) has total angular momentum 3/2 and even parity.

It is, of course, not necessary that any such simple models provide an adequate description of the experiments, particularly of the higher energy data, since the existence of the fourth maximum is ignored and the nature of the third is essentially unknown; non-resonant interactions also appear to be present.

It was suggested by Sakurai (26) that the measurement of the recoil proton in π^o photoproduction would help decide the parity of the second state, since in the Peierls model the interference between the two lower resonant states (of opposite parity) would be expected to produce large polarizations at 90 degrees in the center-of-mass system at energies between the resonances where the resonant phases were properly related. The measurements carried out at Cornell, in Italy, and in the present experiment are in essential agreement: the polarizations near 90 degrees are large and have the predicted sign. (28)

However, G. Stoppini and C. Pelligrini presented an informal calculation which seemed to show that one could expect to obtain high polarization even if the Wilson parity assignment were correct, by interference of the two even-parity resonant states with the non-resonant s-wave amplitude which appears to be present. (31) L. F. Landovitz and L. Marshall suggested that the polarization observed at energies below the second maximum might arise by interference between second and third resonances, if the states had opposite parity. (32) No specific calculations were presented; and there was no published attempt to demonstrate that any of the models offered as alternates to that of Peierls were actually consistent in detail with the energy and angular dependence of the photoproduction cross sections.

Efforts to test the consistency of the various models with the observed angular distributions in the three photoproduction reactions,

$$\gamma + p \rightarrow \pi^+ + n$$

$$\gamma + p \rightarrow \pi^o + p$$

$$\gamma + n \rightarrow \pi^- + p,$$

were made at Caltech by Professor Jon Mathews and Dr. Gerry Neugebauer. The resonant photoproduction amplitudes were obtained from simple resonance formulas, and the non-resonance amplitudes from the Born approximation. It was found that with the assumptions made the angular distributions were not well fitted by any of the models at all energies. It was found especially difficult to fit the angular distributions for charged pion production, where the retardation effect plays a large role. The calculations were not entirely conclusive, since the number of alternatives was too large to investigate each of them in detail.

The present discussion is limited to the neutral pion production, to avoid the complications of the retardation effect. The distributions, unlike those for the charged pions, can be fitted by simple polynomials in the cosine of the center of mass angle, quadratic up to about 600 Mev and quartic up to about 1000 Mev, the highest energy for which detailed measurements exist. One concludes that only low angular momenta contribute. Although the π^o data are not as complete or as widely agreed upon as the π^+ data, there are a number of features which are sufficiently well determined to provide tests of the models; it appears possible, in fact, to decide that the parity of the second resonance must be odd, if the energy and angular dependence of the cross section, and the sign and magnitude of the polarization, are to be consistent with the observations.

The experimental angular distributions are usually represented by the polynomial coefficients in the least squares fits to the angular

distributions, given as functions of laboratory photon energy. It is more convenient to discuss the behavior of these coefficients rather than of the actual distributions. It is necessary, of course, to recognize that some of the coefficients, particularly those of higher order, are poorly determined, and that at best only those features reproduced in the results of independent experiments can be considered real.

The angular distributions in π^o photoproduction have been measured at Caltech and Cornell, usually by observation of the recoil proton alone. The distributions obtained have been analyzed into polynomials in the cosine of the center-of-mass angle; the experimental values of the A, B, C polynomial coefficients in the expansion $\sigma(\theta) = A + Bx + Cx^2 + Dx^3 + Ex^4$, where $x = \cos \theta_{c.m.}$, are shown as functions of laboratory photon energy in fig. 25. At energies at which fits of polynomials of different degree were obtained, only the coefficients of the better fit are shown. The smooth curves are model fits, to be discussed.

The A (isotropic) and C (quadratic) coefficients have opposite sign at low energy, indicating that production in a state of total angular momentum 3/2 by dipole radiation predominates. The B (linear) coefficient is small and poorly determined, but its sign and small magnitude seem to be reproducible. For example, the maxima of the fits to the angular distributions obtained by Vette (14) at 585 and 690 Mev, and by Worlock (15) at 600 and 700 Mev occur in the backward hemisphere at an angle very close to 90 degrees, confirming that the B coefficient is zero or slightly negative in the region of the second resonance. The D (cubic) and E (quartic) coefficients, not

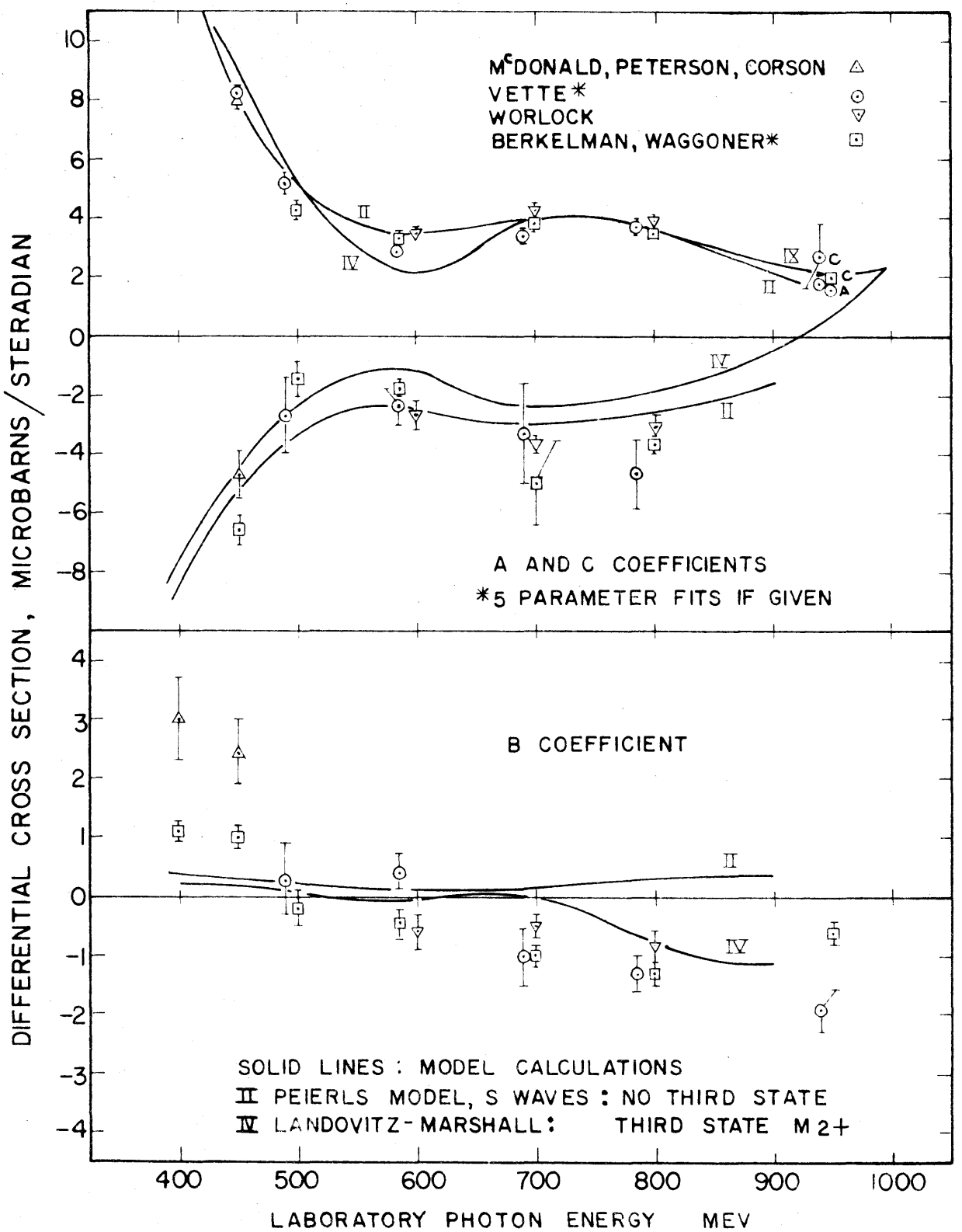

FIGURE 25

A,B,C COEFFICIENTS IN LEAST-SQUARES FITS TO ANGULAR DISTRIBUTIONS IN REACTION $\gamma + P \rightarrow P + \pi^0$

$$\frac{d\sigma}{d\Omega} = A + B\cos\theta + C\cos^2\theta + D\cos^3\theta + E\cos^4\theta$$

shown, are uncertain. The D coefficient does appear to be positive, which is reasonable: in most of the models D and B turn out to have opposite sign. If the sign of the E coefficient is in fact positive, it may indicate that octupole, rather than quadrupole, radiation is dominant at higher energy: the distributions for production in a pure state of angular momentum 5/2 have the forms:

Quadrupole radiation:	$1 + 6x^2 - 5x^4$
Octupole radiation:	$5 + 6x^2 + 5x^4$

The expressions for the angular distributions and polarizations for the multipoles included in the models suggested were derived as indicated in Appendix IV; the photoproduction amplitudes and multipole expansion given by Chew, Low, Goldberger, and Nambu (21) were used in the derivations. In their notation, electric or magnetic multipole amplitudes are denoted by symbols E or M with subscripts ℓ_+ and ℓ_-, indicating a partial wave of orbital angular momentum ℓ and total angular momentum $j = \ell \pm 1/2$ respectively. For example, M_{1+} is the magnetic multipole amplitude leading to a p-state of total angular momentum 3/2, necessarily magnetic dipole. This notation is convenient, since the parity is given by $-(-1)^{\ell}$.

Similar multipole expansions have been given by Peierls, with a different notation and normalization. (24) In Table II the expressions obtained for the polynomial coefficients and polarization at 90° are given. Only the interferences actually needed between the following multipoles are included:

TABLE II

MULTIPOLE EXPANSIONS OF POLYNOMIAL COEFFICIENTS USED IN MODEL CALCULATIONS

Coefficient in $\frac{d\sigma}{d\Omega} = A + Bx + Cx^2 + Dx^3 + Ex^4$, $x = \cos\theta_{c.m.}$

Multipole Term	A	B	C	D	E
$\lvert E_{o+}\rvert^2$	1	0	0	0	0
$\lvert M_{1+}\rvert^2$	5/2	0	-3/2	0	0
$\lvert E_{2-}\rvert^2$	5/2	0	-3/2	0	0
$\lvert M_{2-}\rvert^2$	9/2	0	9/2	0	0
$\lvert M_{2+}\rvert^2$	9/2	0	27	0	-45/2
$\lvert E_{3-}\rvert^2$	9/2	0	27	0	-45/2
$\lvert E_{2+}\rvert^2$	45/4	0	27/2	0	45/4
$\lvert M_{3-}\rvert^2$	45/4	0	27/2	0	45/4
$\mathrm{Re}E^*_{o+}M_{1+}$	0	2	0	0	0
$\mathrm{Re}E^*_{o+}E_{2-}$	-1	0	3	0	0
$\mathrm{Re}E^*_{o+}M_{2-}$	3	0	-9	0	0
$\mathrm{Re}E^*_{o+}M_{2+}$	-3	0	9	0	0
$\mathrm{Re}E^*_{o+}E_{3-}$	0	-9	0	15	0
$\mathrm{Re}E^*_{o+}E_{2+}$	-6	0	18	0	0
$\mathrm{Re}E^*_{o+}M_{3-}$	0	18	0	-30	0
$\mathrm{Re}M^*_{1+}E_{2-}$	0	2	0	0	0
$\mathrm{Re}M^*_{1+}M_{2-}$	0	12	0	-18	0
$\mathrm{Re}M^*_{1+}M_{2+}$	0	18	0	-12	0
$\mathrm{Re}M^*_{1+}E_{3-}$	-3	0	9	0	0
$\mathrm{Re}M^*_{1+}E_{2+}$	0	-18	0	30	0
$\mathrm{Re}M^*_{1+}M_{3-}$	-15/2	0	63	0	-135/2

Table II (Continued)

Multipole Term	A	B	C	D	E
$ReE^*_{2-}M_{2-}$	3	0	-9	0	0
$ReE^*_{2-}M_{2+}$	-3	0	9	0	0
$ReE^*_{2-}E_{3-}$	0	18	0	-12	0
$ReE^*_{2-}E_{2+}$	15/2	0	-63	0	135/2
$ReE^*_{2-}M_{3-}$	0	18	0	-30	0

AP = Polarization at 90 degrees times cross section at 90 degrees

$ImE^*_{o+}M_{1+}$	-1
$ImE^*_{o+}E_{3-}$	-3
$ImE^*_{o+}M_{3-}$	6
$ImM^*_{1+}E_{2-}$	4
$ImM^*_{1+}M_{2-}$	6
$ImM^*_{1+}M_{2+}$	-6
$ImM^*_{1+}E_{2+}$	3/2
$ImE^*_{2-}E_{3-}$	6
$ImE^*_{2-}M_{3-}$	3/2

The polarizations given are positive in the direction $\underline{k} \times \underline{q}$, where $\underline{k}$ and $\underline{q}$ are the momenta of the incident photon and the pion. (The sign convention is opposite to the experimental one.)

CLGN Notation $M_{\ell\pm}$	Usual Notation $M_{j_\gamma,2j}$	Multipole Name	Multipole Order j	j_γ	ℓ	Wave	Parity
E_{o+}	E_{11}	Electric Dipole	1/2	1	0	s	Odd
M_{1+}	M_{13}	Magnetic Dipole	3/2	1	1	p	Even
E_{2-}	E_{13}	Electric Dipole	3/2	1	2	d	Odd
M_{2-}	E_{23}	Magnetic Quadrupole	3/2	2	2	d	Odd
M_{2+}	E_{25}	Magnetic Quadrupole	5/2	2	2	d	Odd
E_{3-}	E_{25}	Electric Quadrupole	5/2	2	3	f	Even
E_{2+}	E_{35}	Electric Octupole	5/2	3	2	d	Odd
M_{3-}	M_{35}	Magnetic Octupole	5/2	3	3	f	Even

Qualitative conclusions regarding the validity of the various models have been reached by comparing the coefficients and polarizations in Table II with the experimental values, and in some cases by numerical evaluation of the coefficients using amplitudes and phases derived from simple resonance formulas. These conclusions may be summarized as follows:

1. If the second resonance is taken to have even parity, the observed polarization cannot possibly arise by interference of two resonant M_{1+} amplitudes with the E_{o+} s-wave amplitude, as suggested by Stoppini and Pelligrini; neither the magnitude nor the sign of the predicted polarizations are consistent with the observed polarizations and angular distri-

butions.

2. Of the four alternatives suggested by Landovitz and Marshall (third state amplitude E_{2-}, M_{2-}, M_{2+} or E_{2+}) two possibilities (E_{2-} and E_{2+}) may be ruled out at once, because the predicted angular distributions or polarizations are either very different from those observed or inconsistent in sign. The other two models are more plausible, but the magnitude of the polarization at low energy is less than that observed; if s-waves, which appear to be present, are included, the polarization is reduced further.

3. All of the even-parity models necessarily show interferences between the two M_{1+} amplitudes in the A and C coefficients and the total cross section which do not seem to be present in the observations.

4. On the other hand, if the second resonance has odd parity, as suggested by Peierls, the observed and predicted polarizations and angular distributions are consistent in magnitude, energy dependence, and sign; a numerical calculation, including the s-wave amplitude which seems to be present, produces a plausible, although not good, fit to the angular distributions and polarizations up to about 800 Mev. Fair agreement with the π^+ data has also been obtained by R. L. Walker and J. Link.

The conclusions listed are based on the following considerations:

In the model of Stoppini and Pelligrini, the 90 degree polarization is as follows:

$$P = \frac{\mathrm{Im} E_{o+}^{*} M_{1+}}{5/2\,|M_{1+}|^2 + |E_{o+}|^2}$$

It is obvious that this expression has a maximum, which occurs when the two amplitudes are relatively imaginary and when their magnitudes satisfy the unlikely ratio $|E_{o+}|/|M_{1+}| = (5/2)^{1/2}$. The maximum value of the polarization is then $(10)^{-1/2}$ or 0.316, significantly less than most of the values observed.

The total magnetic dipole amplitude in the Wilson model or its modifications is the sum of the amplitudes of the first two resonant states:

$$M_{1+} = M_{1+}^{1} + M_{1+}^{2}$$

The superscripts indicate the resonance. In the region of the second maximum, the phase of M_{1+}^{1} is close to 180 degrees, while that of M_{1+}^{2} must pass through 90 degrees if the state is resonant. For two reasons, the sign of M_{1}^{2} must be chosen to be the same as that of M_{1}^{1}: First, if the signs were opposite, the polarization from the two states would tend to cancel, regardless of the nature of the odd-parity amplitude which interferes with them unless its phase lies continually between the two resonant phases. Second, the B coefficient is negative at threshold and becomes positive at the energy of the first resonance, indicating that the phase of the interfering amplitude must lag the resonant phase by 90 degrees, that is, it must be near zero. In order that the B coefficient may turn negative again at about 600 Mev, as it is observed to do, the sign of M_{1+}^{2} must be the same as M_{1+}^{1}, unless the s-wave phase suddenly increases through 90 degrees.

The s-wave amplitude must therefore be taken negative and essentially real to produce agreement of this model with the observed B

coefficient; the sign of the predicted polarization is then, however, opposite to that observed.*

The polarization cannot, then, arise from an interference of two even-parity states with s-waves alone; both the sign and the magnitude of the polarization are incorrect. A reasonable model, however, should include the s-wave; enough positive polarization must then be provided by another interference to overcome the negative polarization generated by the s-wave interference. This condition has been found difficult to meet if the second resonance has even parity.

If the third state has odd parity, it is also possible to obtain polarization by interference with two lower even-parity states, as pointed out by Landovitz and Marshall. Four possible choices for the amplitude of the third state have been examined: electric dipole (E_{2-}) or magnetic quadrupole (M_{2-}), with total angular momentum 3/2; magnetic quadrupole (M_{2+} or electric octupole (E_{2+}), with total angular momentum 5/2. The maximum polarizations obtained by interference of each of these four amplitudes with M_{1+} are as follows:

Interfering Multipoles	Maximum Polarization (Relative Phase 90°)	Condition on Magnitudes
M_{1+}, E_{2-}	$4/5 = 0.800$	$\lvert M_{1+}\rvert / \lvert E_{2-}\rvert = 1$
M_{1+}, M_{2-}	$2/\sqrt{5} = 0.895$	$\lvert M_{1+}\rvert / \lvert M_{2-}\rvert = 3/\sqrt{5}$
M_{1+}, M_{2+}	$2/\sqrt{5} = 0.895$	$\lvert M_{1+}\rvert / \lvert M_{2+}\rvert = 3/\sqrt{5}$
M_{1+}, E_{2+}	$\sqrt{2}/10 = 0.141$	$\lvert M_{1+}\rvert / \lvert E_{2+}\rvert = \sqrt{2}/3$

*I am indebted to V. Z. Peterson and C. Pelligrini for an independent check of this argument; they found that the original calculation of Stoppini and Pelligrini was in error, both in magnitude and sign.

Since the maximum polarization obtainable by interference of M_{1+} and E_{2+} is only 14 per cent, the observed polarization cannot arise from this source. The maximum polarization from the interference with E_{2-} is large, but the angular distribution at energies greater than about 800 Mev shows a sudden increase of the C coefficient to positive values, so that it seems quite unlikely that the third state could be excited by dipole radiation. (The latter argument is originally due to Peierls.)

The other two alternatives have been examined by crude numerical fits to the data, deriving the resonant amplitudes and phases from a resonance formula similar to that used successfully to fit the total cross section near the first resonance by Gell-Mann and Watson. (82) The forms and parameters used are listed in Table III. The resonance widths of the two higher states were obtained by fitting the resonance formulas to the recent Berkeley $\pi^- + p$ total scattering cross sections.(7) The maximum polarizations obtained in the neighborhood of 700 Mev are significantly smaller than the observed values even if s-wave is not included, and the fits to the coefficients are not very convincing.

Such difficulties do not arise if the second state has odd parity, as suggested by Peierls. The first and second states interfere to produce large polarizations at 90 degrees, and the contributions to the polarization and the B coefficient from this interference are consistent in sign below the second maximum. The addition of an s-wave amplitude to the model does not cause any fundamental difficulty.

Numerical calculation with resonance formulas produces fair agreement with the data, although no effort was made to adjust the magnitudes or phases of the amplitudes assumed to provide a better fit; a

TABLE III
RESONANCE FORMS*

1. Photoproduction Amplitudes:

$$M = |M| e^{i\delta} \qquad |M|^2 = \frac{1}{ka} \frac{\Gamma_r}{\Gamma_t} \sin^2\delta$$

$$\tan\delta = \frac{1/2\ \Gamma_s}{E_o - E}$$

E_o = Center of mass energy of resonance

k = Center of mass photon energy, pion mass units

Γ_r = Reaction width, constant except for the first resonance, where formula of Gell-Mann and Watson (82) was used, with $f_\gamma = 0.22$ Mev

Γ_t = Total width $\approx$ scattering width $\Gamma_s = 2x v_\ell(x)\gamma$

$x = qa$

q = Pion center-of-mass momentum

a = Channel radius

$v_\ell(x)$ = Non-relativistic centrifugal barrier factor given by Feshbach, Peaslee, and Weisskopf (83)

γ = Reduced width

2. Parameters: $a = 0.88$ pion compton wavelength
$= 0.88\ \hbar/\mu c$ (μ = pion mass)

State	E_o Bev c.m.	ℓ	γ Mev	Γ_r 10^{-27} cm^2-Mev/ster.	
I	1.24	1	58	(ref. 81, symbol $f_\gamma = 0.22$ Mev)	
II	1.50	1	22	0.72	Amplitude positive
	1.56	1	22	1.43	Amplitude negative
	1.53	2	30	1.36	
III	1.69	2	18	0.25	
	1.71	3	35	0.49	

s-wave E_{o+}: real, $|E_o^+|^2 = 0.30 \times 10^{-30}$ cm^2/ster.

*Units $\hbar = c = 1$.

rather arbitrary normalization to the total cross section was used.* Without adjustment it is difficult to obtain a very good fit, especially to the B coefficient, which is sensitive to the magnitude and phase of the s-waves present. In figs. 24 and 25 some typical values of the polarizations and the polynomial coefficients are plotted.

An effort was made to investigate the possible choices for the amplitude of the third state, given that the second state has odd parity; it is apparent from the data that the third state, and perhaps the fourth state as well, affect the distributions energies above about 700 Mev. Four multipole amplitudes were investigated: M_{2+}, E_{2+}, M_{3-}, and E_{3-}. It was found that if the signs of these amplitudes were chosen to fit the B and D coefficients at high energy (that is, to agree approximately rather than disagree violently), the polarization tended to become negative at about 900 Mev unless the M_{3-} amplitude was used. Recent results on the polarization at high energy obtained by Frascati (78) indicate that the polarization may continue large and positive; this result contradicts the earlier value of 9 ± 9 per cent obtained by Stein.

The importance of including the third or higher states is indicated by attempts at numerical fits to the angular distribution data of Vette and Worlock; typical efforts are shown in fig. 26. The calculated angular distributions are shown for the Peierls model, with s-wave included (amplitudes M_{1+}, E_{2-}, E_{2+}) and also with the addition of a resonant M_{2+} amplitude for the third state. The curves differ, but neither fits well; when the M_{2+} amplitude is added, the A and C coefficients are reduced at high energy by an interference between the two

*I am grateful to Mr. David Loebakka and Mr. John Link for assistance with the numerical computations.

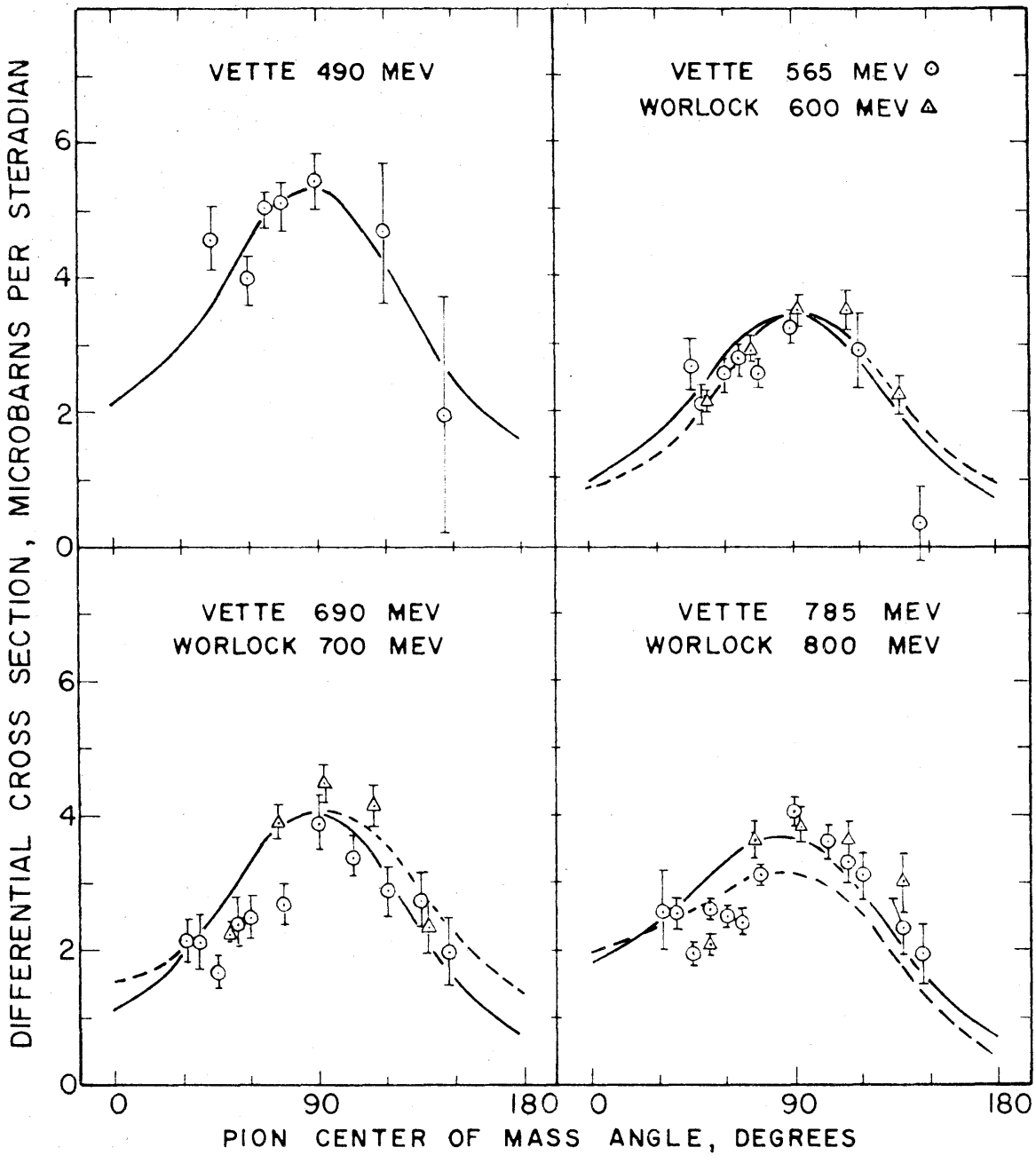

FIGURE 26

ANGULAR DISTRIBUTIONS $\gamma + P \rightarrow \pi^{\circ} + P$

CURVES: MODEL CALCULATIONS

PEIERLS MODEL: WITH S-WAVE E_{0+} ———

WITH THIRD LEVEL M_{2+} - - - -

resonant odd-parity amplitudes, E_{2-}, M_{2+}. It may be that the E_{3-} amplitude is better for the third state, a result indicated by the study of the π^+ distributions made by Link.

Similar conclusions follow from the recent 600-750 Mev π^--p scattering data of J. I. Schonle (84), who finds that (a) the third state seems to have total angular momentum 5/2; (b) the second and third states, if resonant, seem to have opposite parity; (c) strong non-resonant amplitudes are present.

One concludes that although the second state, if resonant, must have odd parity if the polarizations and distributions are to be qualitatively fit, it seems likely that a quantitative fit will not be obtained until more and better data are obtained, particularly at high energy, and that the third state will be found to have even parity.

IX. CONCLUSION AND SUGGESTIONS FOR FURTHER WORK

The polarization of the recoil protons from the photoproduction of neutral pions has been measured using nuclear emulsion as the scatterer and detector. The measured values agree with those of others, and with the predictions of Sakurai based on the Peierls model of the second resonance.

The combination of the Stanford Linear Accelerator, 180 degree spectrometer, and emulsion has proved successful in gathering significant information with a modest expenditure of acceleration time. Further exposures at higher and perhaps at lower energy are desirable.

It may still prove convenient to allow the electron beam to pass through the hydrogen target. However, to reduce the uncertainties caused by electropion production, the contribution from radiative electron scattering, and the exposure time, the radiator should be made thicker. Dr. Friedman has suggested a possible arrangement, with a cooled radiator, of perhaps 0.1 radiation length, close to the end of a short target cell. The increased intensity of the bremsstrahlung would reduce the exposure times to a few hours.*

It is recommended that new exposures be made with G-5, rather then K-5, emulsion. The developed grains are larger in G-5, and the tracks are more visible. The tracks should be developed as heavily as clarity of the plates allows, and precautions taken to avoid fading or

*Electron beam intensities like those in the present exposures would produce, in 0.1 radiation length, a bremsstrahlung intensity of 1.7×10^{17} Mev per hour, or about 1.7×10^{5} Caltech BIP's per hour. The synchrotron delivers, typically, 100 BIPs per hour.

etching of the grains. The use of thicker emulsion should be investigated, as an attempt to improve the area-scanning rate, or, in case the track-following method proves more useful at high energy.

To guarantee the absence of spurious asymmetry caused by scanning bias, the exposures should be made with half of the pellicles reversed.

A further gain in efficiency can be realized by improving the quality of the present emulsion grid. None of the three available grids, Chicago, Berkeley, or CERN, are entirely satisfactory. The Chicago grid was used in the present work, and has the lowest density of markings. However, the grid was made by photographing typewritten numbers, and the contrast of the negative is low, so that an exposure long enough to print the numbers adequately also exposes the background to some extent. It is estimated that about one man-month would be required to ink a grid master, photographs of which would be equivalent in contrast to the Berkeley and CERN grids but with an acceptable density of markings. Efforts to photograph typewritten numbers have not been very successful.

V. Z. Peterson has pointed out that because of the smaller proportion of inelastic scattering from the heavier elements, a heavy liquid bubble chamber is also a useful instrument in measuring proton polarization, especially when operated with a synchrotron with a low repetition rate.

It is, finally, interesting to consider the possibility of measuring the polarization of the recoil neutron in positive photopion production, especially the polarization caused by interference with the retardation

amplitude. To fix the energy of the neutron, coincidence with the π^+ is required, so that the experiment must be performed with counters, and cannot be done at Stanford, where such coincidence measurements are essentially impossible because of the short beam duration and high intensity. Counting rates will be exceedingly low if the conventional pair of counters to left and right of the scatterer are used, since the scatterer and counters must be made narrow to avoid spurious asymmetries.* The principal source of bias is the rapid variation of the kinematics in the production plane, which is also the plane of asymmetric scattering. It is worth pointing out that this difficulty may perhaps be circumvented, by using a magnetic field along the direction of recoil to precess the nucleon spin into the production plane, first to one side and then to the other, a technique developed at Harwell. (46) A single counter can then, in principle, be used to measure the scattering above or below the production plane, reversing the field, and the direction of the moment, between runs. With this arrangement it should be possible to make the scatterer and detectors larger and thicker, since the azimuthal variation of the kinematics is slow.

*The experimental design has been examined by C. Peck.

REFERENCES

1. H. A. Bethe and F. DeHoffman, Mesons and Fields, vol. II (Row, Peterson and Company, Evanston, Illinois, 1955).

2. S. J. Lindenbaum and L. C. L. Yuan, Phys. Rev. 100, 306 (1955).

3. Cool, Piccioni, and Clark, Phys. Rev. 103, 1082 (1956).

4. Burrowes, Caldwell, Frisch, Hill, Ritson, Schluter, and Wahlig, Phys. Rev. Lett. 2, 119 (1959).

5. Brisson, Detoef, Falk-Vairant, van Rossum, Valladas, and Yuan, Phys. Rev. Lett. 3, 561 (1959).

6. Longo, Helland, Hess, Moyer, and Perez-Mendez, Phys. Rev. Lett. 3, 568 (1959).

7. Devlin, Barish, Hess, Perez-Mendez, and Solomon, Phys. Rev. Lett. 4, 242 (1960).

8. Crittenden, Scandrett, Shepard, Walker, and Ballam, Phys. Rev. Lett. 2, 121 (1959).

9. Goodwin, Kenney, and Perez-Mendez, Phys. Rev. Lett. 3, 522 (1959).

10. McDonald, Peterson, and Corson, Phys. Rev. 107, 577 (1957).

11. DeWire, Jackson, and Littauer, Phys. Rev. 110, 1208 (1958).

12. P. C. Stein and K. C. Rogers, Phys. Rev. 110, 1209 (1958).

13. Heinberg, McClelland, Turkot, Wilson, Woodward, and Zipoy, Phys. Rev. 110, 1211 (1958).

14. J. I. Vette, Phys. Rev. 111, 622 (1958).

15. R. M. Worlock, Phys. Rev. 117, 537 (1960).

16. K. Berkelman and J. A. Waggoner, Phys. Rev. 117, 1364 (1960).

17. F. P. Dixon and R. L. Walker, Phys. Rev. Lett. 1, 142 (1958).

18. G. F. Chew, Phys. Rev. 95, 1669 (1954).

19. G. F. Chew and F. E. Low, Phys. Rev. 101, 1570 and 1579 (1956).

20. G. C. Wick, Revs. Modern Phys. 27, 339 (1955).

21. Chew, Low, Goldberger, and Nambu, Phys. Rev. 106, 1345 (1957).

22. R. R. Wilson, Phys. Rev. 110, 1212 (1958).

23. R. F. Peierls, Phys. Rev. Lett. 1, 174 (1958).

24. R. F. Peierls, Phys. Rev. 117, 325 (1960).

25. B. T. Feld, Phys. Rev. 89, 330 (1953).

26. J. J. Sakurai, Phys. Rev. Lett. 1, 258 (1958).

27. P. L. Connolly and R. Weill, Bull. Am. Phys. Soc. Ser. II, 4, 23 (1959).

28. P. C. Stein, Phys. Rev. Lett. 3, 473 (1959).

29. B. T. Feld and B. C. Maglić, Phys. Rev. Lett. 1, 375 (1958).

30. J. Rutherglen, private communication to V. Z. Peterson (to be published).

31. G. Stoppini and C. Pelligrini, Proceedings of the Ninth Annual Conference on High Energy Physics, Kiev, 1959.

32. L. F. Landovitz and L. Marshall, Phys. Rev. Lett. 3, 190 (1959).

33. Walker, Davis, and Shepard, Phys. Rev. 118, 1612 (1960).

34. L. Wolfenstein, Ann. Rev. Nuc. Sci. 6, 43 (1956).

35. B. Rose, private communication to V. Z. Peterson.

36. J. M. Dickson and D. C. Salter, Nuovo Cimento 6, 235 (1957).

37. Dickson, Rose, and Salter, Proc. Phys. Soc. (London) 68A, 361 (1955).

38. Tyrén, Hillman, and Johansson, Nuclear Phys. 3, 336 (1957).

39. Alphonce, Johansson, and Tibell, Nuclear Phys. 3, 185 (1957).

40. Chesnut, Hafner, and Roberts, Phys. Rev. 104, 449 (1956).

41. E. M. Hafner, Phys. Rev. 111, 297 (1957).

42. Johansson, Tibell, and Hillman, Nuclear Phys. 11, 540 (1959).

43. Alphonce, Johansson, and Tibell, Nuclear Phys. 4, 672 (1957).

44. Hillman, Johansson, and Tyrén, Nuclear Phys. 4, 648 (1957).

45. M. J. Brinkworth and B. Rose, Nuovo Cimento 3, 195 (1956).

46. Hillman, Stafford, and Whitehead, Nuovo Cimento 4, 67 (1956).

47. H. Tyrén and Th. A. J. Maris, Nuclear Phys. 3, 52 (1957).

48. H. Tyrén and Th. A. J. Maris, Nuclear Phys. 4, 637 (1957).

49. H. Tyrén and Th. A. J. Maris, Nuclear Phys. 6, 82 (1957).

50. H. Tyrén and Th. A. J. Maris, Nuclear Phys. 7, 24 (1958).

51. K. Strauch and F. Titus, Phys. Rev. 103, 200 (1956).

52. J. I. Friedman, Phys. Rev. 104, 794 (1956).

53. Chodorow, Ginzton, Hansen, Kyhl, Neal, Panofsky, et al., Rev. Sci. Instr. 26, 134 (1955).

54. R. Hofstadter, Revs. Modern Phys. 28, 214 (1956).

55. E. E. Chambers and R. Hofstadter, Phys. Rev. 103, 1454 (1956).

56. K. Brown and G. W. Tautfest, Rev. Sci. Instr. 27, 696 (1956).

57. G. W. Tautfest and H. R. Fechter, Rev. Sci. Instr. 26, 229 (1955).

58. J. I. Friedman, private communication.

59. Dilworth, Occhialini, and Vermaesen, Bulletin du Centre de Physique Nucleaire de L'Université Libre de Bruxelles, No. 13a (1950).

60. Powell, Fowler, and Perkins, The Study of Elementary Particles by the Photographic Method (Pergamon Press, New York, 1959), p. 92.

61. D. L. Judd, Rev. Sci. Instr. 21, 213 (1950).

62. H. A. Cramér, Mathematical Methods of Statistics, (Princeton University Press, 1946).

63. Barkas, Barrett, Cuer, Heckman, Smith and Ticho, UCRL 3768 (1957); Barkas, UCRL 3769 (1957).

64. M. N. Rosenbluth, Phys. Rev. 79, 615 (1950).

65. J. Schwinger, Phys. Rev. 75, 898 (1949).

66. L. I. Schiff, Phys. Rev. 87 750 (1952).

67. G. W. Tautfest and W. K. H. Panofsky, Phys. Rev. 105, 1356 (1957).

68. H. A. Bethe and J. Ashkin, Experimental Nuclear Physics, vol. 1, E. Segre, editor, (John Wiley and Sons, New York, 1953), p. 166.

69. Becker, Destaebler, and Panofsky, HEPL Internal Memorandum 202, unpublished (1960).

70. J. A. Wheeler and W. E. Lamb, Jr., Phys. Rev. 55, 858 (1939).

71. R. P. Feynman, notes in Quantum Electrodynamics, unpublished (1953).

72. Bethe, Schweber, and DeHoffman, Mesons and Fields, vol. I (Row, Peterson and Company, Evanston, Illinois, 1955) pp. 45-53.

73. R. H. Dalitz and D. R. Yennie, Phys. Rev. 105, 1598 (1957).

74. Panofsky, Newton, and Yodh, Phys. Rev. 98, 753 (1955).

75. Panofsky, Woodward, and Yodh, Phys. Rev. 102, 1392 (1956).

76. G. B. Yodh and W. K. H. Panofsky, Phys. Rev. 105, 731 (1957).

77. W. K. H. Panofsky and E. A. Allton, Phys. Rev. 110, 1155 (1958).

78. G. Salvini and R. Querzoli, private communication to V. Z. Peterson.

79. Brisson, Detoef, Falk-Vairant, van Rossum, and Valladas, Nuovo Cimento (to be published).

80. P. Carruthers, Phys. Rev. Lett. 4, 303 (1960).

81. R. F. Peierls, Phys. Rev. Lett. 5, 166 (1960).

82. M. Gell-Mann and K. Watson, Ann. Rev. Nuc. Sci. 4, 219 (1954).

83. Feshbach, Peaslee, and Weisskopf, Phys. Rev. 71, 145 (1947).

84. J. I. Shonle, Phys. Rev. Lett. 5, 156 (1960).

85. B. Rossi, High Energy Particles (Prentice-Hall, Inc. New York, 1952) pp. 66-77.

86. L. Voyvodić and E. Pickup, Phys. Rev. 85, 91 (1952).

87. D. M. Skyrme, Phil. Mag. 44, 191 (1953).

88. J. S. Ball, UCRL 8858 (1959).

APPENDIX I

SCANNING METHODS

The initial scanning of the Stanford exposures, using the Feld-Maglić method, was carried out as follows by Professor Peterson: The distribution of the projected angles and dips of the tracks near the entering edge (at a depth of 3 mm) was measured in each plate; the median of the projected angle distribution was taken as the angular reference for projected angles in that plate. The projected angles and dips at a greater depth (23 mm) were measured; at this depth the protons had lost 30 Mev. After subtracting the number of tracks which entered at wide angles, the number of tracks to the left and right at angles more than 6 degrees from the median direction were compared. The magnitude of the asymmetries obtained seemed to bear out the statement, in the Letter by Feld and Maglić (29), that tracks which deviated by more than 5 degrees from the incident beam direction could be ascribed to single scattering in the emulsion; an estimate of the multiple scattering contribution, later found to be quite optimistic, also supported this statement. The polarization obtained at 660 Mev was in fair agreement with the value of Stein at 700 Mev, but the value obtained at 585 Mev disagreed even in sign.

Precautions were taken to avoid left-right bias from angular misalignment; the median of the entering distribution was checked by comparing it with the median of the central, multiply-scattered, part of the distribution at 23 mm. Good agreement between the two medians was generally obtained, within the accuracy required by the slope of the

single-scattering cross section.

It was eventually discovered that the multiple scattering had been underestimated; the negative asymmetry was found to be caused by the propagation of a small asymmetry in the incident beam to wide angles by multiple scattering. At this point, a thorough investigation of scanning methods was undertaken, since it appeared that the method recommended by Feld and Maglić was unreliable.

The question of the reliability of the Feld-Maglić method necessarily involves the question of the reliability of their calibration of emulsion as a polarization analyzer. It has already been said that their calibration is almost certainly incorrect, since it differs materially from measurements made on pure elements under more favorable conditions and agreed upon by a number of laboratories.

Before calculating the asymmetry, Feld and Maglić subtracted an estimated multiple scattering background. The scattering seems to have been underestimated. Fig. 27 shows the distribution of plane projected angles of the protons tracks in one of the stacks exposed at Stanford (A). The solid curve is the calculated multiple scattering, obtained by folding Gaussian multiple scattering with a rectangular incoming distribution. The width of the rectangular distribution was taken to be 2.2 degrees,* and the width of the Gaussian 3.2 degrees, using the simple formula of Rossi, allowing for energy loss. (85) In this energy region and for this thickness of emulsion the width agrees within a few

*A width of 2.6 degrees is now thought to be more representative. The change lowers the peak value by about 3 per cent; the distribution is essentially unaffected at wide angles.

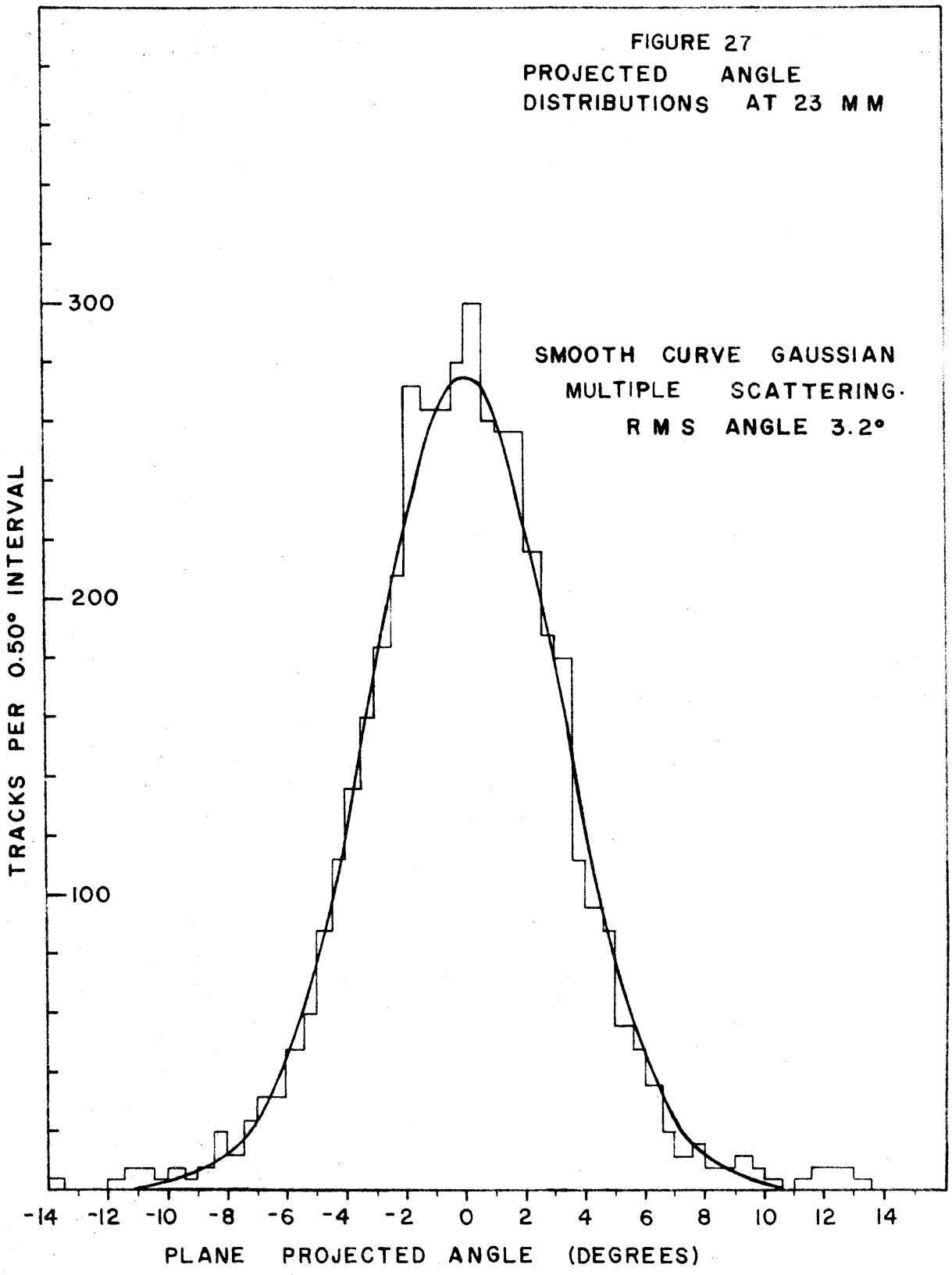
FIGURE 27
PROJECTED ANGLE
DISTRIBUTIONS AT 23 MM
SMOOTH CURVE GAUSSIAN
MULTIPLE SCATTERING.
R M S ANGLE 3.2°
TRACKS PER 0.50° INTERVAL
300
200
100
-14 -12 -10 -8 -6 -4 -2 0 2 4 6 8 10 12 14
PLANE PROJECTED ANGLE (DEGREES)

per cent with the Molière scattering width given by Voyvodić and Pickup, checked experimentally for 147 Mev protons in emulsion by Skyrme. (86, 87) The agreement between the curve and the data provides a strong indication that the scattering measured by Feld and Maglić at angles within the first diffraction maximum from 6 to 12 degrees was predominantly multiple scattering, so that a subtraction of multiple scattering could not be done significantly.

To avoid this difficulty, one may follow each wide angle track found at greater depth back to the incident edge, to eliminate the multiply-scattered tracks: the "follow-back" method. In a trial of the method, tracks found at 23 mm whose projected angle differed from the median angle by more than 5 degrees were followed back. The scanners found

193 tracks with no scatters whose projected angle change was greater than 3^{o}.

53 tracks with one scatter whose projected angle change was greater than 3^{o} and less than 12^{o}.

35 tracks with one scatter whose projected angle change was greater than 5^{o} and less than 12^{o}.

1 track with two scatters whose projected angle changes were greater than 3^{o} and less than 12^{o}.

This measurement shows that only 15 per cent of the scattering into the interval from 5 to 12 degrees is actually single scattering. The conditions under which this measurement was made were very similar to those of the Feld-Maglić experiment; the principal difference was that the angular width of the beam in dip was 8 degrees instead of 1.8 degrees, a difference which should not greatly affect the projected angle distribution.

Large asymmetries found with the Feld-Maglić method under these conditions must be almost entirely spurious, since the multiple scattering is symmetric.

Spurious asymmetries can arise from two sources: First, even if the incoming beam is perfectly symmetric, a small error in the determination of the central angle--the angle of symmetry--can produce quite large biases, since the scattering, multiple or single, decreases sharply with increasing angle. Second, if the beam is not symmetric, the "central" angle depends on the details of the distribution, and is in general unknown.

In the present study it was found by trial that it was difficult to fix the median of the angular distribution in a given plate with an accuracy greater than 0.3-0.4 degrees. The uncertainty arises partly from the statistical uncertainty in the median and partly from the dispersions in angular measurements. If the plate must be removed from the stage, or the protractor setting disturbed so that it must be reset, additional errors are introduced.

If one assumes that the angular distribution consists entirely of Gaussian multiple scattering, one can estimate the first-order asymmetry caused by an angular misalignment of magnitude δ upon the relative numbers, L and R, of events observed in "Left" and "Right" bins of width $d\theta$, at angles $\theta - \delta$ and $\theta + \delta$ from the beam center

$$\epsilon = \frac{L - R}{L + R} = \frac{\theta\delta}{\sigma^2}$$

In this formula σ^2 is the mean square projected angle of multiple

scattering. If σ = 3 degrees, θ = 9 degrees, and δ = 0.3 degrees, one obtains a spurious asymmetry of 30 per cent.

More insidious are the effects of asymmetries in the incoming beam. It is doubtful that a very large asymmetry could arise under the conditions given by Feld and Maglić (greater, say, than 5 per cent), but the following artificial example has been constructed to demonstrate the possible magnitude of the effect in the Stanford exposures: Consider that the beam is made up of a symmetric part and an additional asymmetric part consisting of two Gaussian peaks in the incoming distribution, at angles of -0.625 and 1.250 degrees, and of relative strengths 0.555 and 0.445 respectively; each Gaussian has a root-mean-square angle of 0.5 degrees. The median of this distribution is zero; but after folding it with 3 degree Gaussian multiple scattering, the areas under the tails at angles greater than 6 degrees are different; the asymmetry is 16 per cent. The example may be made more plausible by adding an arbitrary symmetric part, reducing the asymmetry. The corresponding error in the polarization is about twice the spurious asymmetry.

One concludes that the scanning procedure suggested by Feld and Maglić is invalid at small angles, so that asymmetries found with this method are very likely spurious. The feasibility of accepting only large angles, or of using a thinner scattering thickness, was investigated; it was concluded that the sacrifice in yield was so large that the method became less attractive than the more reliable methods.

Although the follow-back method can be used to eliminate the multiple-scattering contamination, it is also subject to misalignment errors, to a somewhat smaller extent. Many of the single scatterings are not detected; only the wide angle tracks are traced back, and multiple scattering along a track which also displays a single scattering may cause it to scatter out of the acceptance interval. This inefficiency makes it possible for angular misalignments to produce a spurious asymmetry, whose magnitude can be estimated as follows:

The relative numbers of tracks, which in fact undergo a single scattering with projected angle change θ^*, and which are later found to lie at a projected angle θ with respect to the incident beam, is approximately

$$p(\theta^*;\theta) = g(\theta-\theta^*)\sigma_p(\theta^*)$$

where $g(\theta)$ is the projected multiple scattering distribution, whose root-mean-square angle is σ; $\sigma_p(\theta)$ is the <u>projected</u> single scattering cross section. It is assumed that the incoming beam consists of parallel tracks, and that the scattering angles are small.

Using this formula, the detection efficiency, which is the normalized probability that the scattering of angle θ^* will be detected by tracing back tracks whose projected angle is greater than θ_1 is

$$p(\theta^*;\theta_1) = \frac{\int_{\theta_1}^{\infty} g(\theta-\theta^*)\sigma_p(\theta^*)d\theta + \int_{-\infty}^{-\theta_1} g(\theta-\theta^*)\sigma_p(\theta^*)d\theta}{\int_{-\infty}^{\infty} g(\theta-\theta^*)\sigma_p(\theta^*)d\theta}$$

Dividing out $\sigma_p(\theta^*)$, and making use of the unit normalization of $g(\theta)$,

one obtains

$$p(\theta^*;\theta_1) = 1 - \int_{\theta_1}^{\theta} g(\theta - \theta^*)d\theta$$

A spurious asymmetry occurs if the left and right limits $\pm \theta_1$ are misaligned by an angle δ, and is given to first order by

$$\epsilon = \frac{g(\theta^* - \theta_1) + g(\theta^* + \theta_1)}{p(\theta^*;\theta)} \delta$$

Assuming that the multiple scattering is Gaussian, that the angle θ_1 is 5 degrees, and that the root-mean-square multiple scattering angle is 3 degrees, the efficiency and bias are given as functions of the projected angle for single scattering θ^* as follows:

Scattering Angle θ^*, Degrees	Detection Efficiency Per Cent	Bias Per Cent/Degree
5	50	14.3
6	64	13.0
7	75	10.8
8	84	8.0
9	95	3.2
12	99	0.8

The method is not particularly efficient in detecting scattering in the first diffraction maximum, where the analyzing power is known with greatest accuracy; the bias effects are also largest in this region. The bias can be controlled, by reducing the instrumental misalignment errors, and also by comparing the numbers of multiply-scattered tracks traced on the left and right side; the bias in the multiple scattering is

larger than the single scattering bias, so that a misalignment is sensitively detected. There are about 30-50 such tracks in a plate; the statistical confidence in the asymmetry is therefore about 15 per cent. In the conditions of the Stanford exposure, the corresponding uncertainty in the mm angular reference is about 0. 25 degrees; it is necessary to average the results over a number of plates to eliminate bias effects.

It was discovered in the trials that the follow-back method is not particularly rapid, because of the time required to trace tracks from plate to plate. Six observer-weeks were consumed in collecting the data quoted, not including the time required to determine the central angle.

Measurements were also made of the rate at which tracks could be followed forward. In the polarization measurement of Friedman at 300 Mev (52), the average track following rate was 45 cm per hour. With the 400 micron emulsions used in the present experiment, however, the wide distribution of incoming dip angles, and the larger multiple scattering, the average distance traveled by a track in a single pellicle was only about 1 cm. In the trials the best rate obtained was about 20 cm per hour.

With the available plates it therefore seemed best to use the area scanning technique, described in detail in the text, since the initial trials indicated that it was more rapid than track following, and there was no obvious source of bias.

APPENDIX II

SPIN PRECESSION

The formula relating the scalar product of the moment vector $\underline{\mu}$ and the unit vector $\underline{n}$ normal to the scattering plane to the precession of the moment in the spectrometer is derived in this Appendix. It will be shown the quantity to be calculated is the conditional mean of $\underline{n} \cdot \underline{\mu}$ given the values of the projected angles and dip immediately before scattering, and the required formula will be derived.

1. Definitions

a. Coordinates: Let (x, y, z) be a right-handed rectangular system in the laboratory, with the y axis normal to the exit aperture of the spectrometer and positive in the direction of motion of the particles. The z axis is positive upwards (c. f. fig. 10).

b. Symbols:

θ_p Projected angle in (x, y) plane, measured from y axis.

γ Dip angle in unprocessed emulsion above (x, y) plane, positive if particle moves upward.

Φ Bending angle

Φ_o Bending angle on central trajectory

θ Laboratory angle of center of entrance aperture

Ω Precession frequency/cyclotron frequency

μ Unit moment vector

M Angular magnification

c. Subscripts for θ_p:

0 At entrance of spectrometer

1 At entrance of emulsion stack

2 Immediately before scattering

3 Immediately after scattering

2. Spin components, to first order where justified in θ_p, γ:

a. At entrance of spectrometer

$$\mu_x = -\gamma_o \cot \theta$$

$$\mu_y = \gamma_o$$

$$\mu_z = (1 - \theta_{p_o} \cos \theta \cot \theta)$$

b. At exit of spectrometer

$$\mu_x = -\gamma_o \cot \theta$$

$$\mu_y = (1 - \theta_{p_o} \cos \theta \cot \theta) \sin (\Omega\Phi + \gamma_o)$$

$$\mu_z = (1 - \theta_{p_o} \cos \theta \cot \theta) \cos(\Omega\Phi + \gamma_o)$$

where

$$\Omega\Phi + \gamma_o = \Omega\Phi_o + \Omega(\Phi - \Phi_o) + \gamma_o = \Omega\Phi_o + [1 - \Omega(1+M)]\,\gamma_1/M$$

$$\theta_{p_o} = \theta_{p_1}/M$$

3. Scattering Probability:

$$\frac{d\sigma}{d\Omega} = \int \sigma(\theta)[1 + a(\theta) P\underline{n} \cdot \underline{\mu}] f_\mu(\theta_{p_1}, \gamma_1) d\theta_{p_1} d\gamma_1$$

$$= \sigma(\theta)[1 + a(\theta) P\underline{n} \cdot \underline{\mu}]$$

where $f(\theta_{p_1}, \gamma_1)$ is the probability that $\underline{\mu}$ lies in the angular interval $(d\theta_{p_1}, d\gamma_1)$, and μ_i = expected value of μ_i:

$$\mu_i = \int \mu_i f_\mu(\theta_{p_1}, \gamma_1) d\theta_{p_1} d\gamma_1 .$$

This formula shows that the mean value of $\underline{n} \cdot \underline{\mu}$ is the quantity to be used if $\underline{n} \cdot \underline{\mu}$ is not directly measured. The information provided by the measurement of the dip and projected angle before scattering (not uniquely related to the orientation of the moment because of multiple scattering) can be used if the conditional mean of $\underline{n} \cdot \underline{\mu}$ is calculated from the measured values.

4. Conditional distribution of moments, given the observed dip and projected angle:

$$f_\mu(\theta_{p_1}, \gamma_1 \mid \theta_{p_2}, \gamma_2) = f(\theta_{p_1} \mid \theta_{p_2}) f(\gamma_1 \mid \gamma_2)/[\Omega(1+M)-1]$$

where $f(\gamma_1 \mid \gamma_2)$ and $f(\theta_{p_1} \mid \theta_{p_2})$ are the conditional distributions of the dips and projected angles at the entrance of the stack given the values measured before scattering.

5. Conditional distributions of dip and projected angle:

Derivation for dip angle given:

a. $f(\gamma_1 \mid \gamma_2) = f(\gamma_1) f(\gamma_2 \mid \gamma_1) / \int f(\gamma_1) f(\gamma_2 \mid \gamma_1) d\gamma_1$; Cramér (62), pp. 267-269.

b. $f(\gamma_1)$ is assumed to be rectangular of width $2v$; $2v$ = angular slit width multiplied by calculated angular magnification.

c. $f(\gamma_2 \mid \gamma_1)$ is assumed to be Gaussian:

$$f(\gamma_2 \mid \gamma_1) = (2\pi)^{-1/2} \sigma^{-1/2} \exp -(\gamma_2 - \gamma_1)^2 / 2\sigma^2 = g(\gamma_2 - \gamma_1)$$

and

$$G(x) = \int_0^x g(t)dt = \text{normal probability integral.}$$

d. Root-mean-square projected angle σ is obtained from the approximate formula of Rossi (81):

$$\sigma = (21\ \text{Mev})t^{1/2}/2^{1/2}p\beta c \quad \text{(radians)}$$

t = scattering thickness in radiation lengths

6. Expectation values of the spin components:

a. Expand μ_y, μ_z to second order in γ_1:

$$\mu_y = (1-\frac{1}{M}\theta_{p_1}\cos\theta\cot\theta)[\sin\Omega\Phi_o + k\gamma_1\cos\Omega\Phi_o - \frac{1}{2}k^2\gamma_1^2\sin\Omega\Phi_o]$$

$$\mu_z = (1-\frac{1}{M}\theta_{p_1}\cos\theta\cot\theta)[\cos\Omega\Phi_o - k\gamma_1\sin\Omega\Phi_o - \frac{1}{2}k^2\gamma_1^2\cos\Omega\Phi_o]$$

where $k = [1 - \Omega(1 + \mathbf{M})]\,M^{-1}$

The second order expansion is quite adequate over the range of argument allowed.

7. Evaluation of mean components: obtain the conditional means of θ_{p_1} given θ_{p_2}, of γ_1 and γ_1^2, given γ_2, and substitute in the above expansions; the procedure is justified by the theorems on the means of sums and products given by Cramér (62, pp. 170-174). Formulas given for dip only; result for projected angle is similar.

$$\gamma_1|\gamma_2 = \gamma_2 + \sigma\left[\frac{g(\gamma_2+v) - g(\gamma_2-v)}{G(\gamma_2+v) - G(\gamma_2-v)}\right]$$

$$\gamma_1^2|\gamma_2 = \sigma^2\left\{1 - \left[\frac{g(\gamma_2+v) - g(\gamma_2-v)}{G(\gamma_2+v) - G(\gamma_2-v)}\right]^2 + \frac{(\gamma_2-v)g(\gamma_2-v) - (\gamma_2+v)g(\gamma_2+v)}{G(\gamma_2+v) - G(\gamma_2-v)}\right\} + (\gamma_1|\gamma_2)^2$$

8. Final evaluation of scalar product $\underline{n} \cdot \underline{\mu}$: Having calculated the expected value of each component of the moment vector, form the scalar product $\underline{n} \cdot \underline{\mu}$.

9. Calculation procedure for each event:

a. Obtain σ, θ_{p_2}, γ_2.

b. Compute $g(\gamma_2 \pm v)$, etc.

c. Compute $\gamma_1|\gamma_2$, $\gamma_1^2|\gamma_2$, $\theta_{p_1}|\theta_p$.

d. Form mean components.

e. Form scalar product.

APPENDIX III

ELECTROPION PRODUCTION KINEMATICS

1. Notation for particle momenta :

Four-Momentum	Definition	(Momentum, Energy) Lab	c. m.*	Mass
p_μ	Incident electron momentum	$(\underline{p}, p_o)$	$(\underline{P}, P_o)$	m
p'_μ	Scattered electron momentum	$(\underline{p}', p'_o)$	$(\underline{P}', P'_o)$	m
q_μ	Pion momentum	$(\underline{q}, q_o)$	$(\underline{Q}, Q_o)$	μ
t_μ	Target proton momentum	$(\underline{t}=0, t_o)$	$(\underline{T}, T_o)$	M
r_μ	Recoil proton momentum	$(\underline{r}, r_o)$	$(\underline{R}, R_o)$	M
k_μ	Momentum transfer: $p_\mu - p'_\mu$	$(\underline{k}, k_o)$	$(\underline{K}, K_o)$	--
d_μ	Center of mass momentum: $k_\mu + t_\mu = r_\mu + q_\mu$	$(\underline{d}, d_o)$	$(\underline{D}=0, D_o)$	--

2. Definition of angles:

θ_e Angle between $\underline{p}, \underline{p}'$: scattered electron angle in lab.

θ Angle between $\underline{p}, \underline{r}$: recoil proton angle in lab.

ϕ Angle between $\underline{p}, \underline{r}$ plane and $\underline{p}, \underline{p}'$ plane.

3. Magnitude of scattered electron momentum:

$$p_\mu + t_\mu = p'_\mu + q_\mu + r_\mu \quad \text{(conservation of momentum)}$$

Eliminating q_μ by the relation $q^\mu q_\mu = -\mu^2$, one obtains after expression of the four-momenta in terms of momentum and

*The c. m. system is that of the pion and proton center of mass.

energy, and putting $p \approx p_o$, $p' \approx p_o'$, the following formula:

$$p' = \frac{rp\cos\theta - r_o(p + M) - \mu^2/2}{p(1 - \cos\theta_e) + r(\cos\theta\cos\theta_e + \sin\theta\sin\theta_e\cos\phi) - r_o}$$

4. Invariant momentum transfer

$$k^\mu k_\mu = (p^\mu - p'^\mu)(p_\mu - p_\mu')$$

$$= -2(m^2 + \underline{p}\cdot\underline{p}' - p_o p_o')$$

$$\approx 2pp'(1 - \cos\theta_e) + m^2(p - p')^2/pp'$$

5. Evaluation of c. m. quantities (upper case letters) from lab quantities (lower case letters): Method used by Dalitz and Yennie (73).

a. Energy

$$A_o = \frac{A_o D_o}{D_o} = \frac{a^\mu d_\mu}{\sqrt{-d^\mu d_\mu}}$$

$$d_\mu = k_\mu + t_\mu = (\underline{k}, M + k_o)$$

D_o = total c. m. energy

$$= \sqrt{-d_\mu d_\mu} = \sqrt{-(k^\mu k_\mu + 2k^\mu t_\mu + t^\mu k_\mu)}$$

$$= \sqrt{-k^\mu k_\mu + 2k_o M + M^2}$$

b. Momentum

$$A = \sqrt{a^\mu a_\mu + A_o^2}$$

c. Scalar product

$$\underline{A} \cdot \underline{B} = a^{\mu} b_{\mu} + A_o B_o = \underline{a} \cdot \underline{b} - a_o b_o + A_o B_o$$

6. Evaluation of "equivalent" real photon energy to give c. m. energy D_o in photoproduction.

Electroproduction:

$$D_o^2 = - d^{\mu} d_{\mu} = -k^{\mu} k_{\mu} + 2k_o M + M^2$$

Photoproduction: k_2 = laboratory photon energy

$$D_o^2 = 2k_L M + M^2 \qquad k^{\mu} k_{\mu} = 0 \text{ for real photon}$$

Therefore, if D_o is computed, k_L is given by

$$k_L = \frac{D_o^2 - M^2}{2M}$$

APPENDIX IV

MULTIPOLE EXPANSIONS OF PHOTOPRODUCTION CROSS SECTIONS AND POLARIZATIONS

Reference: Chew, Low, Goldberger, and Nambu (21).

1. Photoproduction amplitude: most general two-component form:

$$f = i\underline{\sigma}\cdot\underline{e}f_1 + \underline{\sigma}\cdot\underline{q}\underline{\sigma}\cdot\underline{k}x\underline{e}f_2 + i\underline{\sigma}\cdot\underline{k}\underline{q}\cdot\underline{e}f_3 + i\underline{\sigma}\cdot\underline{q}\underline{q}\cdot\underline{e}f_4$$

where

$\underline{\sigma}$ = Pauli spin operator

$\underline{e}$ = unit vector in direction of photon polarization

$\underline{k}$ = unit vector in direction of photon momentum

$\underline{q}$ = unit vector in direction of pion momentum

2. Cross section, if u_f and u_i are initial and final proton wave functions

$$\frac{d\sigma}{d\Omega} = \frac{1}{4}\frac{q}{k}\sum_{\substack{\text{initial}\\\text{spins}}}\sum_{\substack{\text{final}\\\text{spins}}}\sum_{\substack{\text{photon}\\\text{polari-}\\\text{zations}}} |\langle u_f|f|u_i\rangle|^2$$

$$\frac{1}{4}\frac{q}{k}\sum_{\substack{\text{photon}\\\text{polarizations}}} \text{Trace } f^+f$$

3. Polarization

$$P\frac{d\sigma}{d\Omega} = \frac{1}{4}\frac{q}{k}\sum_{\substack{\text{photon}\\ \text{polarizations}}} \text{Trace } f^{+}\underline{\sigma}\cdot\underline{n}f$$

where $\underline{n}$ = unit vector normal to production plane:

$$\underline{n} = \underline{k}\times\underline{q}/|\underline{k}\times\underline{q}|$$

4. Multipole expansion of amplitudes: see also the report by Ball (88)

$$f_1 = \sum_{\ell=0}^{\infty} [\ell M_{\ell+} + E_{\ell+}] P'_{\ell+1}(x) + [(\ell+1)M_{\ell-} + E_{\ell-}] P'_{\ell-1}(x)$$

$$f_2 = \sum_{\ell=1}^{\infty} [(\ell+1)M_{\ell+} + \ell M_{\ell-}] P'_{\ell}(x)$$

$$f_3 = \sum_{\ell=1}^{\infty} [E_{\ell+} - M_{\ell+}] P''_{\ell+1}(x) + [E_{\ell-} + M_{\ell-}] P''_{\ell-1}(x)$$

$$f_3 = \sum_{\ell=1}^{\infty} [M_{\ell+} - E_{\ell+} - M_{\ell-} - E_{\ell-}] P''_{\ell}(x)$$

P_ℓ = Legendre polynomial of order ℓ; primes indicate differentiation with respect to $x_L = \cos\theta_{\text{c.m.}}$

5. Explicit evaluation for the cases found useful are given in Table II of the text; the expansions are given in full by Peierls (24), with a different normalization.